

**An evaluation of the effect of food quality
on heterotrophic protists with a critical
assessment of a new measuring technique
(Flow CAM)**

**Dissertation
zur Erlangung des Doktorgrades**

der Mathematisch-Naturwissenschaftlichen Fakultät

**der Christian-Albrechts-Universität
zu Kiel**

vorgelegt von

Florian Matthias Hantzsche

Kiel 2010

Referent: Prof. Dr. Maarten Boersma

Koreferent: Prof. Dr. Franciscus Colijn

Tag der mündlichen Prüfung: 01.10.2010

Zum Druck genehmigt: 01.10.2010

CONTENTS

CHAPTER I	4
General introduction.....	4
List of manuscripts	10
CHAPTER II.....	11
Some fundamental Flow CAM measurement basics for plankton ecological surveys in the fluorescence triggered image mode.....	11
CHAPTER III.....	34
Use of the Flow CAM for plankton abundance estimations in the field and a critical assessment of the applied method	34
CHAPTER IV	62
Dietary induced responses in the phagotrophic flagellate <i>Oxyrrhis marina</i>	62
CHAPTER V.....	82
No food selection, but compensatory feeding in the phagotrophic flagellate <i>Oxyrrhis marina</i>	82
CHAPTER VI	100
General Discussion.....	100
SUMMARY	112
ZUSAMMENFASSUNG.....	114
REFERENCES.....	117
DANKSAGUNG.....	128
CURRICULUM VITAE	129
PUBLIKATIONEN.....	130
ERKLÄRUNG	131

CHAPTER I

General introduction

The marine pelagic food web

Marine pelagic food webs are complex and dynamic networks of many species which are linked in manifold interactions driven by chemical and physical factors. Some of the species interact indirectly, competing for the same resource; some of them interact directly via consumption and predation. The human need for simplification and classification has forced many of the interacting species into different trophic levels, consuming the levels below, and being eaten by the level above. We also know, however, that these classifications are dynamic in time and space, which means that a consumer might switch between food from different trophic levels depending on prey availability, ingestibility and food quality (Sommer et al. 2002).

Phytoplankton, at the base of the pelagic food web, comprises a huge variety of different algal species, which supply the ecosystem with energy. Light, nutrients and inorganic carbon are the resources that regulate the quantity, distribution, and structure of the phytoplankton community (Diehl 2002). Light serves as the primary energy source through photosynthesis. Light and nutrients differ fundamentally, because nutrients can be recycled and mostly do not leave the ecosystem, whereas absorbed light is transformed into energy and only flows in one direction within the food web, ultimately disappearing again as heat. For a long time the main consumers of the phytoplankton were thought to be the highly visible crustacean mesozooplankters, which, in turn, are the most important food source for higher trophic levels, such as fish (Cushing 1995). Since the 1970s it has become clear that herbivorous and bacterivorous protists such as heterotrophic nanoflagellates (HNF), heterotrophic/mixotrophic dinoflagellates and ciliates play a central role in the lower pelagic food web (Pomeroy 1974; Fenchel 1982c; Azam et al. 1983; Fenchel 2008), and that the microbial loop is of great importance in the transfer of material and energy to higher trophic levels. It is by now well established that protistan predation can be a significant source of mortality for suspended bacteria and phytoplankton in marine ecosystems. Protists, in turn, can be a significant food source for metazooplankton (Fenchel 1982b; Kleppel 1993; Sherr and Sherr 1994; Kiorboe 1998; Landry and Calbet 2004).

Ecological stoichiometry

Traditionally, in aquatic ecology there has been a distinction between bottom-up and top-down control of population dynamics of species, often extended to the whole ecosystem. It is important to realise, however, that top-down control (predation determines population dynamics) in one trophic level is likely to lead to bottom-up control (food availability determines population dynamics) on the next level. Therefore, comprehending the predatory (grazing) interaction between two adjacent trophic levels is of paramount importance for our understanding of the functioning of the ecosystem as a whole. The theory of ecological stoichiometry has proven to be a very useful framework to advance our knowledge of trophic interactions (Sterner and Elser 2002). Ecological stoichiometry, the study of ratios of important nutrients in food and consumers, uses these ratios to explain the interactions between different trophic levels and such processes as the transfer of material and energy through the food web.

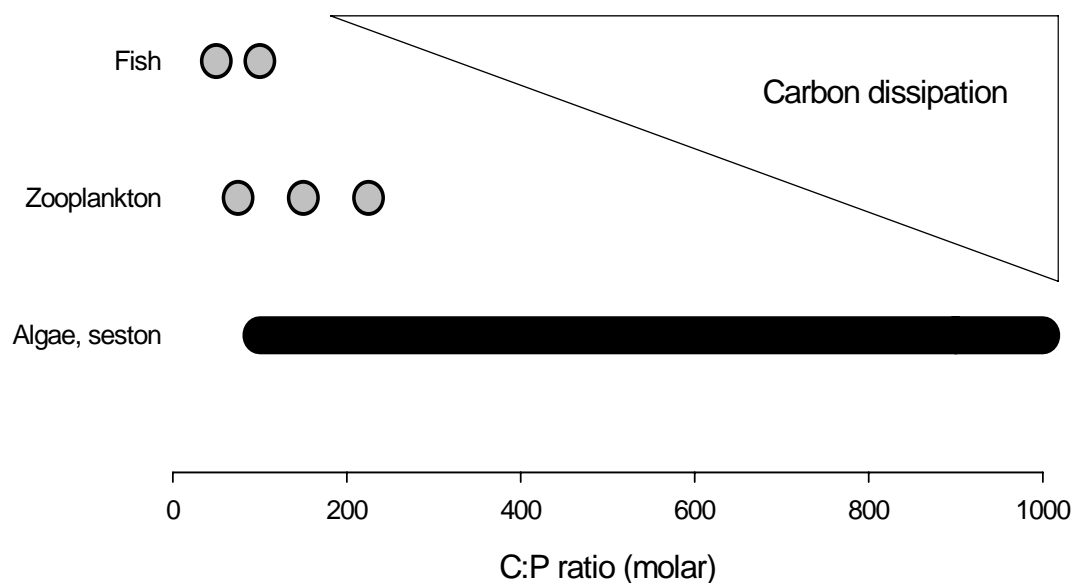


Figure 1: C:P ratio of different trophic levels in an aquatic system. Redrawn from Sterner and Elser (2002).

Previous studies have shown that a substantial difference exists in the nutrient composition between autotrophs and heterotrophs. While the elemental composition of autotrophs follows the availability of nutrients in the environment quite closely, heterotrophs have a more constant body composition, *i.e.* are more homeostatic with respect to the ratio of the main nutrients, carbon (C), nitrogen (N) and phosphorus (P). Obviously, this mismatch in availability and demand between autotrophs and herbivores affects the transfer efficiency of

energy and organic material through the food web. As stated above, not only the quantity of nutrients but rather the ratio of macronutrients (N, P, Si, (Fe)) for which autotrophs compete, determines the composition of the phytoplankton community and its elemental food quality (Tilman et al. 1982; Sommer et al. 2002). Even though heterotrophs are more homeostatic, the different species of heterotrophs differ in their elemental composition, and species higher up in the food chain tend to have lower amounts of carbon in their tissue relative to nitrogen and phosphorus than those species lower in the food chain (Fig. 1). Hence, especially from a herbivore point of view the elemental composition of its food source is highly variable depending on the nutrient availability of the algae, their growth phase, and the availability of light and carbon. Several mechanisms have evolved in herbivorous consumers to deal with nutritional imbalances. Essentially, these mechanisms can be divided into two groups: pre-gut and post-gut mechanisms. Pre-gut adaptations include selective feeding and selective transfer of material from the gut into the body. Post-gut adaptations include differential assimilation of different substances and respiratory and excretion processes. In most feeding processes food is taken up as a package and not as single nutrients, and thus the ecological stoichiometry framework mostly assumes that the majority of the processes to deal with nutritional imbalances are post-gut (Anderson et al. 2005). Therefore optimal food quality is defined as the food which meets the consumer's elemental ratios most closely, resulting in the lowest amounts of excreted products. Consequently food quality is lower when the consumer is faced with imbalances in the nutrient ratios, leading to decreased assimilation rates and/or increased excretion rates. As there might be a cost to these processes this could affect growth and reproduction of the consumer (Boersma 2000; Jensen et al. 2006).

Effects of food quality on heterotrophic protists

As stated above, we now know that a large fraction of the primary production is not consumed directly by crustacean mesozooplankton (in contrast to the classical food chain by Ryther (1969)) but rather by phagotrophic or heterotrophic protists (Fenchel 1982c; Azam et al. 1983; Sanders et al. 1992; Sanders et al. 2000). Heterotrophic bacteria compete with phytoplankton for nutrients such as nitrogen and phosphorus and are dependent on carbon sources which they receive from all trophic levels within the pelagic food web as DOC or detritus (Jumars et al. 1989; Thingstad et al. 1993; Caron et al. 2000). The discovery of these complex interactions (Fenchel 1982a; Fenchel 1988) resulted in a discussion about whether the microbial food web is a sink or a link within the pelagic food web in terms of energy/carbon transfer (Sommer et al. 2002; Fenchel 2008). Sink indicates a loss of energy

available to higher trophic levels as the energy is used by the microbes. Moreover, if a major transfer of energy takes place through the microbial loop this means an elongation of the food chain, with the resulting loss of efficiency for production in higher trophic levels. In contrast, carbon fixed by picophytoplankton ($<2\mu\text{m}$) or recycled by heterotrophic bacteria is not normally available for higher trophic levels as these organisms are too small to be consumed. Grazing by heterotrophic nanoflagellates (HNFs) and ciliates, which in turn can be eaten by mesozooplankton would make this energy available for higher trophic levels again, thus making the microbial food web a link. Most likely, both processes are of importance and depending on the availability of other nutrients, the sink function might be more important than the link function or vice versa. Indeed several laboratory studies have shown that copepods efficiently feed, grow, and reproduce on a diet consisting of heterotrophic protists and are able to switch to heterotrophic prey when phytoplankton quality is low (Wiadnyana and Rassoulzadegan 1989; Stoecker and Capuzzo 1990; Kleppel 1993; Gismervik and Andersen 1997).

Even though there is a wealth of information on the effects of stoichiometric imbalances of the food on growth and reproduction of herbivores closer inspection reveals that most of these studies have focussed on crustaceans, and of these most dealt with the freshwater cladoceran *Daphnia* (e.g. Sterner 1993; Urabe et al. 1997; DeMott et al. 1998; DeMott and Gulati 1999). In the marine environment the main focus of studies dealing with food quality effects on herbivores focussed on the biochemical composition of different food sources (Ederington et al. 1995; Kleppel and Burkart 1995; Klein-Breteler et al. 1999), while only a few studies dealing with food quality issues in a stoichiometrical context exist (Augustin and Boersma 2006; Malzahn et al. 2007; Malzahn et al. 2010). Even fewer studies used protists as the main herbivore and to date we know virtually nothing on the effects of food quality in a stoichiometric context on growth and reproduction of these organisms (Sterner and Elser 2002; Grover and Chrzanowski 2006). Filling this gap was one of the major aims of this thesis, on the one hand by experimental approaches under controlled conditions and on the other hand by improving our observational capacity of natural systems.

Use of the Flow CAM for plankton surveys

As already indicated by Haeckel in the late 1900s counting phytoplankton cannot be done without ruin of mind and body (Haeckel 1890). Despite this, the methods of counting and identifying plankton have changed little since Utermöhl established the techniques for the light microscope (Utermöhl 1958). Recently, however, there has been a renewed interest in

trying to establish methods which can automatically identify and enumerate planktonic communities. Since the traditional process of counting and classifying individual cells is slow, tedious and subject to a number of potential sources of error (e.g. fixation artefacts and human error), automated systems which might be able to measure particles promptly and “alive” (Benfield et al. 2007) are the way forward. With the invention of particle counters to quantify particles or cells in defined size ranges in order to establish the contribution of each size class in samples (Simons 1970; Zimmermann et al. 1980; Wenger et al. 1982; Harfield and Wharton 1988; Goransson 1990) and the progression of computer hard- and software development promising new techniques are now available which might ultimately replace traditional counting methods.

One of those promising approaches is the Flow CAM (Sieracki et al. 1998), a combination of a flow cytometer and a microscope, equipped with a computer processor and a digital camera. The water sample is placed in a sample funnel and pumped through a transparent glass capillary (flowcell). Digital pictures are taken by the Flow CAM as soon as particles pass the field of view. By combining the different techniques it is possible to differentiate between different algal groups, and potentially even between different growth stages within one species, as size, fluorescence, shape and optical density may differ between different growth phases in one species. To date, however, only a few publications have appeared that used the Flow CAM in such experiments and/or in standard surveys of phytoplankton communities (Sieracki et al. 1998; See et al. 2005; Buskey and Hyatt 2006; Ide et al. 2008). Hence, establishing the conditions under which the Flow CAM yields proper results is of great importance, and the second major aim of this thesis.

Outline of the thesis

One of my research aims was to test the Flow CAM as an automated plankton recognition system to replace the tedious, traditional methods such as microscopic counts. The long time plankton series at Helgoland Roads (North Sea, 54°11.3'N, 7°54.0'E) was initiated in 1962, and is destined for such automated plankton counting and recognition systems as measurement are taken on a work-daily basis (Wiltshire and Manly 2004). With the growing interest in long term plankton studies as a means to study the effects of global warming on aquatic communities, plankton monitoring and surveys will most likely become even more important in the future. The use of the Flow CAM is not trivial. Many different parameters can be changed, the effects of which are not always predictable. Therefore, Chapter II deals with the exhaustive testing of the instrument, using the algae *Rhodomonas*

salina and changing different Flow CAM parameters such as pump speed, camera exposure, fluorescence amplifier and threshold. Furthermore the potential of the Flow CAM to discriminate between differently grown *R. salina* was investigated.

In Chapter III, weekly water samples from Helgoland Roads were measured with the Flow CAM from July 2007 until January 2009. I present an application of the Flow CAM for the field using three different flowcell sizes and three different magnifications. The Flow CAM data are then correlated with the microscopic counts, chlorophyll content and water transparency to test the reliability of the Flow CAM measurements.

In Chapter IV, the effect of food quality on the phagotrophic flagellate *Oxyrrhis marina* in terms of food uptake and growth using different nutrient defined *Rhodomonas salina* as algal prey was examined. Additionally, possible excretion processes and the level of homeostasis of *O. marina* are shown.

In Chapter V the Flow CAM was used to investigate the ability of *O. marina* to select between different nutritionally defined *R. salina* dependent on the food source *O. marina* was previously cultured on (pre-gut selection). In a second step the potential of *O. marina* to recognize the elemental deficiency both in their own cells and the food cells was tested. Dependent on the precondition of *O. marina* the potential to compensate unbalanced food when food of higher quality was available was examined.

In Chapter VI, I discussed the results and give suggestions for further research.

List of manuscripts

This thesis consists of four manuscripts which are in preparation for submission (in prep.), submitted or published.

1.) Some fundamental Flow CAM measurement basics for plankton ecological surveys in the fluorescence triggered image mode (in prep.)

Florian Matthias Hantzsche, Friedhelm Schroeder, Karen Helen Wiltshire & Maarten Boersma

All analyses, the text writing and graphical presentation were done by Florian Matthias Hantzsche under the supervision of Prof. Dr. Maarten Boersma, Prof. Dr. Karen H. Wiltshire and Dr. Friedhelm Schroeder.

2.) Use of the Flow CAM for plankton abundance estimations in the field and critical assessment of applied method (in prep.)

Florian Matthias Hantzsche, Friedhelm Schroeder, Silvia Peters, Kristine Carstens, Karen Helen Wiltshire & Maarten Boersma

All analyses, the text writing and graphical presentation were done by Florian Matthias Hantzsche under the supervision of Prof. Dr. Maarten Boersma, Prof. Dr. Karen H. Wiltshire and Dr. Friedhelm Schroeder. Silvia Peters provided phytoplankton and microzooplankton data (microscope counts) and Kristine Carstens measured chlorophyll (H.P.L.C).

3.) Dietary-induced responses in the phagotrophic flagellate *Oxyrrhis marina* (published 2010)

Florian Matthias Hantzsche & Maarten Boersma

All analyses, the text writing and graphical presentation were done by Florian Matthias Hantzsche under the supervision of Prof. Dr. Maarten Boersma.

4.) No food selection, but compensatory feeding in the phagotrophic flagellate *Oxyrrhis marina* (submitted)

Florian Matthias Hantzsche, Cedric Meunier, Julia Haafke, Arne Michael Malzahn, Maarten Boersma

All analyses, the text writing and graphical presentation were done by Florian Matthias Hantzsche under the supervision of Prof. Dr. Maarten Boersma and Dr. Arne Malzahn. Cedric Meunier assisted during the experiments and Julia Haafke measured the nutrient data (C,N,P).

CHAPTER II

Some fundamental Flow CAM measurement basics for plankton ecological surveys in the fluorescence triggered image mode

Florian Matthias Hantzsche, Friedhelm Schroeder, Karen Helen Wiltshire & Maarten
Boersma

ABSTRACT

Despite the fact that there is strong demand for the development of automated plankton recognition systems in planktology to replace traditional time intensive counting techniques, such as light microscopy, little is known about the exact measurement mechanisms and limits of available systems. Publications on quality control applications do almost not exist which would be imperative as such systems are used solving ecological problems in the field and in experimental setups. We evaluated one such system-the “Flow CAM”. With this we hope to help other users to understand the fundamental measurement mechanisms in the fluorescence triggered image mode, the mode which is most commonly used for counting fluorescent particles such as phytoplankton. Due to the high variety of different Flow CAM measurement options, their wide range of adjustment possibilities, we focused first on one flowcell (100 μm) and objective (20 X) combination. The effect of flowcell illumination, cell density and pump speed were examined on the accuracy of Flow CAM measurements and demonstrated that all of these factors significantly influenced the accuracy of the measurement. Furthermore, how fluorescence is actually measured by the Flow CAM mainly dependent on the particle speed was discussed. It is understood that this system cannot be evaluated in all of its facets. It was hoped to improve the application success and to encourage other users to develop applications for precise Flow CAM measurements in the fluorescence triggered image mode, with this work.

INTRODUCTION

Already in the late nineteen-hundreds when Haeckel started the first research on planktonic communities, an accurate and timely counting of the many organisms present in one drop of water posed many difficulties. Indeed Haeckel himself stated that counting of phytoplankton ‘could not be achieved without ruining one’s mind and body’ (Haeckel 1890). This is still the case today, and even though several (semi-) automatic ways of counting phytoplankton were developed in the past, much of the counting is still done using the traditional Utermöhl microscope method (Utermöhl 1958). As a result, every new development in this area is usually met with a mixture of scepticism and enthusiasm. The initial publication with a detailed description of the newly developed Flow CAM technology by Sieracki et al. (1998), combined with the rapid marketing of a ready-to-use version of the system, and the subsequent sale of several hundred Flow CAM machines, led the scientific community to hope that finally a system which would be able to automatically identify and quantify phytoplankton was on the market.

Surprisingly, the number of publications with Flow CAM applications available from ISI’s Web of Science is still very low. Only seven publications are available, all with very specific aims, and the description of the methods and modes is difficult to follow for the interested reader. Essentially, the Flow CAM can be operated in three different counting modes:

- The fluorescence triggered image mode (+laser), which counts based on fluorescence of the particles, thus theoretically counting algae only (fluorescence triggered).
- The light scattered image mode (+laser) which counts every particle scattering the laser, thus counting additionally to the fluorescence algae everything (+non fluorescent particles) which pass the flowcell.
- The AutoImage mode (-laser) which counts every particle (similar to the light scattered image mode), however not “live”, but in distinct time intervals. This mode is the actual, automatic counting mode where the Flow CAM calculates the density of particles based on particle frequency and pump speed.

Sieracki et al. (1998), Buskey & Hyatt (2006), Ide et al. (2008) and Littman et al. (2008) used the Flow CAM in the fluorescence triggered image mode, whereas the remaining authors used the AutoImage mode (See et al. 2005, Zarauz & Irigoien 2008) or light scatter image mode (Sterling Jr. et al. 2004). So, with the Flow CAM marketed as an automated plankton recognition system or auxiliary tool for plankton ecological surveys it seems strange that a

clear description of effects and consequences of the large variety of possible adjustments and measurement modes provided by the Flow CAM technology is missing from the literature. Here, we aim to rectify this and shed some light on the possibilities and pitfalls of Flow CAM technology with the aim to further this interesting new technology.

The Flow CAM can be run in three different modes as stated above. The mode that is most appropriate for natural algal samples is the fluorescence triggered mode, as the auto-fluorescence of the particles that pass the lens trigger the camera and data collection. The AutoImage mode simply measures every particle, with the definite disadvantage for natural samples that all other particles (detritus, animals, marine snow) are also collected, which results in an unmanageably high number of measured particles. Reliable data acquisition and time efficiency are the basic requirements for the use of in flow imaging systems over time consuming traditional techniques such as light microscopy (Benfield et al. 2007). It is stated in the Flow CAM manual of Fluid Imaging that many parameters affect measurement accuracy. Particle density, pump speed, fluorescent properties of the measured particles and the illumination of the used flowcell/objective combination all influence the results, but unfortunately no detailed information about the effects of changing individual parameters is available. The only exception is the recommendation by the manufacturers to use a sample density $<100 \text{ ind ml}^{-1}$ for the fluorescence triggered image mode and $>100 \text{ ind ml}^{-1}$ for the AutoImage mode. The problem with all these parameters is that the effects of changes in one of them depend on the values of the other parameters, and standardized testing of changes in these parameters have not been published. Apart from the methodological problems identified above, the general specification of a desired cell concentration of $<100 \text{ cells ml}^{-1}$ for correct Flow CAM measurements in the fluorescence triggered image mode is unrealistic for most cases in plankton surveys. This normally means that high dilutions of water samples are necessary, as particle densities are seldom even in the range of 100 ind ml^{-1} , especially in coastal systems, where densities are easily an order of magnitude higher. Smaller particles (e.g. $<15 \mu\text{m}$) are usually much more abundant than particles above $15 \mu\text{m}$, as particle frequency is usually an inverse power of size (McCave 1984). Surveys of the smallest particles therefore need a much higher dilution for the proper estimation with the Flow CAM, whereas bigger particles (e.g. $>15 \mu\text{m}$) should be counted in an undiluted sample. Consequently, the nature of the particle distribution in the field has to be known by the researcher before being able to use the Flow CAM and as a result a measurement with the Flow CAM is anything but trivial.

Sieracki et al. (1998) stated that the bottleneck of the Flow CAM system is the fluorescence detector itself, which might be limited to two detections per second. As a result, the density of particles and the pump speed will affect the accuracy of the Flow CAM measurements in the fluorescence triggered image mode. Moreover, the fluorescence signal of a fluorescent particle is measured as the relative fluorescence after passing the laser beam in 10 micro second units. This means that also the relative fluorescence is highly dependent on the pump speed.

Hence, in this study we set out to investigate the effects of several settings of the Flow CAM system on the amount of counted particles per ml. The implications of changing these settings have not been studied before, and are absent from the manual. We will show that changing the pump speed for example has large effects on the amount of counted particles, and that this effect is dependent on the densities of the tested particles. Secondly, we demonstrate that the potential of the Flow CAM to discriminate between different fluorescent particles is large, whose magnitude however is also highly dependent on the pump rate. We used the Flow CAM system in the fluorescence triggered image mode with defined concentrations of the cryptophyte *Rhodomonas salina* with a 100µm/20 X flowcell/objective combination. The aim was to improve the usability of the Flow CAM for further investigations.

MATERIAL AND METHODS

A portable black and white Flow CAM (www.fluidimaging.com-VisualSpreadsheet Version 1.5.16) with a green laser beam for the fluorescence triggered image mode and a 100 µm flowcell with 20X objective combination was used. For further technical Flow CAM details see Sieracki et al. (1998). A defined cell concentration of the cryptophyte *Rhodomonas salina* was used for the experiments. *R. salina* is suitable for the fluorescence triggered image mode as it contains two photopigments that can be measured with the Flow CAM (chlorophyll a (detectable with channel 1) and phycoerythrin (detectable with channel 2)). The batch culture of *R. salina* was grown in f/2 medium (Guillard 1975) (16:8 light cycle) under sufficient light conditions ($185 \mu\text{mol m}^{-2} \text{s}^{-1}$) at 20°C. Under those conditions the culture *R. salina* had a deep red colour (Rho f/2) (phycoerythrin and chlorophyll a). Consequently, the Flow CAM fluorescence detector could receive an algal signal in both channels. Nitrogen depleted *R. salina* were also prepared as a second culture under the same culture conditions described above but without nitrogen in the culture medium. In the course of four days the nitrogen depleted *R. salina* culture changed its colour (and C:N ratio) from red over orange,

yellow, to green (Rho-N) as the nitrogen depletion caused a visible reduction of phycoerythrin (photoprotein) over time. The Flow CAM fluorescence detector would be expected to receive strong signals in channel 1 (Chl a), but much weaker ones in channel 2 (phycoerythrin) by the end of the depletion phase. To obtain a defined cell concentration for the following Flow CAM measurements, we determined the culture density with a CASY particle counter (Schärfe Systems, Germany) and diluted the samples with 0.2 µm filtered seawater to the desired cell concentrations which were again checked with the CASY before the Flow CAM measurement started.

Because of the fact that the Flow CAM system does not calculate the cell concentration in the fluorescence triggered image mode automatically, the measured volume has to be established, measured and transferred into the provided field of the Visual Spreadsheet Software. All presented regression analyses were done with Sigmaplot 10.0, two-way ANOVA with Sigmastat 3.5.

First, we focused on the measurement precision of the Flow CAM depending on cell concentration and pump rate. As the recommended concentration of <math><100 \text{ cells ml}^{-1}</math> is too low for experimental purposes, we started with the maximum of the recommended cell concentration (100 cells ml⁻¹) and increased the density in 16 steps up the maximum of 390,000 cells ml⁻¹ which we occasionally have measured with the AutoImage mode (=fluorescent + non-fluorescent particles) in the field. The purpose of this study was to find the pump rate at which point the precision of the Flow CAM measurement achieved 100% of the offered cell concentration to decrease measurement time and simultaneously avoid measurement artefacts (double measurements). Additionally, we tested the effect of flowcell illumination (=camgain adjustments) and the role of the fluorescence threshold on the counting success of the Flow CAM.

In the second part of this study we focused on the particle fluorescence measurements. We were interested to see whether the Flow CAM is able to follow changes in cell fluorescence properties of *R. salina* depending on their stoichiometric composition. Pump speed and changes of the fluorescence gain were manipulated to enhance the possibility to discriminate between nutrient replete and nitrogen depleted *R. salina*.

Flowcell illumination, cell concentration and pump speed

As described in the Flow CAM manual, pump speed and sample density might have a negative effect on the accuracy of the Flow CAM measurement because of the fact that the fluorescence detector is limited to only two detections per second. Therefore, when counting

in the fluorescence triggered image mode, a cell concentration below 100 cells ml⁻¹ is recommended in the manual with no indications on the optimal pump speed. Pump speed is, however, important to keep the time used for such measurements as low as possible since cell density determines the capture frequency of the Flow CAM. This means that e.g. at very low cell density and very low pump rate the time which has to be used to capture one single algal cell may last hours. Therefore the contact probability with algal cells at very low concentrations is enhanced with increasing pump rate. Thus, the time for measurements decrease to achieve the requirements of minimum counting standards as described in Lund et al. (1958). Therefore the aim was to find a proper configuration where the Flow CAM counts at least 400 pictures in a manageable time (~10 min). Additionally, the percentage of double or multiple measurements were to stay under 10% during the Flow CAM measurements. Those undesired measurements occur when two cells simultaneously pass the laser (=co-captures) and can be detected through visual inspection of the data sheet after the particle data have been exported into a spreadsheet programme. Particles with identical fluorescence signals in channel 1 and 2 (Peak and TOF) indicate simultaneous measurements of two or more particles and can be sorted out.

We also investigated the effects of the flowcell illumination on the measured concentration of *R. salina*. In initial measurements we had already observed that it was possible to measure densities of around 3,000 cells ml⁻¹, so this was the density we used. The illumination depends on the physical properties of the lens (objective magnification) as well as on the brightness of the LED flash and the light exposure sensitivity of the camera (=camgain). Therefore we set the adjusting screw of the LED flash to maximum and changed the “camgain” of the Flow CAM from its standard configuration of 525 (without units) at the start and, through the range 400-925, to receive different illuminations of the flowcell. We measured for 3 min with a pump speed ~0.15 ml min⁻¹ using a 2 mm (inner diameter) silicon pump tube. The gain (4) (=amplifier) and threshold (100) (=the threshold which has a particle to take to be captured) of the fluorescence detector were kept on the standard configuration to investigate the effect of appropriate cell illumination on Flow CAM counting success.

We also prepared defined cell concentration of Rho f/2 from 100- 390,000 cells ml⁻¹. Cell concentrations lower than 100 ml⁻¹ were not used, because of the experimental time and low measurement success probability in the used time range. At a cell concentration of 100 cells ml⁻¹ at the lowest pump rate (0.019 ml min⁻¹) used, 30 min were required to capture 13 pictures. At the highest used pump rate (0.76 ml min⁻¹) used, 10 min were needed to capture 100 pictures. The highest cell concentration used represents the particle concentration

(living+non living particles) which we occasionally measured in the AutoImage mode during autumn at Helgoland Roads, Germany. To achieve a range of different pump rates we used two tubes (inner diameter 1 and 2 mm) and changed the available pump speed ranges from “Slow” to “Fast” and “Prime”. Eleven different pump steps in “Slow” and “Fast” can be chosen which increase the pump rate linearly. “Prime” stands alone and is the fastest pump speed available. To ensure proper flowcell illumination we set the camgain from 525 (standard) to 700; the fluorescent gain of the fluorescence detector remained set at standard (4), but the fluorescent threshold was set from 100 (standard) to 1 to ensure that even algal cells with low fluorescent properties were measured. Each measurement ran for 3 min except for the low cell concentrations (described above). The loss of counting accuracy was defined as the percentage of the obtained Flow CAM measurement compared to the offered cell density. This loss was related to the pump speed, thus enabling us to calculate which pump rate at given cell concentrations would yield 100 % consistency (=measurement success) between Flow CAM counts and offered cell density.

Theoretically, the amount of pictures taken should increase linearly with increasing pump speed if the fluorescence detector is not blocked because of excessive demand (>2 captures sec^{-1}). Hence, we investigated the number of pictures dependent on the flow rate, as well as the number of double measurements (=co-captures). Such measurement artefacts occur when two or more cells pass the lens simultaneously.

Fluorescence measurement of the Flow CAM, seeing differences

The fluorescence measurement in each channel is measured as a waveform. The peak of the wave represents the signal strength which is generated by the fluorescent particle and which might be adjustable through the fluorescent gain of the Flow CAM detector. The waveform width is determined by the time (time of flight= TOF) at half peak maximum (measured in 10 μs units). Therefore, two main properties have to be considered in the fluorescence triggered image mode- the fluorescence power of the algal cell itself and the velocity of a fluorescent particle in terms of used pump speed which might have an effect on the fluorescence detector of the Flow CAM.

To investigate whether, and at which settings, the Flow CAM is capable of differentiating between different fluorescent properties of algal cells we prepared a first experiment with nitrogen depleted *R. salina* culture (green Rho-N) as described above. We inverted the limitation process through the addition of the lacking nitrogen (full N- pulse) to obtain nutrient replete *R. salina* (red Rho f/2). The lack of phycoerythrin in nitrogen depleted

R. salina cells (green) is known to be reversible, and typically cultures change to deep red again within 24 hours. To follow the regeneration process we measured the fluorescence of ~1,000 *R. salina* cells (diluted to 3,000 cells ml⁻¹ end-concentration; 2 mm pump tube; ~0.56 ml min⁻¹ pump rate; camgain 700; fluorescence gain= 4; fluorescence threshold= 100) through the Flow CAM and filtered ~250 µg C on pre-combusted Whatman GF/F filters for C:N analysis. Time step 0 h represents the C:N ratio and the measured fluorescence shortly before the addition of nitrogen to the culture, time steps 1 h, 2.5 h, 4 h, 6 h, 7.5h and 21 h are measurements after the full nitrogen pulse. Each fluorescence measurement at those described time steps is the mean (+std) fluorescence peak measurement of ~1,000 *R. salina* cells in channels 1 and 2.

In a second experiment we were interested in the magnitude of the fluorescence signal detected by the Flow CAM depending on the used pump speed (=particle velocity). Therefore, we prepared both cultures of *R. salina*- nutrient replete and nitrogen depleted (Rho f/2 + Rho-N) with an end concentration of 1,000 cells ml⁻¹ and measured each pump step for 3 min. We changed the pump speed between 0.09- 0.58 ml min⁻¹. The camgain was set at 700, fluorescent gain at 4 and the fluorescent threshold at 1. We measured the cultures as single cultures. The increase of the mean fluorescence with increasing pump rate was best fitted with a saturation curve ($f = a \cdot x / (b + x)$). At which pump rate both cell types (treatment Rho f/2 + Rho-N) might be distinguishable was then analysed using a two- way ANOVA. We could not use the raw data since tests on variance homogeneity and normality failed, even after different transformations. Therefore, we used the means of fluorescence signals and grouped them into 8 pump steps.

In the last experiment we tested the possibility to increase the fluorescence signal in channel 2 with increasing gain of the fluorescence detector (4- 4,095; threshold 1; camgain 700), which might increase the possibility to distinguish between both algal treatments at lower pump rate if both algae treatments are measured in a mixture. Additionally this would prevent the decrease of counting success. Therefore, we used an intermediate, constant pump rate (0.17 ml min⁻¹) and a cell density of 1,000 cells ml⁻¹ with three replicates.

RESULTS

Flowcell illumination, cell concentration and pump speed

The illumination of the used flowcell objective combination (100µm/20X) had a significant effect on the measurement success of the Flow CAM. From the lowest setting (400) up to 630 (including the standard of 525) the illumination of the flowcell was too dark.

The Flow CAM still captured particles but the measurement was highly variable, representing between 33-60% of offered cell concentration. From 640 until 725 the capture success became more stable and obtained 62-74% of offered cell concentration. Camgain adjustments above 725 seemed too bright and measurement success decreased (Fig. 1). However, at any camgain setting, we were unable to achieve a correct Flow CAM measurement of the cell concentration ($3,000 \text{ cells ml}^{-1}$) at any camgain setting, potentially as a result of the combination of too high densities with incompatible pump speeds or the use of a too high fluorescent threshold (100).

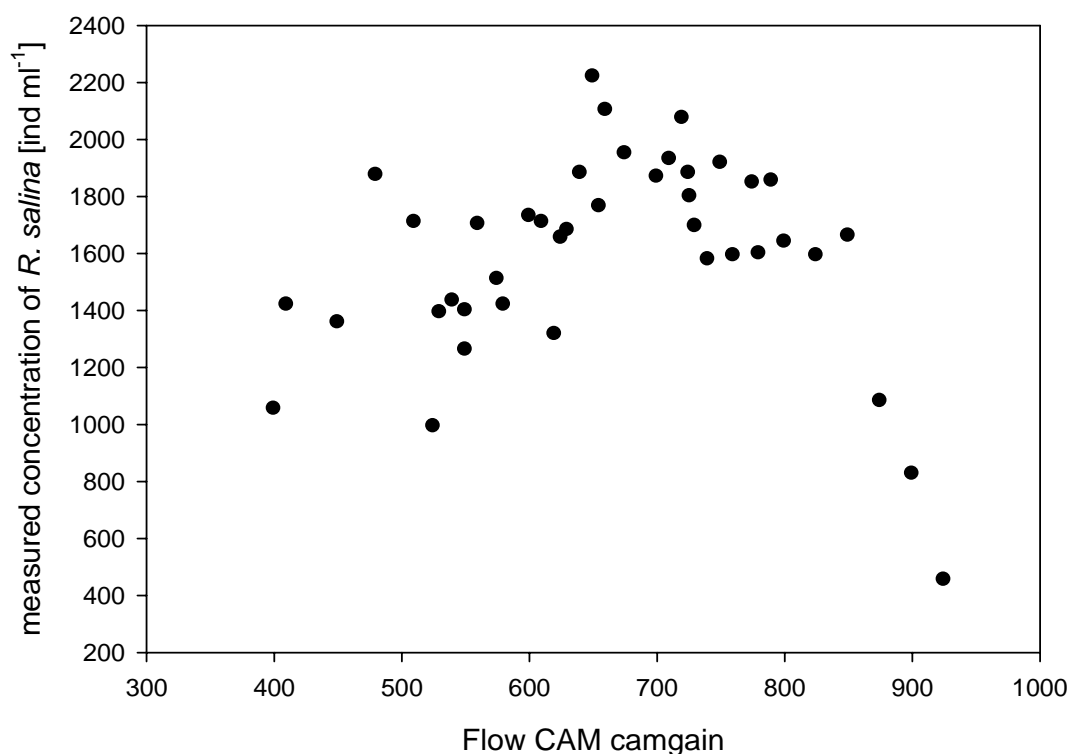


Figure 1: The role of proper flow cell illumination for exact Flow CAM measurements using the 100 μm flowcell/20X. Standard configuration (525) of camgain should be changed to ~ 700 to enhance measurement success.

Pump speed and offered cell density had a large effect on the measurement success (given as % of the initial density) (Fig. 2). We observed that there was no single pump speed that allowed the accurate measurement of all densities, nor was there one density that could be accurately measured with a range of different pump speeds. In general, at higher cell densities, the exponential decrease of the Flow CAM measurement success with increasing pump rate was steeper (Tab. 1). At the lowest pump rate (0.01 ml min^{-1}) we observed an overestimation of the offered cell concentration. Using the highest pump rate (0.76 ml min^{-1}) the relative loss of measurement success was significantly affected by the offered cell

concentration. Although lower sample densities such as the recommended $<100 \text{ ml}^{-1}$ might decrease the risk of an underestimation of the true cell density even when the pump rate is high, a correct Flow CAM measurement cannot be obtained at lower pump rates. Based on Figure 2 we estimated the pump speed at which the Flow CAM theoretically measures 100% (see inlay of Fig. 2). Based on figure 2, one could argue that even higher cell concentrations might be counted properly. Unfortunately, before counting these densities one has to know the densities to count them properly.

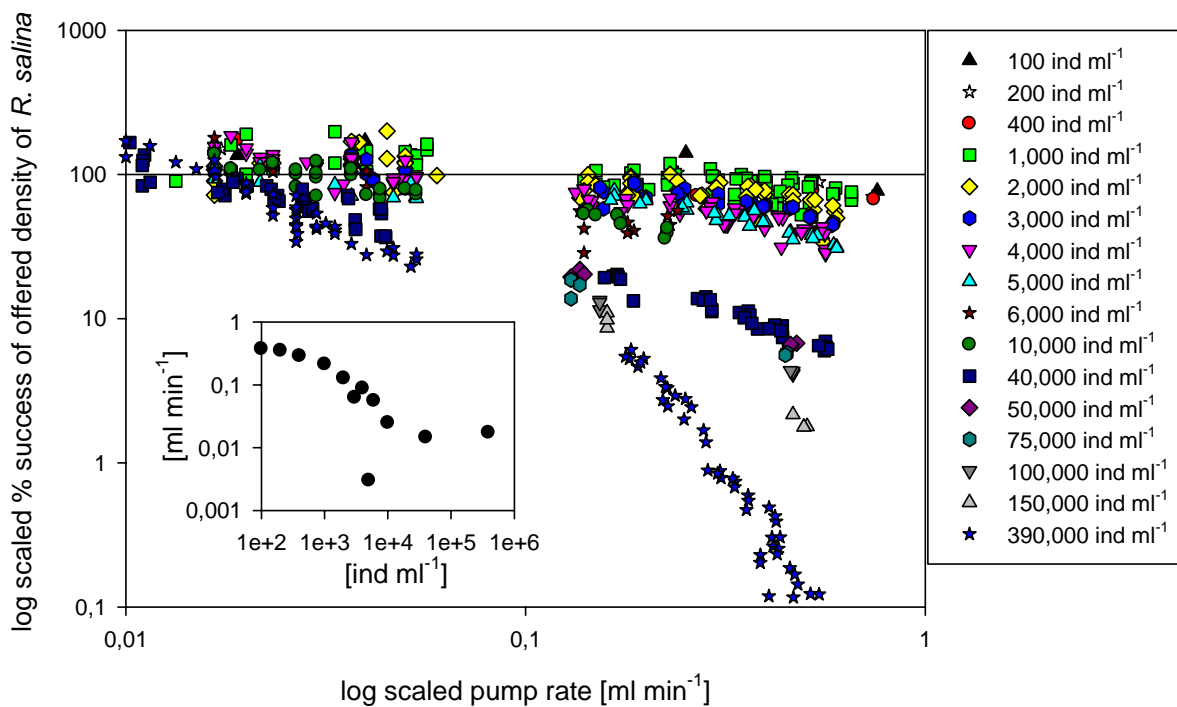


Figure 2: Success of Flow CAM measurement with increasing pump rate (100% line signed) and offered cell density of *R. salina*. All measurements decreased with increasing pump rate. The denser the sample, the heavier decreased the measurement success with the Flow CAM. Graph inlay show however the calculated pump rate $[\text{ml min}^{-1}]$ where offered cell density $[\text{ind ml}^{-1}]$ might be correctly measured with the Flow CAM in fluorescent triggered image mode.

Table 1: Summary of non linear regression analysis ($f=a*\exp(-b*x)$) of used pump speeds and measurement success (%) of Flow CAM with 16 different offered *R. salina* densities [ind ml^{-1}].

Cell density [ind ml^{-1}]	a	s.e.	b	s.e.	R ²	p-value	n-measurements
100	134.9435	24.6591	0,8052	0.6509	0.33	0.2340	6
200	138.1776	9.9855	0.9203	0.2711	0.79	0.0183	6
400	156.0587	17.7586	1.5433	0.5516	0.74	0.0279	6
1,000	129.3736	5.2096	1.2088	0.1559	0.47	<0.0001	72
2,000	122.8644	5.1590	1.6127	0.2027	0.56	<0.0001	63
3,000	110.3534	3.5953	1.5662	0.1436	0.79	<0.0001	39
4,000	128.7820	4.3011	2.8604	0.2406	0.78	<0.0001	66
5,000	100.6646	3.2034	2.0443	0.1583	0.85	<0.0001	39
6,000	148,6248	10.2770	7.0621	1.1307	0.81	<0.0001	18
10,000	114.4111	5.0898	5.4053	0.7477	0.76	<0.0001	30
40,000	152.4241	10.9368	28.7884	3.1498	0.86	<0.0001	65
50,000	32.6054	1.8753	3.4139	0.2982	0.98	<0.0001	6
75,000	25.6732	2.9701	3.3500	0.6001	0.93	0.0017	6
100,000	21.51	1.4368	3.4841	0.3212	0.98	0.0001	6
150,000	21.7551	3.1220	4.9733	0.7855	0.97	0.0003	6
390,000	306.1290	11.8373	64.4829	2.2150	0.97	<0.0001	99

Double measurements (=co-captures) were possible at all concentrations, were however under 10% of the captured images at concentrations up to 10,000 cells ml^{-1} . This might be due to the fact that even at low cell densities *R. salina* was not homogenously distributed in the flow cell. Thus, even at very slow pump speeds and low cell concentrations co-captures of simultaneously passing cells occurred (Fig. 3 A). Higher cell concentrations exacerbated the problem of co-captures and caused a steep increase reaching ~70% at the highest concentration of 390,000 cells ml^{-1} indicating that co-captures of simultaneously passing *R. salina* were rather density dependent than pump speed dependent. Therefore higher pump speeds at cell concentrations <10,000 cells ml^{-1} had no significant effect on multiple Flow CAM captures and occurred at any cell concentration in this range (Fig. 3 B).

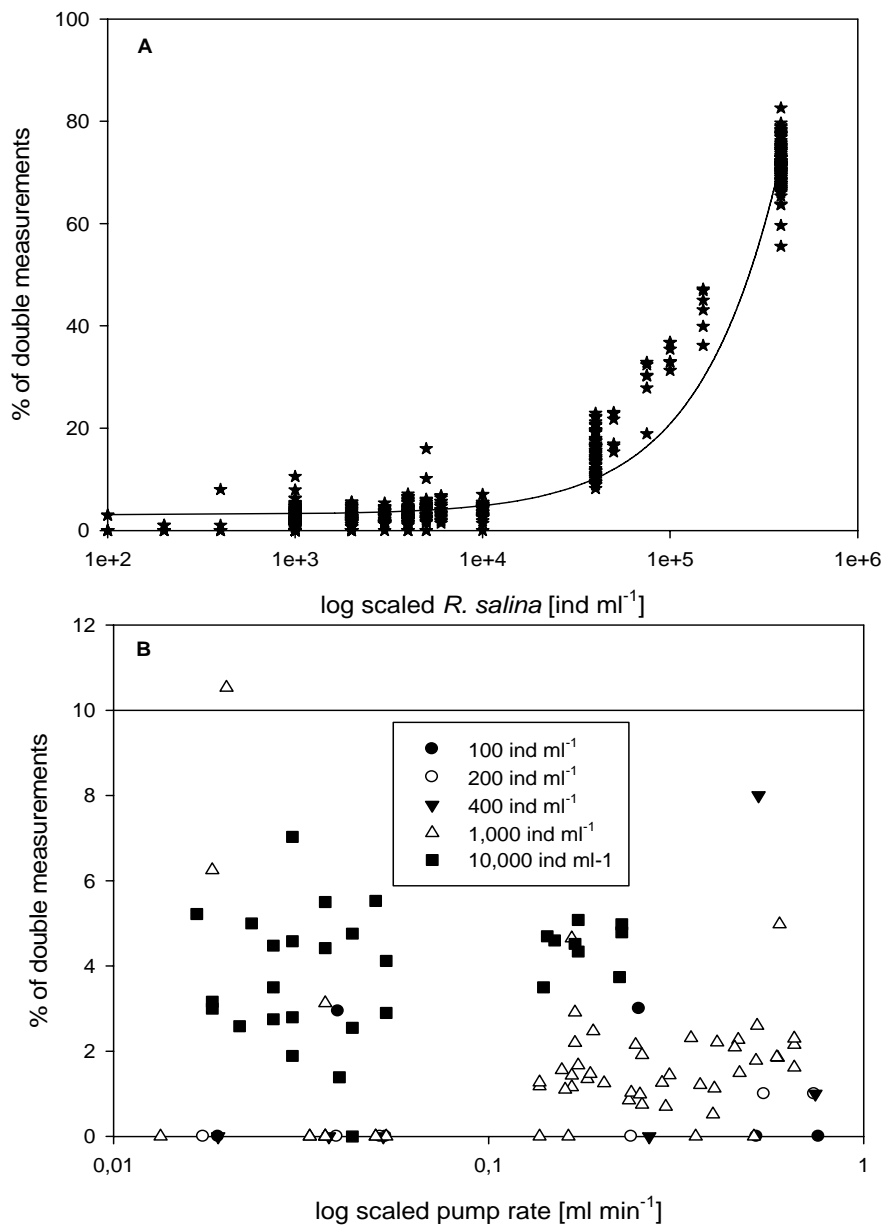


Figure 3: (A) Percentage of double and multiple measurements obtained by the Flow CAM with increasing cell density of *R. salina* (linear regression: $f = y_0 + a \cdot x$; $a = 0.002$, $y_0 = 3.0714$; $R^2 = 0.98$, $p < 0.0001$); (B) Percentage of double and multiple measurements with increasing pump rate [ml min⁻¹] with selected *R. salina* cell concentrations (100, 200, 400, 1,000 and 10,000 cells ml⁻¹).

Besides the accuracy of Flow CAM measurements we were interested in the time efficiency which is mainly coupled with captured cells per time unit [min] to keep overall measurement time as low as possible. The amount of pictures taken min⁻¹ did not linearly increase with increasing pump speed at any cell concentration (Fig. 4 A). With increasing

pump rate a significant loss of cell captures was visible for all cell concentrations up to 150,000 cells ml^{-1} , and thus the relationship was best fitted to a saturation curve (Tab. 2).

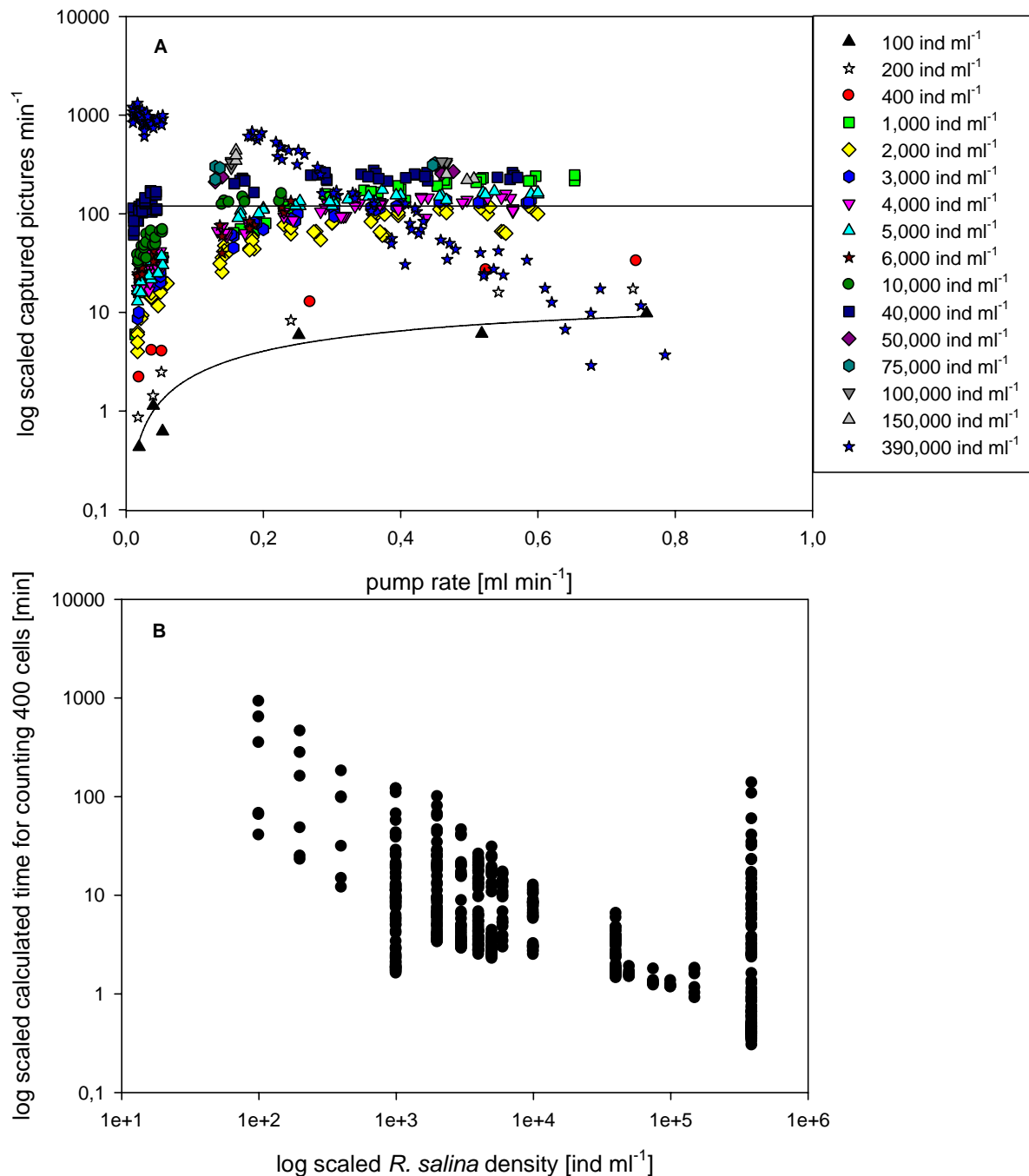


Figure 4: (A) Captured pictures per min with increasing cell density of *R. salina* and pump rate [ml min^{-1}]- black line indicates provided 120 detections min^{-1} ; (B) calculated time for counting 400 cells of *R. salina* with increasing sample density to receive counting standards.

This was surprising because already with a cell density of 100 cells ml⁻¹ the decline of Flow CAM captures with increasing pump rate implies that saturation of the fluorescence detector (2 particles s⁻¹ or 120 particles min⁻¹) could not be the explanation. The pump rate itself might be the reason that particles passed through the flowcell too quickly and thus could not be recognized by the Flow CAM. Only at the highest cell concentration of 390,000 cells ml⁻¹ did the Flow CAM measurements show a significant sign of overstraining of the fluorescence detector which resulted in a significant, almost linear decline of captured cells with increasing pump rate.

Table 2: Summary of regression analysis ($f = a \cdot x / (b + x)$) of captured particles min⁻¹ depending on pump rate [ml min⁻¹] and cell density.

Cell density [ind ml ⁻¹]	a	s.e.	B	s.e.	R ²	p-value
100	16.5695	6.9316	0.6179	0.4819	0.94	0.0013
200	36.1811	5.5858	0.7552	0.2020	0.99	<0.0001
400	129.0175	70.7163	2.0996	1.4795	0.99	<0.0001
1,000	779.8011	165.1049	1.4185	0.3985	0.96	<0.0001
2,000	179.3297	23.4441	0.4312	0.1033	0.87	<0.0001
3,000	242.5552	14.6211	0.4229	0.0479	0.98	<0.0001
4,000	197.8385	12.3788	0.2513	0.0358	0.93	<0.0001
5,000	234.2756	10.8182	0.2356	0.0265	0.98	<0.0001
6,000	204.3950	81.5764	0.2382	0.1638	0.78	<0.0001
10,000	227.0928	12.0686	0.1155	0.0122	0.96	<0.0001
40,000	257.6079	5.4722	0.0303	0.0024	0.89	<0.0001
50,000	279.1497	13.9739	0.0276	0.0116	0.65	0.0532

The calculated time which would have to be used for counting 400 cells averaged ~900 min at lowest pump rate (0.019 ml min⁻¹) with the lowest cell concentration (100 cells ml⁻¹). The used time decreased to ~41 min using the highest pumping (0.76 ml min⁻¹). With increasing cell density the used time obviously decreased. This did not apply to the highest cell concentration of 390,000 cells ml⁻¹. At this concentration there might be a trade-off, where lowest pump rate resulted in lowest time measurement, higher pump speeds to longer measurement time because of the excessive demand of the fluorescent detector at which no further cells might be captured (Fig. 4 B). If we keep our criteria (10 min measuring time, at least 400 cells), no cell concentration less than 1,000 cells ml⁻¹ could be used at any used

pump speed. At a cell concentration of 1,000 cells ml⁻¹ a low pump rate of 0.05 ml min⁻¹ resulted in a measuring time of ~20 min which could be decreased down to ~1.5 min at highest pump rate (0.65 ml min⁻¹).

Summarizing the results of these experiments, we could show that the measurement success of the Flow CAM in the fluorescence triggered image mode (combination 100 µm/20X) is highly dependent on (1) the right illumination of the flowcell (camgain ~640-725) and (2) the cell concentration but only up to a cell concentration of 10,000 cells ml⁻¹ if the used pump speed is adapted to lower pump rates. To obtain a time-efficient and accurate cell count measurement a cell concentration of 1,000 cells ml⁻¹ at low pump rates is recommended.

Fluorescence measurements of the Flow CAM

The Flow CAM could be used to follow the mean fluorescence change of nitrogen depleted *R. salina* during the regeneration process of phycoerythrin after the full nitrogen pulse. The relative fluorescence of nitrogen depleted *R. salina* was ~2,497 at channel 1 (=chlorophyll a) and ~253 at channel 2 (=phycoerythrin) at the start of the experiment. The following visible culture colour change of *R. salina* from green to yellow and finally to red corresponded well with the relative fluorescence measurement of the Flow CAM. After 21 h the mean fluorescence in channel 1 was ~2,987 and in channel 2 ~2,494 respectively. The formerly nitrogen depleted *R. salina* enhanced its fluorescence, especially in channel 2 which means that phycoerythrin was fully regenerated (Fig. 5 A). The change in the fluorescence of *R. salina* could also be confirmed with the change of its C:N- ratio which was ~17 at the start of the experiment and ~5,44 after 21h (Fig. 5 B). Thus, the Flow CAM might be an excellent tool for discriminating different nutrient defined *R. salina* based on the relative fluorescence differences between nutrient replete (+phycoerythrin) and nitrogen depleted algae (-phycoerythrin) in channel 2.

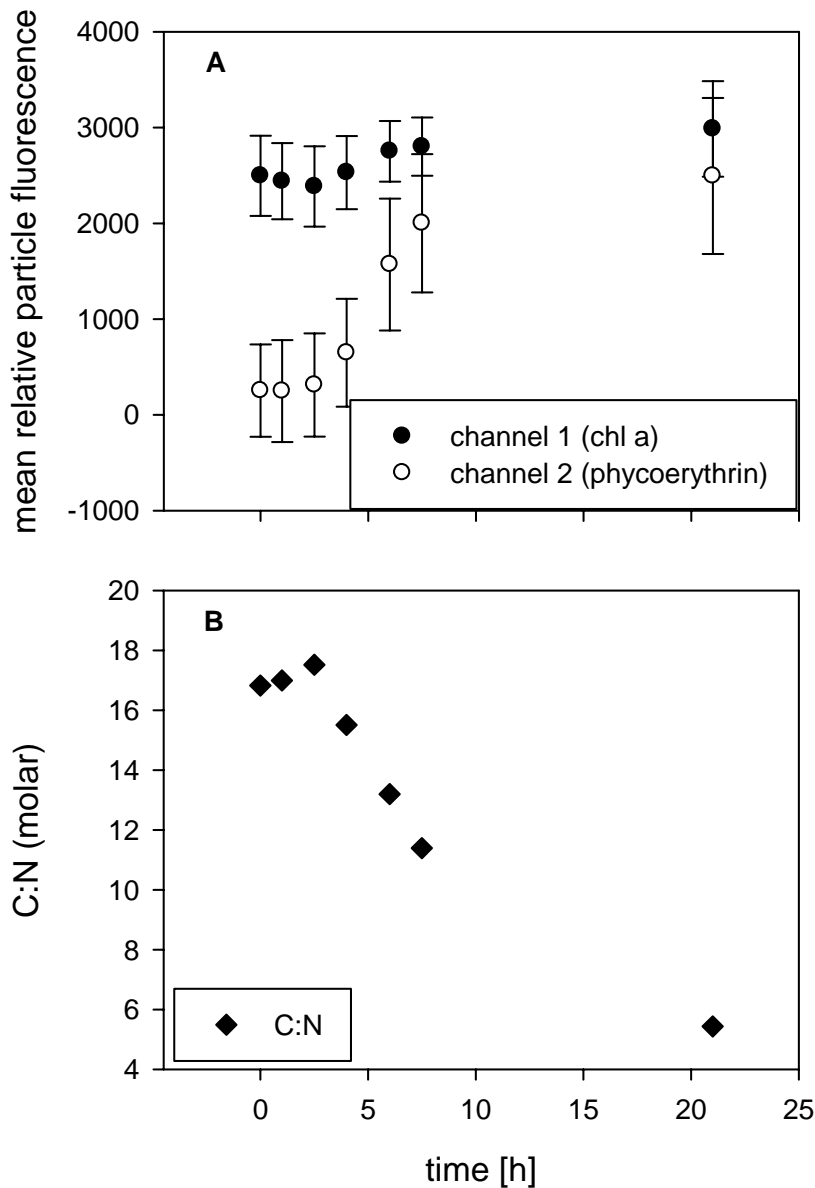


Figure 5: (A) Changing fluorescence property of nitrogen limited *R. salina* (Rho-N) after full nitrogen pulse and (B) its changing C:N ratio over time.

As described previously, however, we recognized that the magnitude of the fluorescence is somehow dependent on the cell velocity (=used pump rate). Indeed, the magnitude of the mean fluorescence in channel 2 changed with increasing pump rate and might be best described by a saturation curve (Tab. 3; Fig 6). The fluorescence of channel 2 was significantly different between algal types for all eight pump steps (Tab. 4 + 5). A discrimination between nutrient replete (Rho f/2) and nitrogen depleted *R. salina* (Rho-N) might be possible at all pump rates as long as the used pump rates are kept constant.

Table 3: Summary of regression analysis ($f= a*x/(b+x)$) of measured fluorescence (channel 2) of nutrient replete (Rho f/2) and nitrogen depleted *R. salina* (Rho-N) with increasing pump rate [ml min^{-1}].

treatment	a	s.e.	B	s.e.	R ²	p-value
Rho f/2	3,699.3954	163.7021	0.4520	0.0363	0.98	<0.0001
Rho-N	282.0007	17.5322	0.0859	0.0164	0.72	<0.0001

Table 4: Summary of two-way ANOVA to test the effects of pump rate [ml min^{-1}] and fluorescence in channel 2 (phycoerythrin) to differentiate between the two algae treatments (Rho f/2 + Rho-N).

ANOVA	Factor	Df	MS	F	p-value
	pump rate [min ml^{-1}]	7	229,625,912	309	<0.001
	treatment	1	1,707,886,386	2,300	<0.001
	pump rate x treatment	7	152,294,137	205	<0.001
	Residual	15,905	742,383		
	Total	15,920	1,285,342		

Table 5: Comparison for factor treatment (Rho f/2 vs Rho-N) within 8 pump rates (ml min^{-1}) based on the fluorescence in channel 2 (two-way ANOVA, Tukey-post hoc test).

Comparison	pump rate [ml min^{-1}]	Difference of means	P	Q	p-value
Rho (f/2) vs. Rho-N	0.018	174.372	2	3.163	0.025
	0.037	218.593	2	5.552	<0.001
	0.050	195.735	2	4.999	<0.001
	0.148	710.974	2	25.882	<0.001
	0.185	942.946	2	27.694	<0.001
	0.300	1,327.943	2	45.451	<0.001
	0.382	1,482.418	2	52.748	<0.001
	0.569	1,752,819	2	89.025	<0.001

An increase of the fluorescence gain in channel 2 at intermediate pump rates had only a weak effect on the magnitude of the fluorescence signal for phycoerythrin (gain 4- 512) to increase the fluorescence of Rho f/2 for better discrimination against Rho-N. With further gain increase of channel 2 (>1,000) we even observed a decrease of the mean fluorescence

signal in channel 2 which is caused by overexposure of higher fluorescent cells (Rho f/2) (Fig. 7). Such cells are as a result not captured by the Flow CAM. Hence, an increase of the fluorescent gain did not yield any promising results in the differentiation between both cell types.

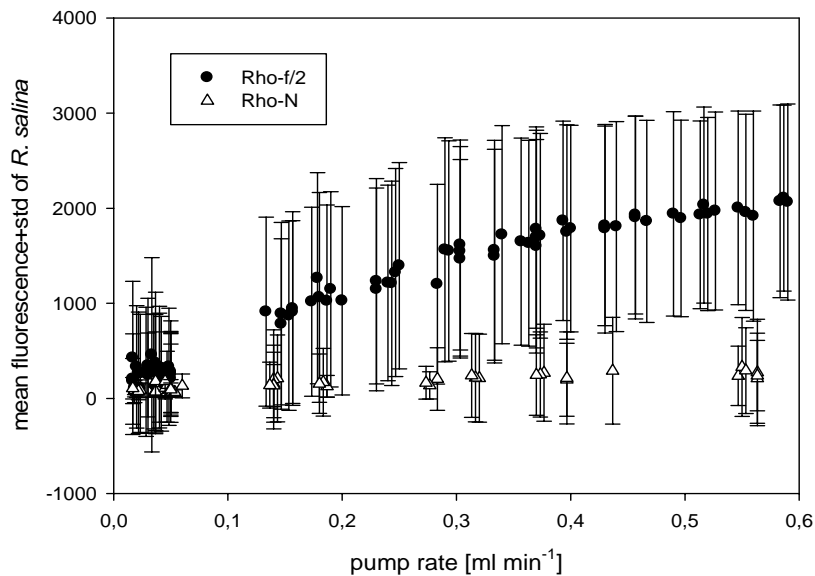


Figure 6: Effect of pump speed on the magnitude of mean fluorescence (+std) of nutrient replete (Rho f/2) and nitrogen depleted *R. salina* (Rho-N) in channel 2.

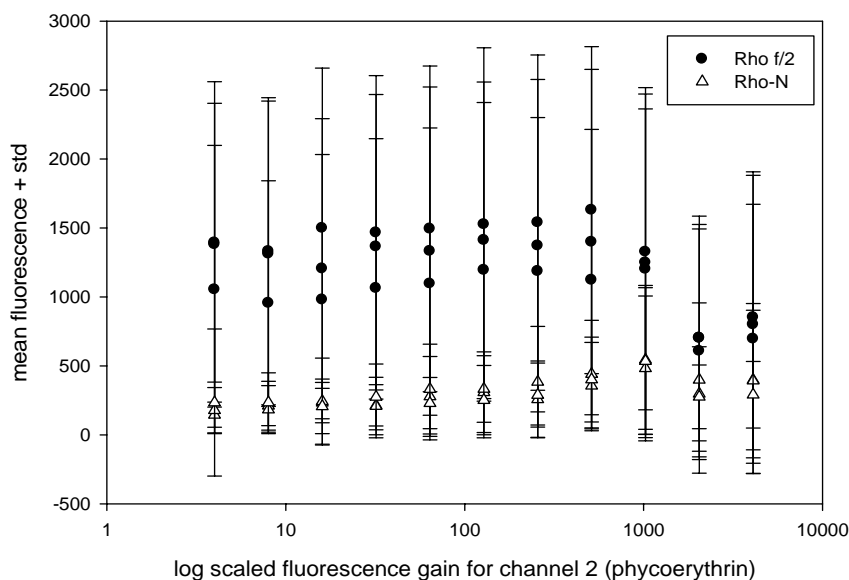


Figure 7: The attempt to increase the fluorescence gain in channel 2 (phycoerythrin) at constant pump rates ($\sim 0.17 \text{ ml min}^{-1}$) to enhance the fluorescence of nutrient replete *R. salina* (Rho f/2) for better discrimination against nitrogen depleted *R. salina* (Rho-N).

DISCUSSION

Despite the attractiveness of the Flow CAM as an automated counting system, using the machine sensibly is by no means trivial. It might be very useful to ‘discover’ a single species of interest in a sample, obtaining robust counting results, however, is much more of a challenge. The major problem with Flow CAM measurements in the fluorescence triggered image mode is that many factors have to be considered all of which affect the counting success. Every minor change of these can have an enormous impact on counts and might be the reasons why there are only three publications available for the fluorescence triggered image mode. Only one author has used our flowcell size/objective combination (100 μm /20X) (Ide et al. 2008), Sieracki et al. (1998) used the 300 μm sized flowcell with 4X objective and Buskey & Hyatt (2006) used the 300 μm sized flowcell with 10X objective. Other flowcell/objective combinations will certainly have different effects on the counting success of the Flow CAM in the fluorescence triggered image mode, but the fundamental results of our paper should be transferable.

The flowcell illumination is highly dependent on the used lens and objective magnification and is not mentioned in previous papers. Since the standard configuration “camgain” in the Visual spreadsheet software is set on 525 for all magnifications/flowcell sizes and since the illumination is adjustable over the LED flash screw (in our model), it is difficult to recommend a “panacea” for proper flowcell illumination. On the one hand, the standard setup of the camgain results in cell captures, but on the other hand, better measurement accuracy can only be achieved with camgain changes. This has to be implemented for each used flowcell/objective combination.

The fluorescence gain and threshold are other adjuster bolts in the Flow CAM. Unfortunately, the exact magnitudes are either not mentioned or called “adapted” in Buskey & Hyatt (2006). Theoretically it might be best to enhance the fluorescence gain to maximum configuration (4095) boosting the fluorescence signal of low fluorescent particles. Simultaneously a decrease of the fluorescence threshold set on minimum configuration (1) should facilitate that measurement of even low fluorescent algae. Ide et al. (2008) stated that they used a fluorescence gain set at highest value (4095) and a lower fluorescence threshold set from 100 to 12 for their measurements. The authors explain that the reason for such changes compared to the standard configuration setup (fluorescence gain= 4; fluorescence threshold= 100) because of the recommended protocol by the Flow CAM Company for their survey. Our presented data in the first part of this paper shows that a decrease of the fluorescence threshold from 100 to 1 increases the measurement success of *R. salina* without

changing the fluorescence gain. In the second part we can show that a moderate increase of the fluorescence gain has only low effects on the fluorescence signal of *R. salina*. An excessive increase of the fluorescence gain however has its limits since higher fluorescent cells of *R. salina* ($\text{Rho } f/2$) are over-amplified and are as a result not captured by the Flow CAM and lost to counting (personal observation).

All of the above described adjustable factors are minor compared to the most effects of the fluorescence triggered image mode: cell concentration and pump speed. Even at comparably low cell concentrations ($100 \text{ cells ml}^{-1}$) the Flow CAM is not able to detect the cell concentration with increasing pump rates correctly. This makes it hard to use and it is in our view not acceptable that the Flow CAM has no pump speed range where accurate and constant measurements are possible. This is due to the Flow CAM detector not being able to recognize cells which pass the laser beam too quickly with increasing pump rates. Unfortunately, even at low pump rates correct and constant measurements are not possible due to co-captures (double measurements) and probably low sample size (<400 pictures) which cause an overestimation of the real cell densities.

The reason for such double measurements is the density of the particles with the consequence that in denser samples the particles are closer to each other and the time and sample volume which is required to contact the next fluorescent particle depends on the cell density and the used pump rate. Theoretically at very low cell densities therefore high pump rates might be useful to increase the contact probability with the next fluorescent particle in order to decrease the used time to shorten the distance between those particles respectively. At higher cell concentrations where the distance to the next fluorescent particle is short the adjustable pump rate should be decreased as much as possible to prevent that the next fluorescent particle is not captured due to excessive demand of the fluorescence detector.

An alternative explanation, however, is that *R. salina* is more heterogeneously than homogeneously distributed within the flowcell, so that co-captures (pump speed independent) simultaneously happened combined with long periods where no cell captures occurred. This may be especially true at low cell concentrations. To go further into details, the “field of view” of the Flow CAM in which *R. salina* is actively captured, is determined by the used flowcell size and objective magnification, and is therefore a sub-sample of the whole sample (means the total flow cell width). If *R. salina* were homogeneously distributed over the whole flowcell width, the proportion of captured *R. salina* by the Flow CAM would allow a correct estimation of *R. salina* cells which have passed the Flow CAM beyond the field of view. Due to the fact that the Flow CAM captured only low amounts of pictures at low concentrations

and low pump speeds in the used measurement time, the Flow CAM apparently overestimated the real cell density due to low sample size and high flowcell factor (which is determined by the flowcell width divided by the width of the field of view).

Running the Flow CAM in the fluorescence triggered image mode requires particle velocity to be triggered by the fluorescence of a passing particle (i.e. the Flow CAM does not capture fluorescent particles when pump speed is zero). The laser triggers the fluorescence of a passing particle but the magnitude of the fluorescence depends on the particle speed. At higher pump speeds the relative fluorescence increases, although we are not completely sure why this is the case. This means that particles which have a low fluorescence could not be captured by the Flow CAM when used pump speed is low and the fluorescence threshold of the detector is high (e.g. standard configuration 100). At higher used pump rates the probability of capture by the Flow CAM of a low fluorescent particle would be therefore increased since the magnitude of the fluorescence signal exceeds the high fluorescent threshold. A significant decrease of the fluorescence threshold (e.g. to 1) would enhance the probability that low fluorescent particles are captured even when pump rates are low. Again such a wide range of information on the sample used is already needed before being able to count the sample, so that one almost has to count it by hand before using the Flow CAM.

All of these findings are in contrast to Sieracki et al. (1998) who showed that correct measurements with low cell concentrations and high pump rates are possible using a 300 μm flow cell/4 X objective combination. In contrast to our flowcell/objective combination where we captured particles in a ~ 263 μm wide and visible section of the flowcell (=“field of view”), they had a $\sim 1,765$ μm wide field of view in their Flow CAM setup. Thus, the probability of capturing fluorescent particles passing the laser beam was ~ 7 -fold higher and might be the reason that they had to dilute monocultures of six different algae cultures (25-100,000 cells ml^{-1}) to < 50 cells ml^{-1} and used a pump rate of 1 ml min^{-1} . Also Buskey & Hyatt (2006) successfully used a 300 μm flowcell/10X objective combination (~ 680 μm wide field of view) and pre-diluted *Karenia brevis* cultures to a cell concentration of < 500 cells ml^{-1} while using a constant pump rate of 0.38 ml min^{-1} . Ide et al. (2008) used our flowcell/objective combination and measured raw water field samples with a maximum of 120 cells ml^{-1} (< 5 μm particles) or ~ 400 cells ml^{-1} during bloom conditions, respectively, without any dilutions, with a pump rate of 1 ml min^{-1} . In comparison to our results, we have never obtained such high pump rates (max ~ 0.7 ml min^{-1}) and if we would have used a cell concentration below 50 cells ml^{-1} , we could have used ~ 80 min to capture 400 cells.

Based on our results, we could calculate an appropriate pump rate at given cell concentration up to $10,000 \text{ ml}^{-1}$ at which correct Flow CAM measurements were possible. Further investigations, however, have to be carried out to clarify whether at these calculated pump rates and cell concentrations double measurements (co-captures) compensate for the lack of not measured particles, or whether these are actually all correct counts.

One of the attractive measurements in the fluorescence triggered image mode is the possibility to differentiate between different nutrient defined *R. salina* (Rho f/2 vs. Rho-N). The magnitude of the fluorescence measurement for chlorophyll a (channel 1) and phycoerythrin (channel 2) is mainly driven by the pump speed and might be only slightly changed by the fluorescence gain when the used pump speed is low. It is therefore obvious that if particles need to be measured with respect to their fluorescent properties that the pump speed needs to be kept constant (Buskey & Hyatt 2006).

From our investigations we have seen that it is possible to count fluorescent particles correctly when a lot of information on the sample is already available. The Flow CAM might be a useful tool for experimental setups with known, constant factors such as cell concentrations, constant pump rates and species which possess different chlorophyll and phycoerythrin contents, as is the case in *R. salina* with different nutrient composition. Whether the Flow CAM is applicable for semi-automated plankton recognition in the field remains to be seen because the information available on the water sample is often so sparse that it might be necessary to count the sample first, before it can be counted automatically with the Flow CAM.

CHAPTER III

Use of the Flow CAM for plankton abundance estimations in the field and a critical assessment of the applied method

Florian Matthias Hantzsche, Friedhelm Schroeder, Silvia Peters, Kristine Carstens, Karen Helen Wiltshire & Maarten Boersma

ABSTRACT

Despite years of progress in our knowledge of the processes that govern planktonic communities, we are essentially still using the same techniques to quantify densities of planktonic organisms as we did 100 years ago. The development of automatic measuring systems is still in its infancy. Although fluorometric probes, pigment analyses and flow cytometry help with the identification of the main groups in the phytoplankton, to date there are no real alternatives to microscopic counting when it comes to the identification of phytoplankton species. The recently developed Flow CAM, as a combination of a flow cytometer and a microscope might at least partly solve this problem. Hence, we tested the Flow CAM for its use in the long-term sampling at Helgoland Roads, Germany, focussing on phytoplankton and microzooplankton. We studied the applicability and reliability of the Flow CAM, especially with regard to cell abundance and plankton composition, compared to the daily microscopic observations and chlorophyll *a* measurements.

We observed that particles appear in a wide size range with a hyperbolic size-frequency distribution which could be measured using the 100 μm flowcell in the AutoImage modus of the Flow CAM. Most particles were non-living and small ($<15 \mu\text{m}$), whose densities correlated well with water transparency but not with chlorophyll and microscopic counts. The main living planktonic component which correlated best with chlorophyll *a* content was larger phytoplankton above 50 μm , measured in the fluorescence triggered image mode. In comparison with microscopic counts, the Flow CAM counts were consistently lower in all used flowcell measurements. Theoretically, the fluorescence triggered image mode only counts fluorescent (algal) particles. We, however, found that this was not the case. First, especially in dense solutions, co-captures between fluorescent and non fluorescent particles occurred in each flow cell causing the non-fluorescent particle to obtain the fluorescence signal of the fluorescent one, and thus inadvertently giving detritus particles a fluorescent signal. Second, to avoid rest chlorophyll in detritus particles to be counted as algae the fluorescence threshold of the Flow CAM detector needs to be fairly high. Unfortunately this also means that algal cells with low fluorescence were not captured efficiently by the Flow CAM. Manual selecting of the counted particle yielded better results, but was very time consuming. The time effort needed for Flow CAM measurements and for the re-processing of captured data was unacceptably high (hours and days!). Before this instrument can be used reliably as a semi-automated plankton recognition system, we need to develop applications clarifying the effects of the plentiful adjustments which are possible with the Flow CAM.

INTRODUCTION

Long-term monitoring data in planktonic communities for climate change shifts have been in the focus of attention in the last decade (Wiltshire and Manly 2004; Wiltshire et al. 2008). The changing environment -increasing temperature and carbon dioxide levels- has challenged scientists in diverse disciplines to predict changes on species and on community structure. Especially the long-term sampling series of planktonic organisms are a very valuable resource to describe and assess the effects of change in the marine ecosystem. Most plankton monitoring data, however, are based on traditional microscopic analysis of preserved samples with known disadvantages, such as changes of plankton composition through fixation, misinterpretation of cell volume (Stoecker et al. 1994; Menden-Deuer et al. 2001; Wiltshire and Dürselen 2004; Zarauz and Irigoien 2008) and the lack of quality control of past observed data (but see Raabe and Wiltshire 2009). In addition, even experts are subject to human restrictions, which may lead to misidentification, counting mistakes and misinterpretation of sampled data (Wiltshire and Dürselen 2004; Culverhouse 2007).

In recent years, many new technologies have been developed for the assessment of algal species presence and abundance, e.g. DNA analysis (e.g. Metfies et al. 2007), HPLC (e.g. Claustre et al. 2004), scanning flow cytometry (Dubelaar et al. 2004) and other automated optical tools (see Benfield et al. 2007). One of those new technologies is the Flow CAM, an imaging-in-flow system for automated analysis, which was successfully established and tested by Sieracki et al. (1998) for microplankton estimations in the size range between 20 and 200 μm . Further Flow CAM applications are found in the literature for the detection of harmful algae (Buskey and Hyatt 2006) and for experiments on animals grazing on algae and microzooplankton (Ide et al. 2008). The Flow CAM is equipped with several flowcells (50-2,000 μm depth) in combination with four different objectives (2-times to 20-times magnification) to measure particles of defined size classes. The water sample is pumped into the system and the Flow CAM takes pictures of particles which pass through the flowcell. For particle measurements, the user can select between two different operation options. One of them is the unselective AutoImage mode which detects all available particles (living and non living particles) and the second is the selective fluorescence triggered image mode which is supposed to capture only those particles that are fluorescent after being excited using a green laser.

In general, particles in natural waters including plankton decrease in abundance as a power of size (McCave 1984), and hence automated systems can only work if they recognize restricted size ranges of the whole size spectrum (Sieracki et al. 1998). The Flow CAM is

optimally suited to deal when different combinations of flowcell and objective (magnification) combinations allow the accurate assessment of particles as small as 5 μm and as large as 1 mm.

In the present paper we selected three of these combinations (100 $\mu\text{m}/20\text{X}$; 300 $\mu\text{m}/10\text{X}$ and 600 $\mu\text{m}/4\text{X}$) in both the AutoImage as well as in the fluorescence triggered image mode. It was our aim to test the Flow CAM for its suitability in routine phytoplankton sample analyses, and therefore we compared the results of the Flow CAM counting with those from the daily routine monitoring observations at the sampling station Helgoland Roads, Germany (Wiltshire and Dürselen 2004; Wiltshire et al. 2008). We assessed the suitability of the instrument both in terms of identification success as well as in terms of handling time of the sample and the post-measuring analysis.

MATERIAL AND METHODS

Sample preparation

One liter of water sampled at the sampling station Helgoland Roads (see Wiltshire and Manly 2004) was prepared for Flow CAM analysis from July 2007 until January 2009 in one-two week intervals. In order to measure the whole size spectrum, we started our measurements with 100 μm (for size range 2-100 μm) and 300 μm (15- 300 μm) flowcells in combination with 20X and 10X magnification respectively. In the course of the running experiment, we recognized that colony forming diatoms, such as *Pseudo-nitzschia* sp., large single celled diatoms, e.g. *Coscinodiscus* sp., and dinoflagellates, e.g. *Ceratium* sp. were either insufficiently captured on Flow CAM pictures (just parts of the real size) or were completely absent during Flow CAM measurements even when present in the water. Therefore, from January 2008 onwards, we used a third flowcell/objective combination (600 $\mu\text{m}/4\text{X}$) for capturing plankton size range between 50 and 600 μm .

One disadvantage of Flow CAM measurements is the need of pre-filtering the water sample depending on the flowcell size to prevent clogging and resultant undesired air bubbles which are captured by the Flow CAM. Therefore, the sample was divided into three sub-samples immediately after sampling. 200 ml were inverse filtered with a 80 μm meshed net for the 100 μm flowcell measurement and 300 ml with a 250 μm net for the 300 μm flowcell measurement. The rest of the 500 ml remained unfiltered for the 600 μm flowcell measurement. Mesozooplankton was removed with a pipette. The sub-samples were stored dark and cold until the measurement with the system started, which was usually 1-4 hours after preparation of the sub-samples.

Flow CAM operation

For our experiment we used a portable black and white Flow CAM (www.fluidimaging.com) with a green laser beam for the fluorescence triggered image mode. Flow CAM details see Sieracki et al. (1998). The user has several opportunities to change settings in the fluorescent mode such as fluorescent gain (=amplifier) and fluorescent threshold of the fluorescence detector. For our measurements and in agreement with the manufacture operator manual we used the standard configurations (gain=4; threshold=100) in all three flow cell/objective combinations and we only changed the field “distance to neighbour” from 5 to 15 μm to prevent cell and colony structure cuttings on the taken Flow CAM pictures. We used neither a fixed pumping speed nor a fixed sample volume for each measurement, but adjusted the speed on the picture frequency around 120 pictures min^{-1} (usually between SLOW 5 and FAST 5) depending on the particle density in the defined particle size range and the used flowcell.

Before each fluorescent measurement 1,000 particles were counted in the AutoImage mode. In this mode, the Flow CAM counts every particle in the defined size range regardless of its fluorescent properties and calculates the total particle density automatically. In the fluorescence triggered image mode, which counts theoretically only living algae, we stopped the measurements after at least 5,000 particles were counted in the 100 μm and 300 μm flowcell measurements and at least 1,000 particles in the 600 μm flowcell measurement. In all of the measurements we used undiluted water samples and the pumped volume was measured after particle capture was finished. The density of fluorescent particles was then calculated with the Flow CAM software “Visualspreadsheet” (Version 1.5.16).

Flow CAM assay for monitoring performance

To test the applicability of the Flow CAM, results were compared with microscopic counts, chlorophyll data (HPLC) and the Secchi depth (SD) all important parameters of the daily routine monitoring of the Helgoland long time series.

RESULTS*Measurement effort with the Flow CAM*

The time needed to count the number of particles with the Flow CAM using the three different combinations of flowcells and magnifications in both measurement modes (AutoImage + fluorescence triggered image mode) was substantial. The time required for each sampling day and flowcell/objective combination as well as the difference in both Flow CAM

measurements (auto=AutoImage; fluor= fluorescent mode) was considerable (Fig. 1). Whereas the 1,000 particle counts in the AutoImage mode (Fig. 1A, C, E) were accomplished in a reasonable time from several minutes to around 1 hour, the time needed in the fluorescent triggered mode (Fig. 1B, D, F) for the 5,000 particle count was rarely under 1 hour and lasted up to 6 hours.

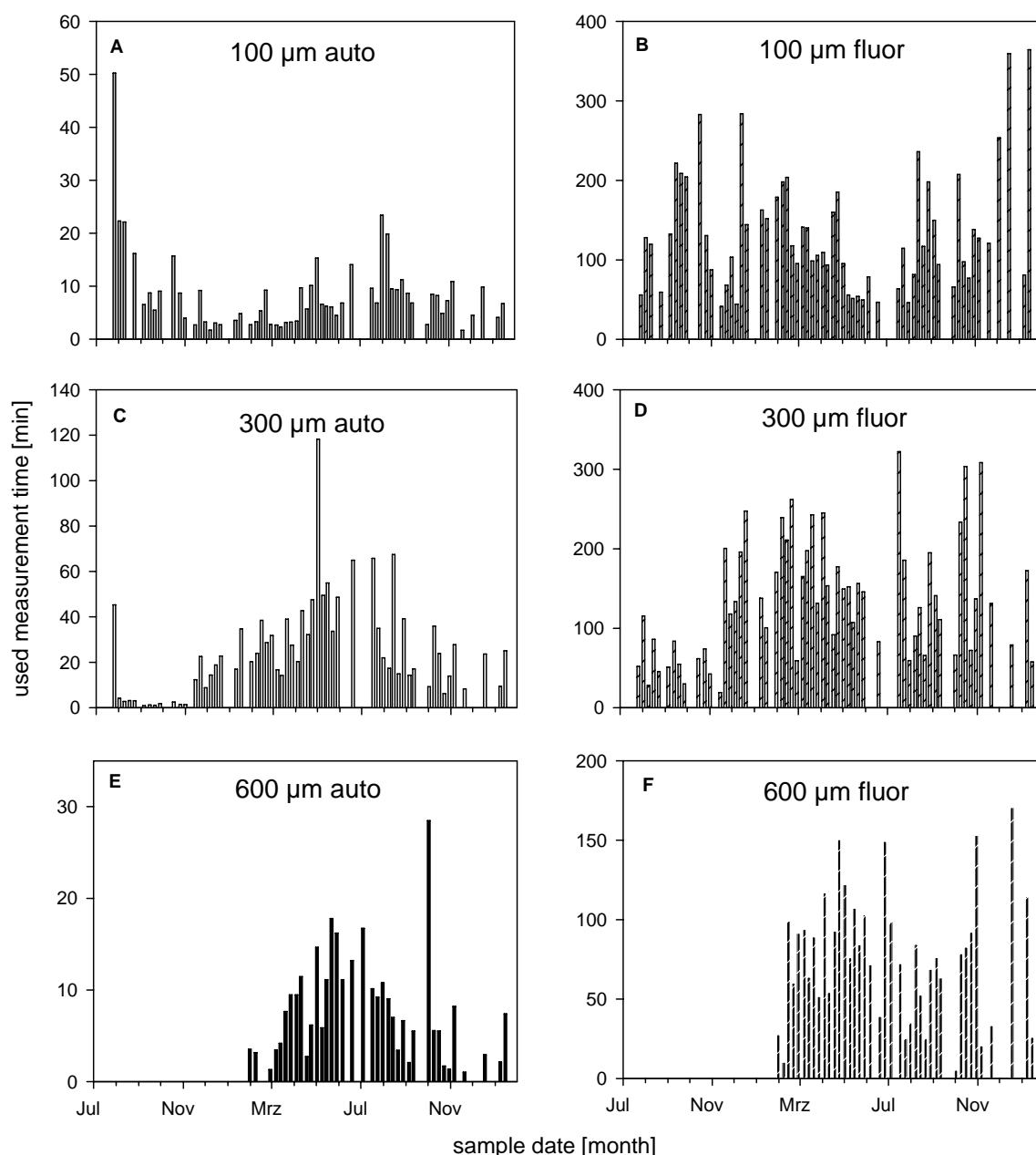


Figure 1: Used time (min) for each flow cell size measurement in the AutoImage (left hand) and fluorescence triggered image mode (right hand): (A, B) 100 μm ; (C, D) 300 μm and (E, F) 600 μm .

The total sample volume needed showed even higher differences between both measurement modes, and the volume increased with the used flowcell size (Fig. 2). In the AutoImage mode (Fig. 2A, C, E) the volume is measured by the Flow CAM, and can be obtained from the software, whereas in the fluorescence triggered mode (Fig. 2B, D, F) it is necessary to measure the volume by hand. Compared to the volume which is usually used for microscopic countings (25-50 ml), the measured volume with the Flow CAM in our set-ups were much higher, in total often around 500 ml, so that we should expect a much more accurate sampling and counting with the Flow CAM.

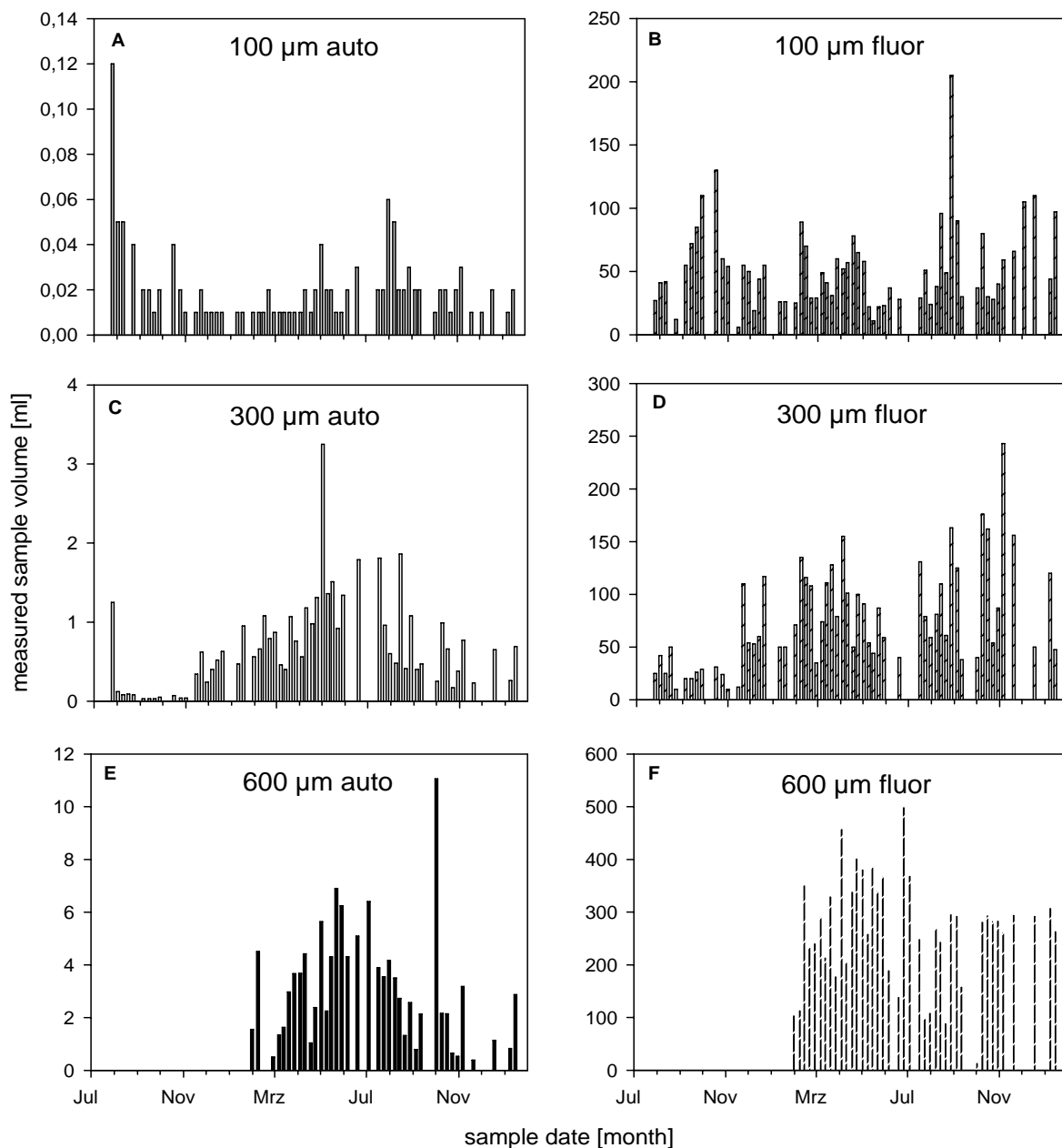


Figure 2: Sample volume (ml) measured in each flow cell size in the AutoImage (left hand) and fluorescence triggered image mode (right hand): (A, B) 100 µm; (C, D) 300 µm and (E, F) 600 µm.

The limit of 5,000 cells counted was based on the saturation curves exemplified in figure 3.

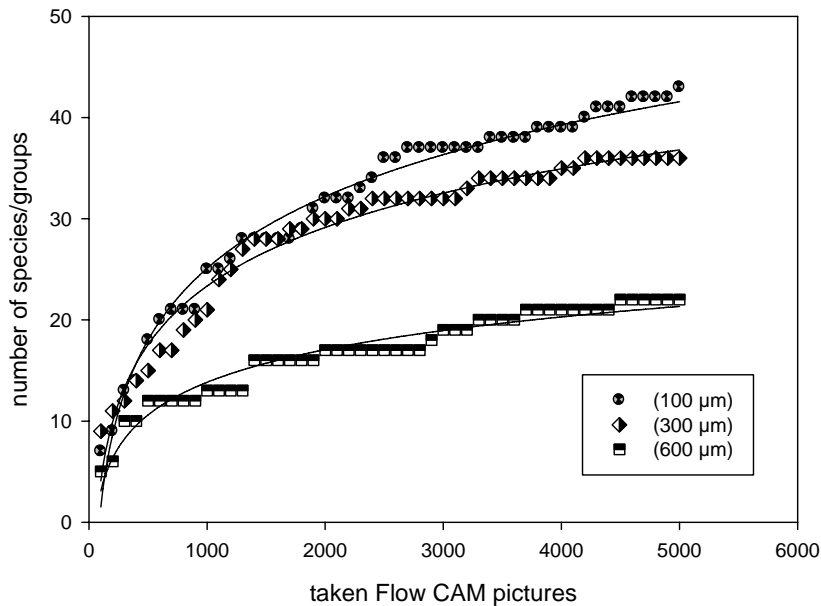


Figure 3: Sample performance of identifiable species/groups with increasing taken Flow CAM pictures (21.08.08) for each flow cell size (100 µm, 300 µm and 600 µm) in the fluorescence triggered image mode.

Especially with the smallest flowcell we saw that the curve relating counted particles with the number of observed individual taxonomic entities only starts to saturate at this number of counted particles. Particle counts with the 300 µm flowcell (size 15- 300 µm) detected less species/groups than with the 100 µm flowcell because of the more restricted particle size range, however, yielded nine new species which were not captured with the 100 µm flowcell. Lowest species/group detection was observed with the 600 µm flowcell (50- 600 µm), and only one more new species which was not seen with the smaller flow cells. The microscopic counts yielded 61 taxa during this particular sampling day, whereas the total number of taxa observed with the Flow CAM was only 53. Thus, despite a much higher effort, both in the total number of particles counted, the total sampling volume and the time spent counting and analyzing the data the output was higher using traditional microscopic counting methods.

Parameter measurements during the sampling period

Secchi-disk transparency of the water fluctuated between less than 1m and over 5m (Fig. 4A). It did not correlate significantly with either chlorophyll a concentrations (Fig. 4B), nor with the microscopic counts (correlations are not shown). Secchi depth was lowest during

autumn and winter (<1.5 m) and highest during the vegetation period during spring and summer (>1.5 m). Most likely, storm events during the non vegetation period caused particle re-suspension from the sediment.

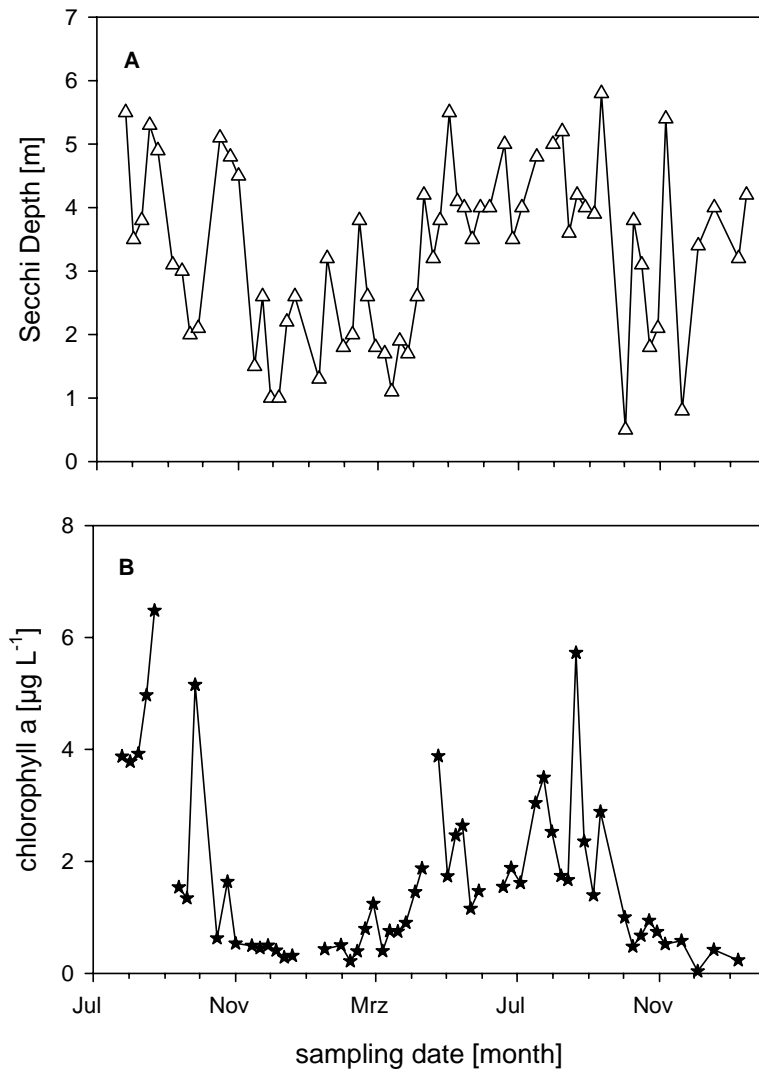


Figure 4: Overview of routine measurements at “Reede” sampling station Helgoland, Germany, during the sampling period between July 2007 and January 2009: (A) Secchi Depth (SD) [meter]; (B) Chlorophyll a content (HPLC) [µg L⁻¹].

At the beginning of the experiment we observed a chlorophyll a content of $\sim 4 \mu\text{g L}^{-1}$ (Fig. 4B). A first maximum was observed at the end of August ($6.5 \mu\text{g L}^{-1}$) followed by a short decrease and a subsequent autumn peak in October 2007. The chlorophyll a content during the rest of the year 2007 until spring 2008 was low ($< 1 \mu\text{g L}^{-1}$). The first noticeable increase started in early April 2008 and chlorophyll peaked at the end of this month ($\sim 4 \mu\text{g L}^{-1}$). After the spring bloom 2008 three following peaks in the summer (in the middle of July $\sim 3.8 \mu\text{g L}^{-1}$ and at the end of August $\sim 6 \mu\text{g L}^{-1}$) and one in autumn (middle of October $\sim 3.5 \mu\text{g L}^{-1}$)

occurred. The winter months until the end of the experiment in January 2009 were characterized by low chlorophyll contents ($< 1 \mu\text{g L}^{-1}$).

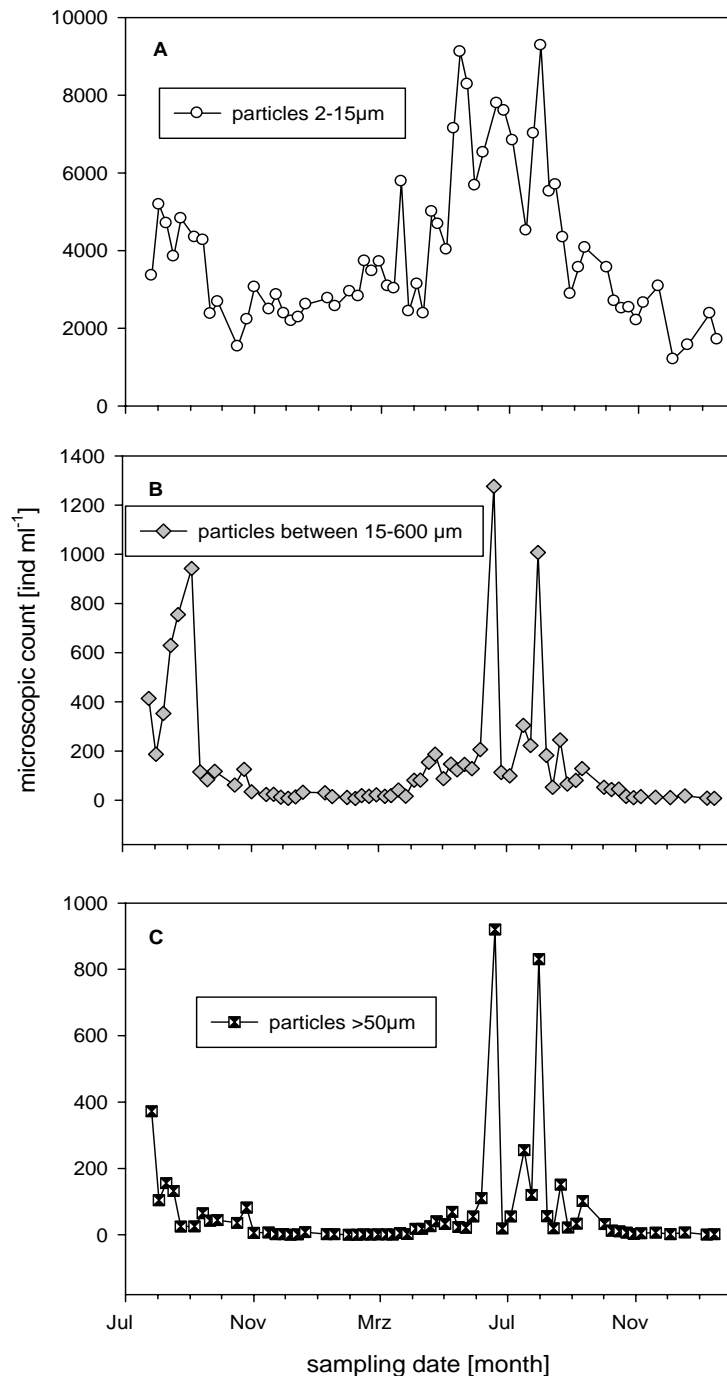


Figure 5: Summary of microscopic counts [ind ml⁻¹] during the sampling period: (A) abundance of phytoplankton species/groups in the size range of 2-15 μm ; (B) in the size range of 15- 600 μm and (C) in the size range of 50-600 μm .

Microscopic counts showed that in terms of abundance phytoplankton in the size range between 2 and 15 μm , consisting of small flagellates (3- 15 μm) and coccolithophorids ($\sim 5 \mu\text{m}$), dominated the phytoplankton community. The densities of fluorescent particles in this

size class were never below 1,000 cells ml⁻¹. Lowest abundance was observed during the autumn and winter months of both years. Highest abundance was found in summer 2007 (~5,000 cells ml⁻¹), in the middle of May and end of July 2008 (~9,000 cells ml⁻¹) (Fig. 5A). The abundances of larger plankton organisms (>15 µm), which mainly consisted of a variety of diatoms (single cells and cell colonies), dinoflagellates and ciliates, were much lower compared to the smaller cells. The cell density of this size class was most of the experimental period below 100 cells ml⁻¹. Three distinct peaks (~900-1,300 cells ml⁻¹) occurred: the first at the beginning of September 2007 (bloom of the diatom *Cylindrotheca closterium*), the second in the middle of June and the third at the end of July 2008 (colony forming diatom *Leptocylindrus minimus*) (Fig 5 B). The abundance of phytoplankton species above the 50 µm size range was even lower, essentially almost always below 1 cell ml⁻¹. In summer 2007 a bloom of the colony forming diatom *Eucampia zoodiacus* (~150 cells ml⁻¹) occurred and in the summer 2008 the colony forming diatom *Leptocylindrus minimus*, which might be several hundred micrometers long, dominated the larger phytoplankton (Fig. 5C).

The unspecific Flow CAM measurements with the AutoImage mode showed that most particles were in the size range between 2 and 15 µm (100 µm flowcell) and were never less than 10,000 particles ml⁻¹ at any time. Two wide peaks over the whole experimental period were detected with lowest densities in the summer (10,000- 50,000 particles ml⁻¹) and highest in autumn and winter (50,000- 240,000 particles ml⁻¹). Most of the captured Flow CAM pictures were non-living (non-fluorescent) particles (~98%) (Fig. 6A). The 300 µm flowcell measurement showed a similar pattern of particle density in a size range between 15 and 300 µm, but with densities two orders of magnitude lower than the observed particle densities in the 2-15 µm size range (100 µm) (170- 4,000 particles ml⁻¹) (Fig. 6B). Lowest particle concentrations were again measured with the 600 µm flowcell (50- 600 µm), varying between <1- 130 particles ml⁻¹ (Fig. 6C).

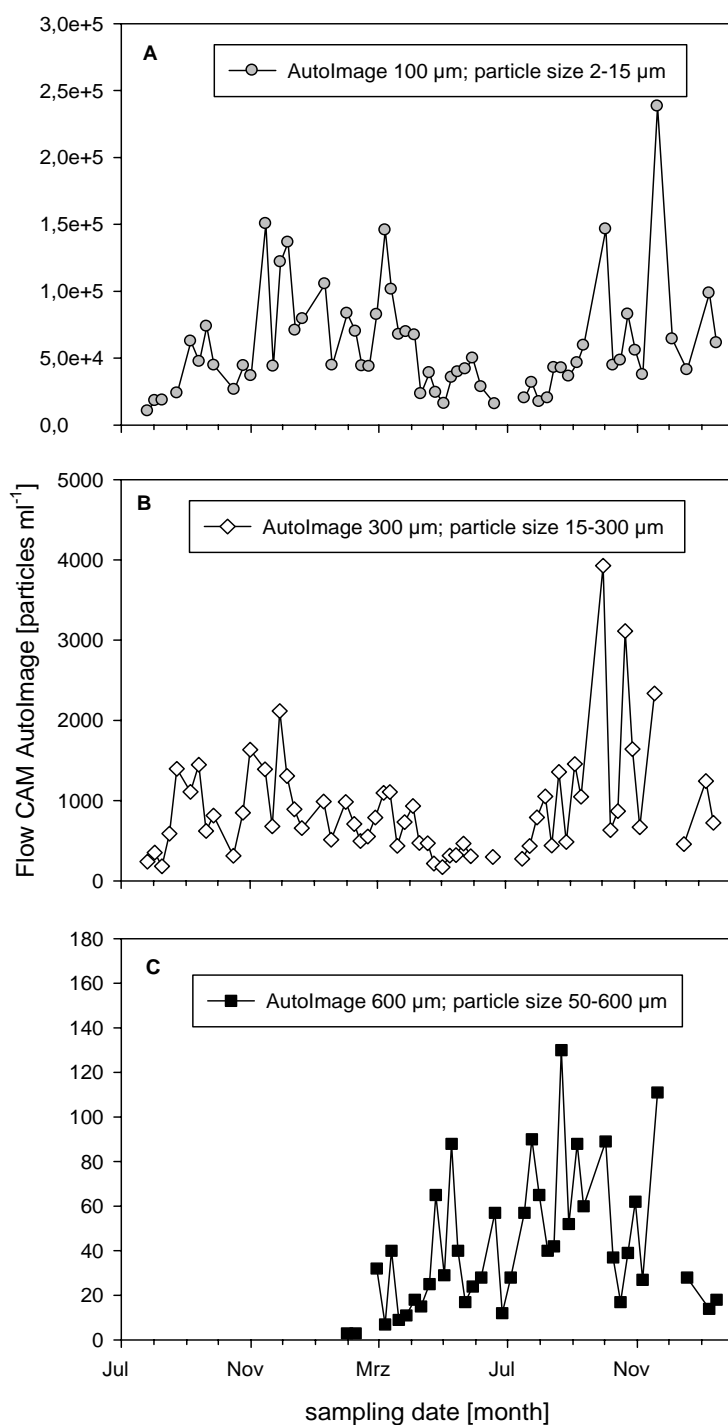


Figure 6: Summary of Flow CAM counts in the AutoImage mode [particles ml⁻¹] during the sampling period: (A) abundance of particles in the size range of 2-15 μm using the 100 μm flow cell/20X objective; (B) in the size range of 15- 300 μm using the 300 μm flow cell/10X objective and (C) in the size range of 50-600 μm using the 600 μm flow cell/4X objective.

In contrast to the unspecific measurements with the AutoImage mode, the fluorescence specific measurements with the fluorescence triggered image mode of the Flow CAM showed much lower densities in each particle size range. Highest densities of fluorescent particles

were measured with the 100 μm flowcell (particle size 2-15 μm : 100- 3,200 ml^{-1}) and did not show the same distribution over the experimental time as observed in the microscopic counts (Fig. 7A).

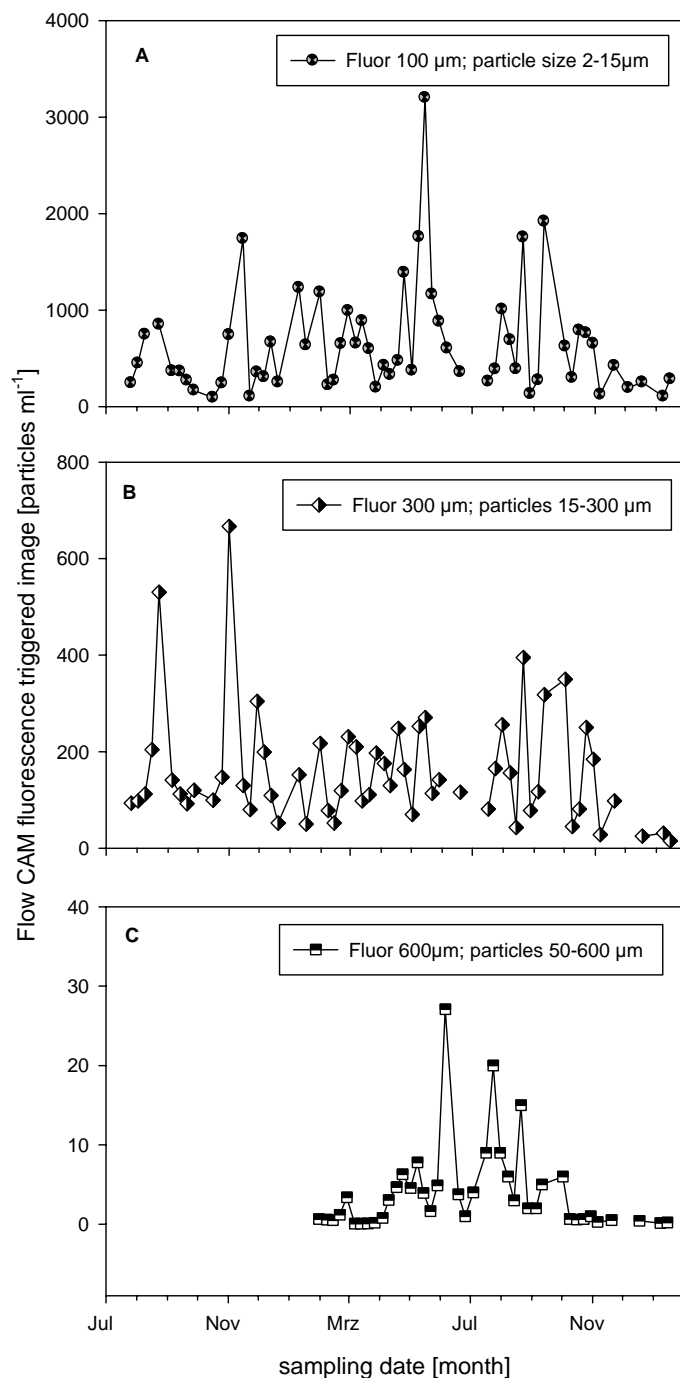


Figure 7: Summary of Flow CAM counts in the fluorescence triggered image mode [particles ml^{-1}] during the sampling period: (A) abundance of particles in the size range of 2-15 μm using the 100 μm flow cell/20X objective; (B) in the size range of 15- 300 μm using the 300 μm flow cell/10X objective and (C) in the size range of 50-600 μm using the 600 μm flow cell/4X objective.

This was the case also for the 300 μm flowcell measurements (particle size 15-300 μm : 15- 700 ml^{-1}) where the highest densities were measured mid of August 2007 and at the beginning

of November 2007 (Fig. 7B). The abundance of particles $>50 \mu\text{m}$ measured with the $600 \mu\text{m}$ flowcell was $<0.1 \text{ ml}^{-1}$ during winter 2008 and 2008/09, and highest during the summer ($15\text{--}28 \text{ ml}^{-1}$) (Fig. 7C).

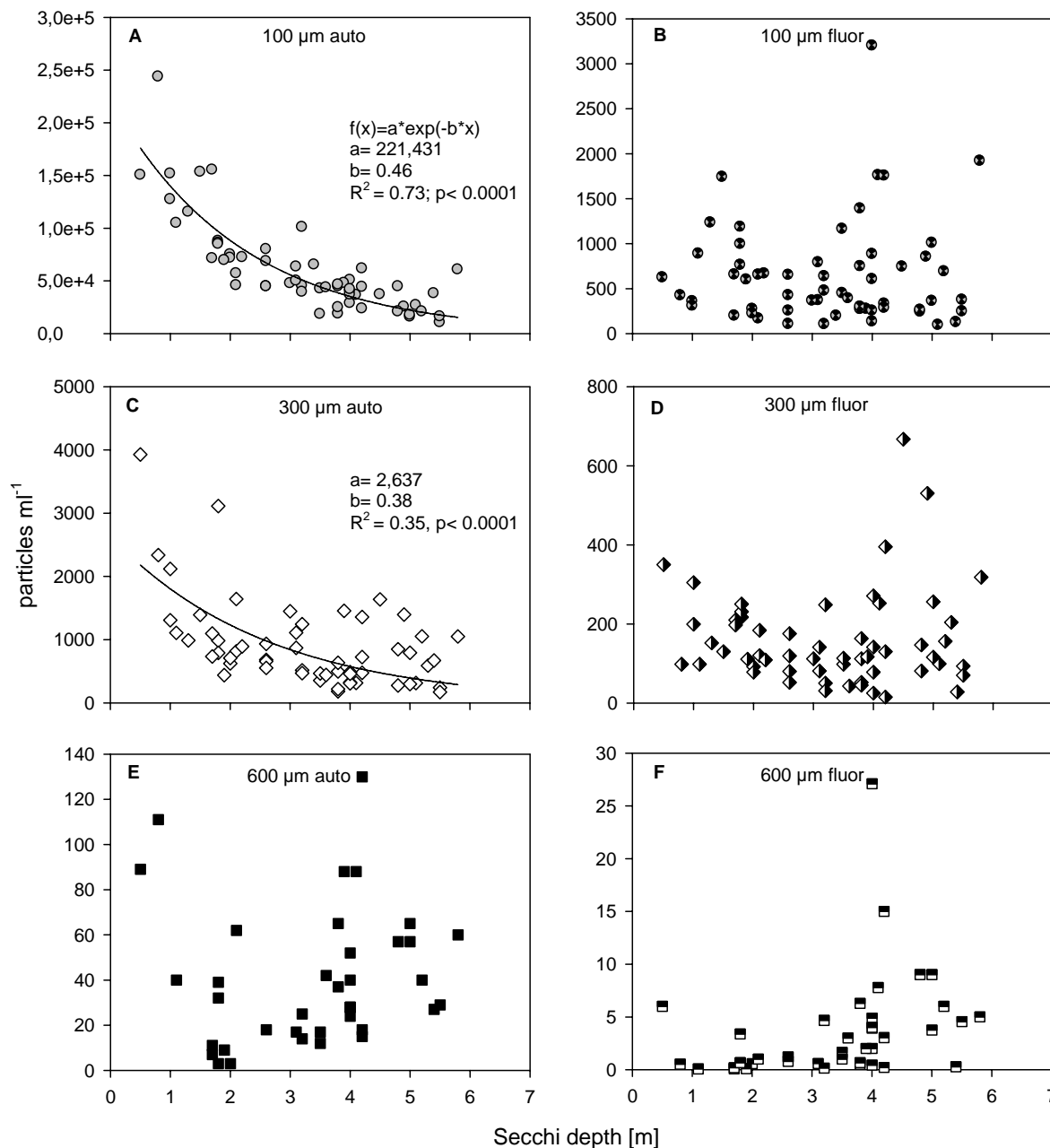


Figure 8: Correlations between measured particles ml^{-1} with the Flow CAM and the Secchi Depth (SD) for each flow cell size (100, 300 and 600 μm). (A, C, E): measured in the AutoImage mode (auto) and (B, D, F) in the fluorescence triggered image mode (flour).

Which parameters correlate with Flow CAM measurements?

When we correlated each flowcell measurement in both Flow CAM modes (AutoImage+fluorescence triggered image mode) with the other parameters measured, we observed a significantly negative correlation of the 100 μm flowcell measurement in the AutoImage and the Secchi depth. Obviously, the densities of the smallest particles (2-15 μm) were the factors which influenced the turbidity of the water column (Fig. 8A). These particles are non-living particles, which can be seen from the measurement in the fluorescence triggered image mode (Fig. 8B) or the microscopic counts (correlations not shown, but see Fig. 10A). Bigger particles (15- 300 μm) which were measured with the 300 μm flowcell in the AutoImage showed also a significant but weaker correlation with the Secchi Depth (Fig. 8C). Also these particles were mainly non fluorescent particles (Fig. 8D and Fig. 11A). The density of the largest particles (50-600 μm) did not show any significant correlations with water transparency both in the AutoImage (Fig. 8E) and the fluorescence triggered image mode (Fig. 8F), but tended to correlate better with microscopic counts (Fig. 12).

Whereas the density of the smallest particles was negatively correlated with increasing chlorophyll a in the AutoImage mode with the 100 μm flowcell (Fig. 9A), no correlations in the fluorescence triggered image mode could be observed (Fig. 9 B). As stated above, these smallest particles (2- 15 μm) were mostly non living particles and hence had no correlation with chlorophyll content. Also, the correlation between the microscopic counts in this particle size range and the chlorophyll content was not significant (not shown). The particles which were measured with the 300 μm flowcell (15-300 μm), showed no significant correlations with increasing chlorophyll a content in both Flow CAM measurement modes (Fig. 9C+9D). Only the largest particles (>50 μm) which were measured with the 600 μm flowcell (Fig 9E+9F) had a positive correlation with chlorophyll content. Corroborating evidence from the microscopic survey (not shown), showed that indeed the occurrence and abundance of large fluorescent particles is responsible for most of the chlorophyll measured in our coastal system.

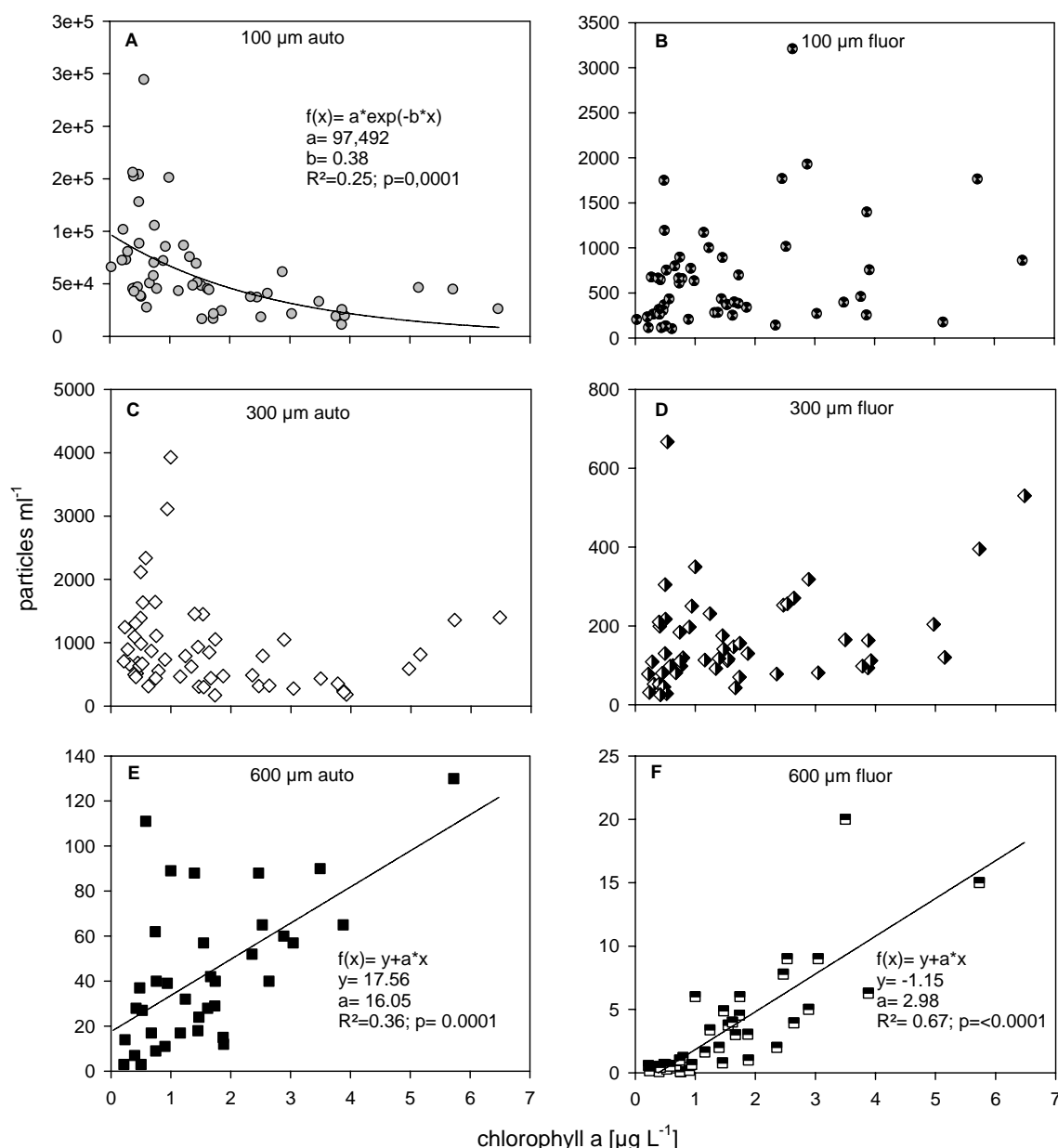


Figure 9: Correlations between measured particles ml^{-1} with the Flow CAM and the chlorophyll a content (HPLC) for each flow cell size (100, 300 and 600 μm). (A, C, E): measured in the AutoImage mode (auto) and (B, D, F) in the fluorescence triggered image mode (flour).

The unselected raw measurements of the Flow CAM in the fluorescence triggered image mode showed no correlations to the microscopic counts in the particle size range 2-15 μm measured with the 100 μm flowcell. The Flow CAM underestimated the abundance of algae (fluorescent particles) in this size fraction by a factor of three-ten even using the raw (all images taken) measurement (Fig. 10B). After a very time-consuming selection of only those particles that were identifiable as algae, still no correlation between the Flow CAM and the

microscopic counts could be observed. The underestimation of the measured Flow CAM abundance was obviously now even higher (factor ~6-15) (Fig. 10C).

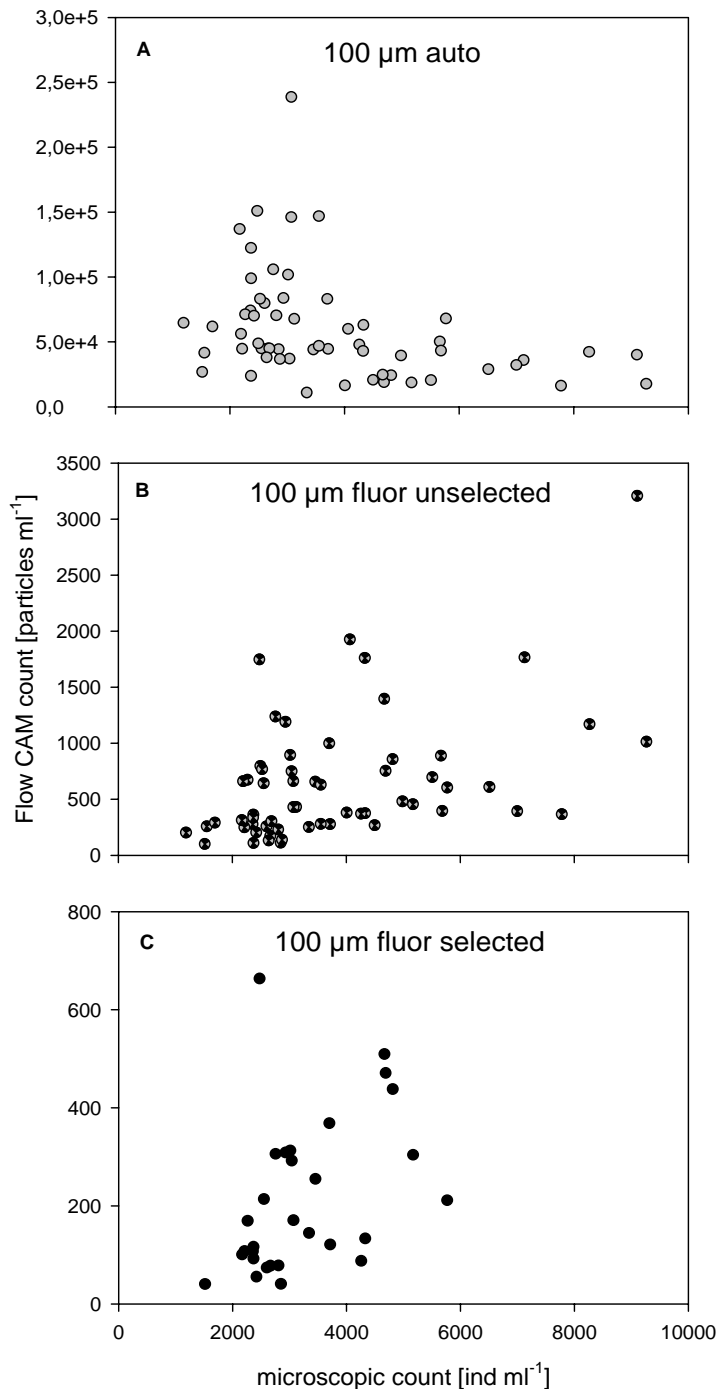


Figure 10: Comparison of Flow CAM measurements with microscopic counts in the particles' size range 2-15 µm (100 µm flow cell): (A) measured in the AutoImage mode; (B) measured in the fluorescence triggered image mode (“unselected” means raw measurements) and (C) measured in the fluorescence triggered image mode after identifiable detritus was out- selected (“selected”).

The difference between the unselected and selected Flow CAM measurement was more obvious with the 300 µm flowcell. No correlations between the unselected Flow CAM

measurements and the microscopic counts in the size range 15- 300 μm were detected (Fig. 11B). The only significant correlation between Flow CAM counts and microscopic counts of all measurements could be achieved after non living particles were excluded (Fig. 11C).

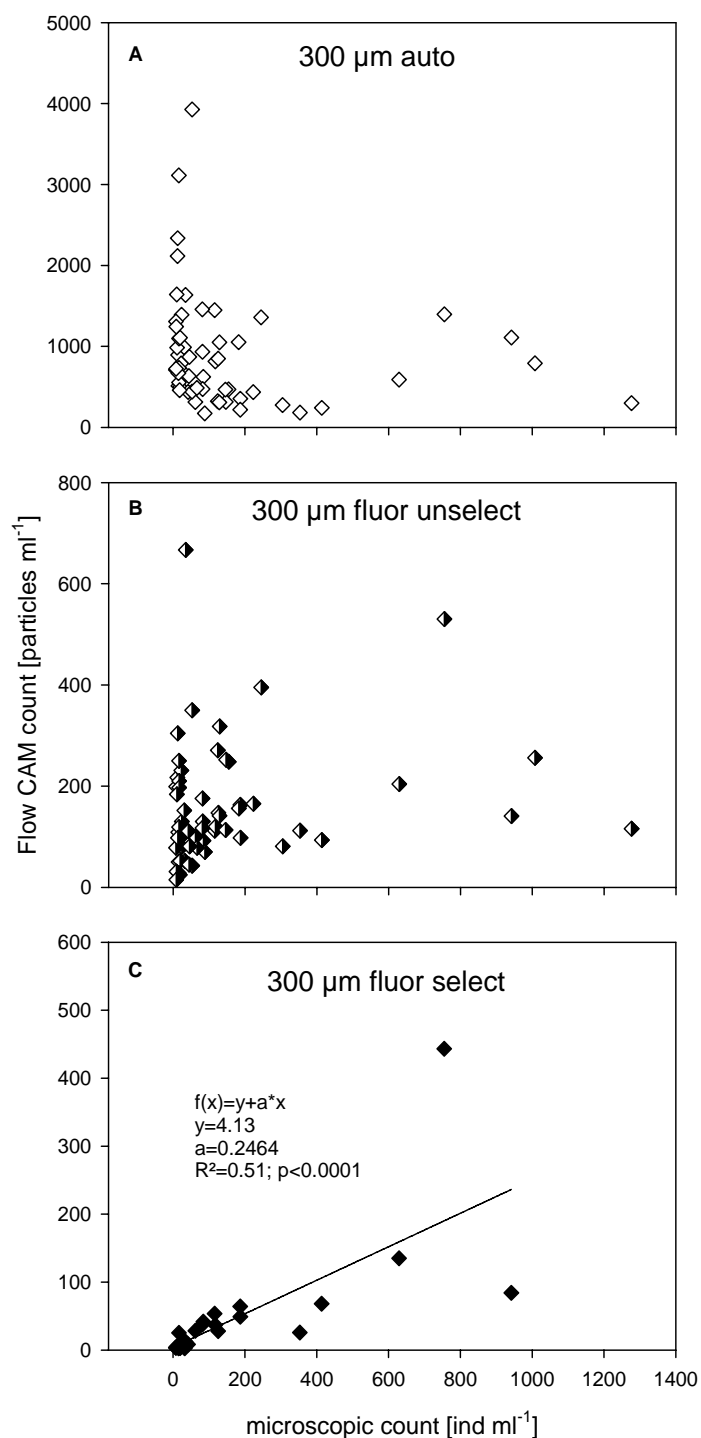


Figure 11: Comparison of Flow CAM measurements with microscopic counts in the particles' size range 15-300 μm (300 μm flow cell): (A) measured in the AutoImage mode; (B) measured in the fluorescence triggered image mode (“unselected” means raw measurements) and (C) measured in the fluorescence triggered image mode after identifiable detritus was out- selected (“selected”).

The underestimation of the particle abundance was less than with the 100 μm flowcell, but still around a factor two. Particles in this size range which were effectively measured with the 300 μm flowcell were single celled dinoflagellates (20-100 μm), ciliates and single celled diatoms. Parts of colony forming diatoms could be captured, but the images did not represent the real size (e.g. *Eucampia zodiacus*, *Rhizosolenia imbricata*).

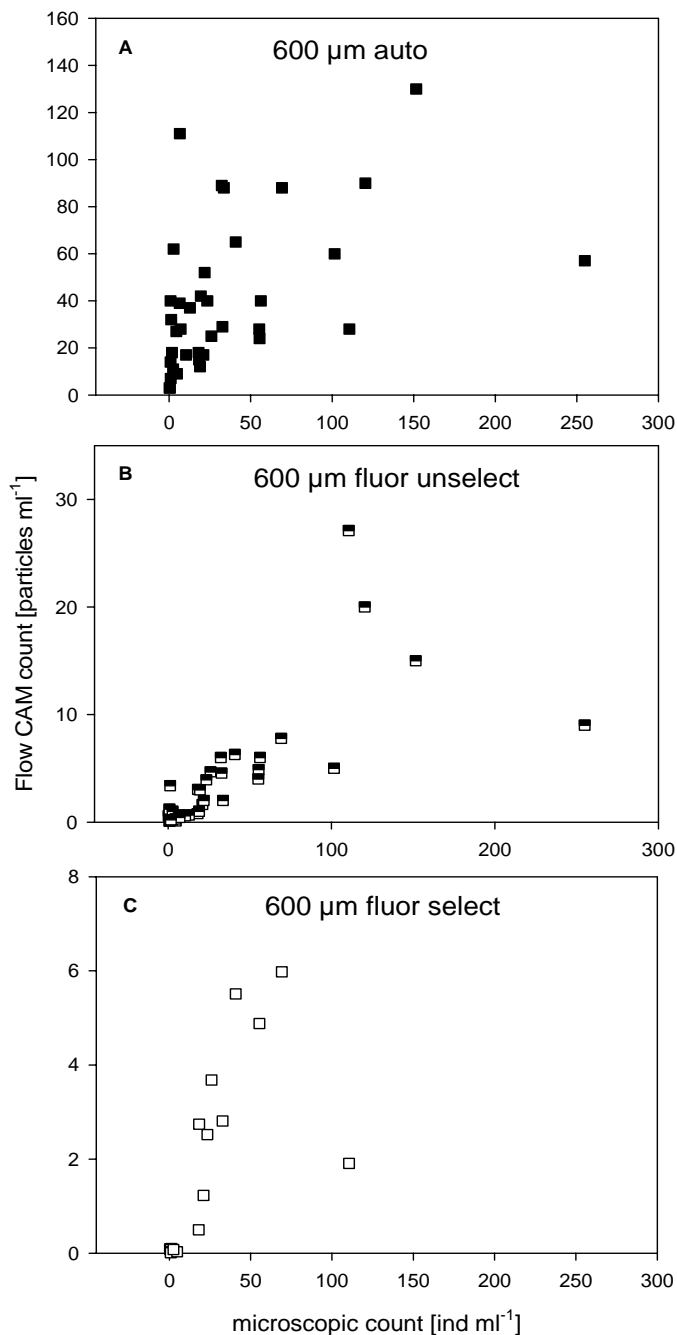


Figure 12: Comparison of Flow CAM measurements with microscopic counts in the particles' size range 50-600 μm (600 μm flow cell): (A) measured in the AutoImage mode; (B) measured in the fluorescence triggered image mode (“unselected” means raw measurements) and (C) measured in the fluorescence triggered image mode after identifiable detritus was out- selected (“selected”).

The measurement with the 600 μm flowcell solved the size problem of the colonies described above and yielded images of whole diatom colonies (e.g. *Bacteriastrum hyalinum*, *Leptocylindrus* sp.) and big sized dinoflagellates (e.g. *Ceratium fusus*, *Noctiluca scintillans*), as well as big sized ciliates ($>50 \mu\text{m}$)(e.g. *Laboea* sp.). As seen with the other two flowcell measurements the Flow CAM underestimated the cell abundance of larger particles (50-600 μm) in comparison with microscopic counts. No strong correlation with the microscopic counts were observed but there seemed to be a tendency that the Flow CAM measured microscopic cell counts in the size fraction 50- 600 μm roughly correct (Fig. 12B+C). To investigate how important these effects really were, we went through the image database of roughly half the total sampling events (this is a major effort with 11,000 images that need to be looked at), and selected only those images that were obviously living organisms. The numbers that emerged from this exercise were then correlated with the microscopic counts in the same size classes.

Why did the Flow CAM underestimate the microscopic counts in the fluorescence triggered image mode?

Apparently a huge amount of particles were non living particles in the water column during the experimental period. Going into further detail using the fluorescence measurement of the Flow CAM for each flow cell size, a large number of non identifiable particles in the size class 2-15 μm were obtained with the 100 μm flowcell (20-75% of total measurements). During the re-processing of captured Flow CAM pictures, it was hard to decide to attribute these particles to either non-living particles (detritus) or living particles due to similar shape of living plankton organisms (flagellates and coccolithophorids). The proportion of living plankton organisms which could be definitely identified was around 25-70%, whereas the amount of identifiable non-living particles was quite low (1-25%). In consideration of the huge amount of non-living particles in this size class, the amount of non identifiable particles might be rather non-living particles than living cells (Fig. 13A). The particles measured in the 300 μm flowcell (15-300 μm) were more easily attributable because of its size. Whereas the amount of living particles during summer and autumn were ~20-80% of total Flow CAM captures, the amount of non-living particles dominated the Flow CAM measurement during winter up to 95% (Fig. 13B). This could even be confirmed with the 600 μm flowcell where most of taken Flow CAM pictures in the fluorescence triggered image mode were non-living particle during the winter months. In early spring however the amount of living organisms continued to increase up to 90% of total captures (Fig. 13C).

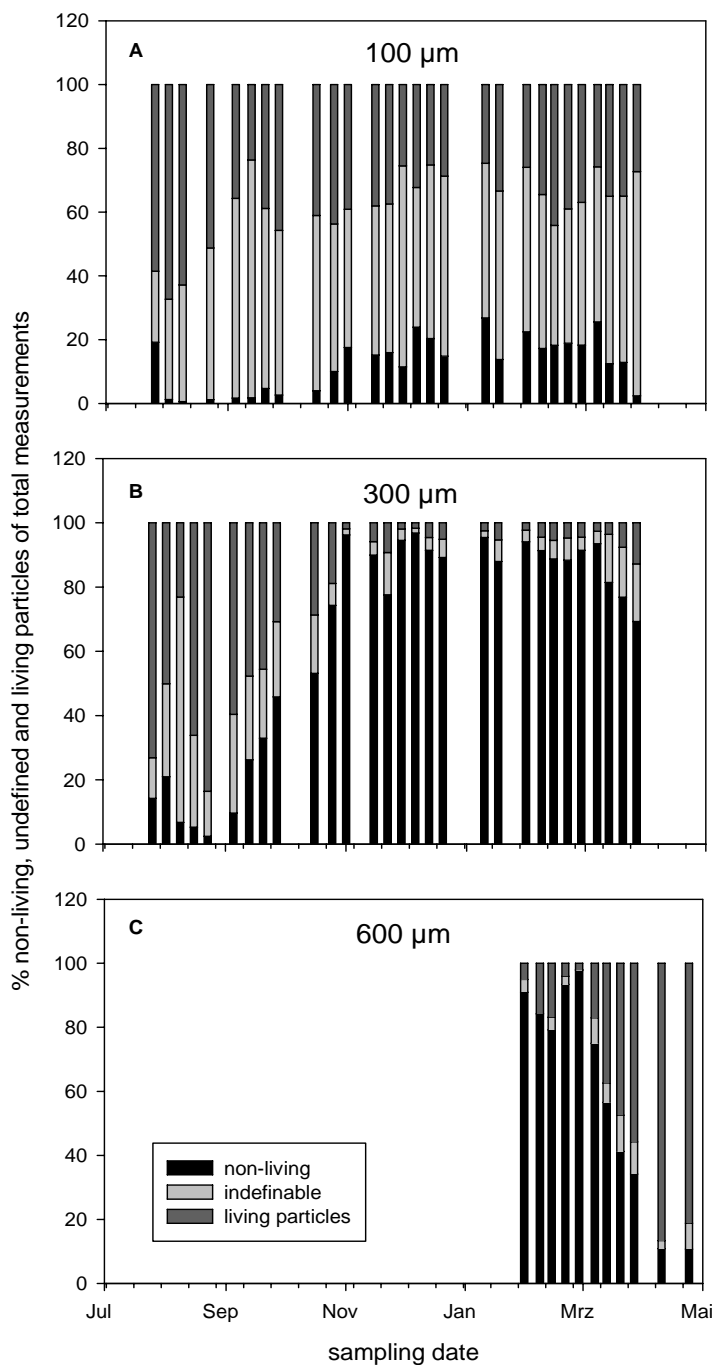


Figure 13: Extract of Flow CAM captures of non-living (detritus), undefinable and living particles for each flowcell size in the fluorescence triggered image mode during the sampling period (July 2007-April 2008): (A) 100 μm ; (B) 300 μm ; (C) 600 μm sized flowcell.

Many particles measured in the fluorescence triggered image mode of the Flow CAM (and thus having fluorescence) were obviously non-living particles. There were several reasons for this. First, every particle that passed the flow cell at the same time a fluorescent particle went through received the fluorescent properties of the particle (co-captures).

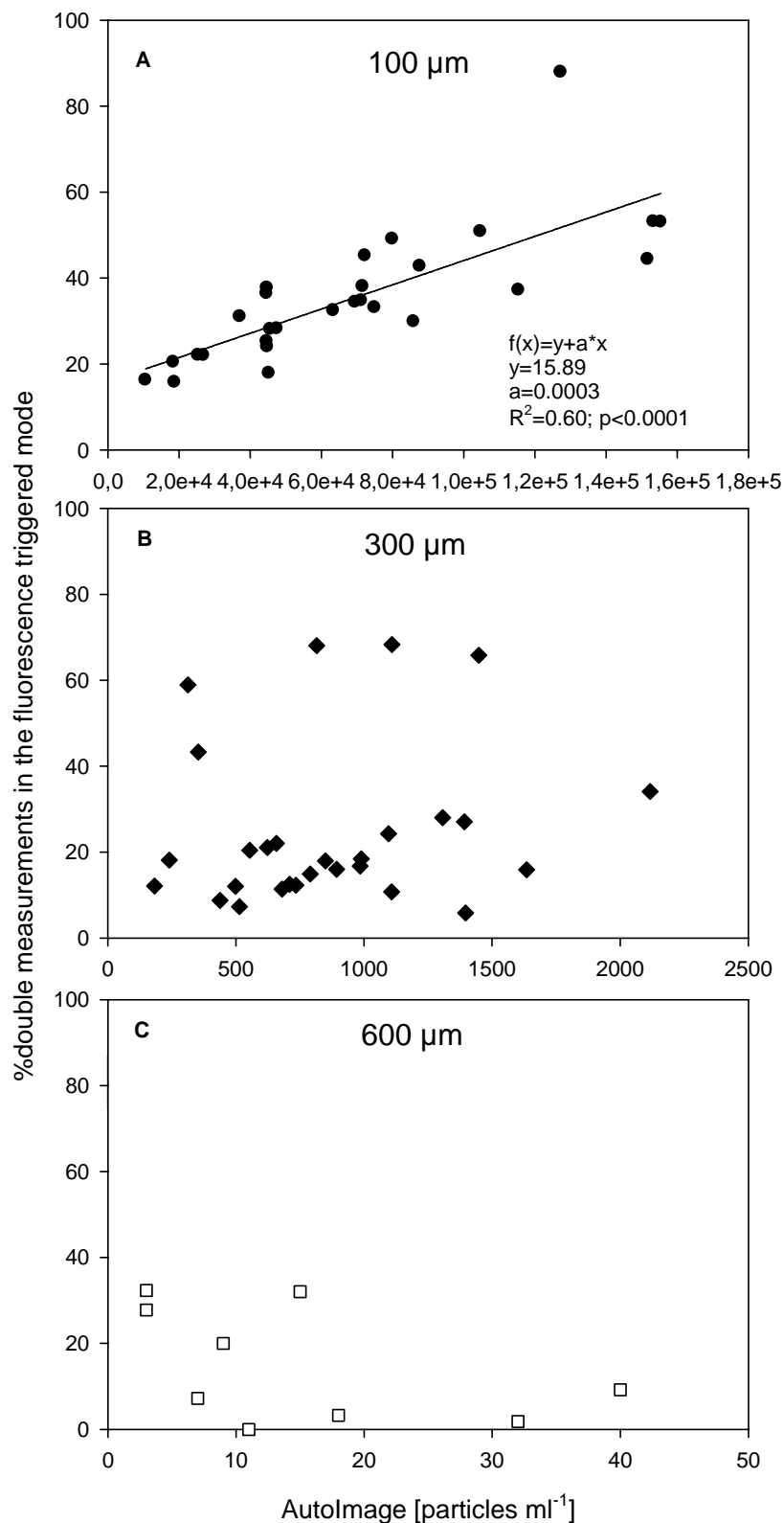


Figure 14: The role of total particle concentration measured in the AutoImage mode and the resultant co-captures (%) of non fluorescent particles with fluorescent particles in the fluorescence triggered image mode during the sampling period (july 2007-april 2008): (A) 100 μm; (B) 300 μm; (C) 600 μm sized flow cell.

Although this is relatively easily detected (but tedious) by visual inspection of the data sheet afterwards, as different particles have identical values for fluorescence, it makes for a substantial number of false hits, and was especially prominent in the 100 μm flowcell measurement. The amount of co-captures (double measurements) in the fluorescence triggered image mode increased linearly with increasing particle concentration measured with the AutoImage mode (Fig. 14 A). Such double measurements were also detectable in the 300 μm flowcell, however occurred most prominently when larger algal species or large colony forming species were present. Due to the fact that smaller sized particles were in such cases always more abundant than larger algal species, multiple captures occurred with smaller sized particles in the wide adjusted measurement size ranged from 15 to 300 μm (Fig. 14B). This might be also the explanation of the double measurements found in the 600 μm flowcell (Fig. 14C). Therefore, the high amount of non-living particles in the 300 and 600 μm flowcell measurements might be affected by the fluorescent property of the particles itself. Recently dead or decaying algal cells might also still show some fluorescence again leading to false hits.

To determine the Flow CAM performance of each flow cell size at a group/taxon level, we selected four examples. The first example is the major group of “flagellata indeterminate” in the size range between 3 and 15 μm measured with the 100 μm flowcell. Flagellates above ~ 5 μm were easily recognized on Flow CAM images because of their cell shape. Below 5 μm it was very difficult to identify a captured particle as a flagellate. We found a weak but significant correlation between the Flow CAM counts and the microscopic counts with detected flagellates of the Flow CAM ($R^2= 0.25$; $p= 0.0045$). Again, however, the Flow CAM measurements underestimated the densities substantially (Fig. 15A). The second example is the large dinoflagellate *Akashiwo sanguinea* (40- 80 μm) which built a bloom in the summer of 2007 and could be measured with two flowcells (100 μm +300 μm). The Flow CAM performance with both flowcells showed a good consistency with the microscopic counts (100 μm : $R^2= 0.64$; $p= 0.0002$; 300 μm : $R^2= 0.49$; $p= 0.0026$), but obviously the number of non-zero counts was fairly low (Fig. 15B). The third example is the large dinoflagellate *Ceratium fusus* (~ 600 $\mu\text{m}/30$ μm) which is a typical summer and autumn species at Helgoland Roads, but occurs in low numbers. This species could be captured with all three flowcell sizes, was however only correctly captured with the 300 μm and 600 μm flowcell. The 20X magnification with the 100 μm flowcell was too high so that only parts of the individuals were captured. All three Flow CAM measurements had a significant correlation with the microscopic counts (100 μm : $R^2= 0.75$; 300 μm : $R^2= 0.80$; 600 μm :

$R^2=0.70$; $p<0.0001$), but again underestimated the abundance which was detected with the microscope (Fig. 15C).

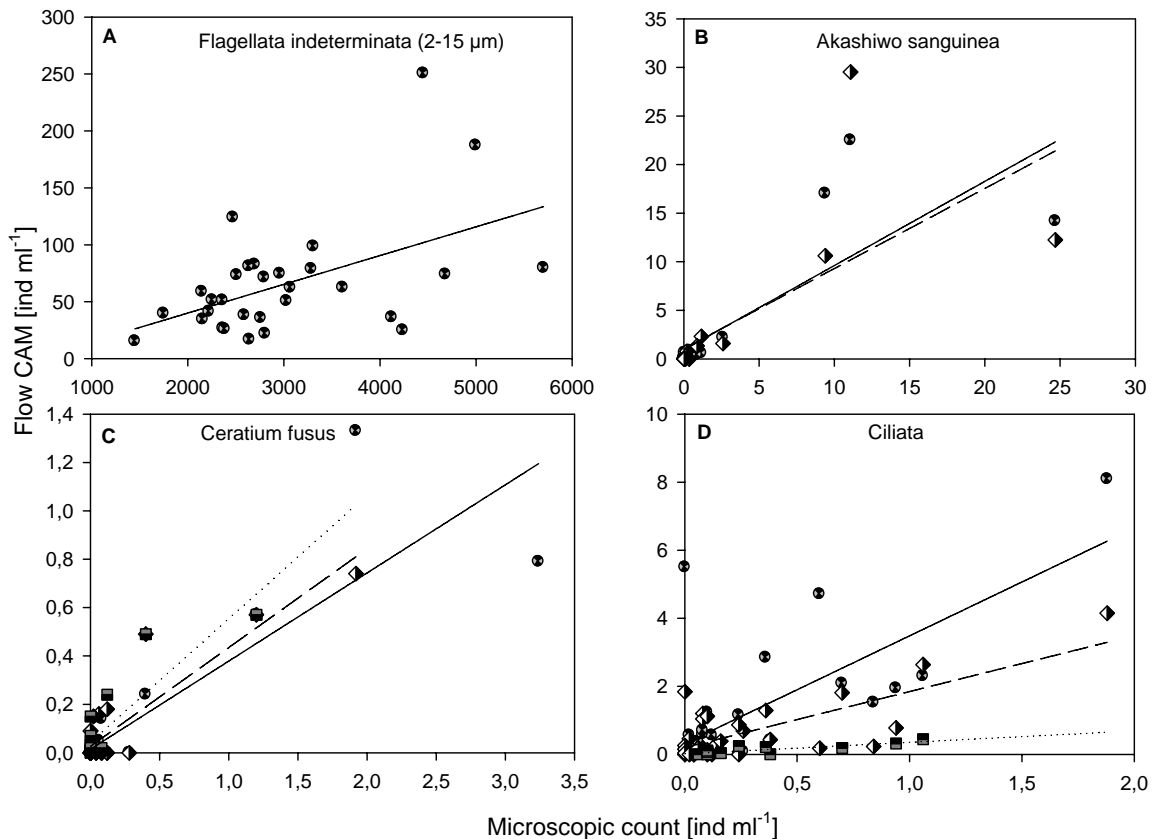


Figure 15: selected species and groups measured with the Flow CAM vs microscopic counts. **A** Flagellata indeterminate (size range 2- 15 μm) measured with the 100 μm flowcell; **B** dinoflagellate *Akashiwo sanguinea* measured with the 100 μm (dots and solid line) and 300 μm (diamonds and dashed line) flowcell. **C** dinoflagellate *Ceratium fusus* measured with the 100 μm , 300 μm and 600 μm (squares and dotted line) flowcells. **D** Ciliata measured with all three flowcell sizes.

The last example is the group “Ciliata indeterminate” which occurs in a huge size range between 15 and 150 μm at Helgoland Roads but also in low numbers depending on their size. All of the three Flow CAM measurements yielded good correlations with the microscopic counts (100 μm : $R^2= 0.51$; $p<0.0001$; 300 μm : $R^2= 0.56$; $p<0.0001$ and 600 μm : $R= 0.69$; $p= 0.0016$). This group is an exception because the Flow CAM yielded higher abundance estimates than the microscopic counts. Some might argue that measuring ciliates in the fluorescence triggered image mode is incorrect. Important ciliate species at Helgoland are mixotrophic (e.g. *Laboea* sp. or *Myrionecta rubra*) which means containing chloroplasts or were fluorescent because their food vacuoles were filled with food algae. A second explanation might be that ciliates were co-captured by the fluorescence incidence described above. The higher ciliate estimates with the Flow CAM was however mainly explained by the

fact that only three different species were counted under the microscope (*Mesodinium* sp., *Myrionecta rubra* and *Laboea* sp.). The Flow CAM detected more than ~20 other ciliate taxa over the whole experimental period, which could be not further identified (Fig. 15D).

DISCUSSION

The portable Flow CAM was tested against the routine sampling of the long-term sampling station at Helgoland Roads, Germany. The first outcome of our investigations is that the time and effort that needs to be invested in one sample, using three flowcell/objective combinations with two Flow CAM measurement modes, is such high that in the same time the sample could have been easily counted using the traditional methods (~1hour).

The AutoImage of the Flow CAM

The automatic counting mode of the Flow CAM is a suitable tool for measuring high particle concentrations in natural field samples. Up until now, water transparency measurements at Helgoland Roads could not be correlated with any other parameters. Here, we have shown that it is well explained by the amount of non-living particles in the water, and not by algal densities or chlorophyll concentration. This is in contrast to lake studies where the Secchi Depth often correlates with chlorophyll. The AutoImage captures only the most abundant particles. The one thousand captured particles which we used for the AutoImage measurement would not have been sufficient to capture sufficient amounts of living plankton organisms since we captured almost exclusively non-living particles in the AutoImage mode. The AutoImage mode is the mode which might be the best choice if detritus is of less importance. The advantage is that in contrast to the fluorescence triggered image mode less considerations into suitable configurations and adjustments of the Flow CAM for accurate measurements have to be taken (Hantzsche et al. in prep, Chapter II). Another advantage is the relatively short time needed for AutoImage measurements, which obviously is an advantage only when the user is interested in non-living particles.

The Flow CAM in the fluorescence triggered image mode

Theoretically, the fluorescence triggered image mode measures only fluorescent particles using a laser to excite the fluorescence and induce the camera to take a picture. Unfortunately, in our study this did not work properly. The first reason might be the used adjustment “fluorescent threshold” (100) of the Flow CAM which determines the fluorescence signal of a passing particle which triggers the Flow CAM. The problem is that

species which are weak fluorescent are not captured because of their weak fluorescence signal to hurdle the adjusted threshold of the fluorescence detector. Such algal cells are then “defined” as non fluorescent particles and are therefore not captured by the Flow CAM. Hantzsche et al. (in prep, Chapter II) showed that a significant decrease of the fluorescence threshold (from 100 to 1) enhanced the possibility to capture low fluorescent *R. salina* which were not efficiently captured by the Flow CAM when the fluorescent threshold was set on 100. Additionally, Hantzsche et al. (in prep, Chapter II) showed that the magnitude of the fluorescence signal of *R. salina* was highly dependent on the pump speeds. This means that if the pump rate is low and the threshold of the fluorescence detector set on 100, low fluorescent algal cells are not captured because the fluorescence signal of such slow and weak fluorescent cells are too low to hurdle this high adjusted fluorescent threshold. With increasing pump rates but equal adjusted threshold, the probability increases that the fluorescent signal of such weak fluorescent algal cells increases. Thus, the Flow CAM is triggered and captures such cells since their fluorescent signal hurdle the adjusted fluorescent threshold. Higher fluorescent particles may hurdle the equal adjusted threshold (100) of the fluorescence detector even at lower pump rates and are therefore selectively captured by the Flow CAM. With increasing pump rates, however, the risk increases that the Flow CAM does not recognize fast passing particles (Hantzsche et al. (in prep, Chapter II)). It might be possible, that higher fluorescent particles are over-amplified through the equal adjusted gain and threshold of the fluorescence detector. Such particles are too bright and are therefore not captured by the Flow CAM.

Therefore, we have to assume that the variable pump rates in our field survey are a second reason that all Flow CAM measurements underestimated (except for ciliates) the abundance which was found in the microscopic counts. Low pump rates decreased the fluorescence signal of passing particles and were therefore not captured because of the high fluorescent threshold. Higher used pump rates probably increased the fluorescence signal of weak fluorescent particles, however enhanced the risk that higher fluorescent particles were over-amplified or that particles passed the laser too quick and thus, were not captured by the Flow CAM. Especially in the 600 μm flow cell where the pump rate had to be high to increase the probability to capture large but less abundant species might be the reason that the Flow CAM underestimated the abundance even at cell concentrations below 100 cells ml^{-1} . A possible response might be to keep the pump rates constant as soon as suitable application protocols are established which clarify the correlation between pump speeds and the adjustable gain and threshold of the fluorescence detector for each flowcell size. The time

effort, however, which has to be used for field samples will increase since the abundance of plankton species change over the year.

Another important difficulty is the large size range and hyperbolic abundance frequency of particles which occurs in marine waters as described by McCave (1984). Single celled phytoplankton which is counted under the microscope differs in its size from 3 μm (e.g. flagellates) until 600 μm and larger (e.g. *Coscinodiscus wailesii*, *Noctiluca scintillans*). Huge colonies of diatoms and *Phaeocystis* colonies reach up to several mm. The observed densities of these described plankton species range between 10,000 ml^{-1} for the smallest and 0.02 ml^{-1} for the largest which means a factor of 500,000. Thus, under optimal conditions the Flow CAM would measure ~500,000 small species in order to capture one large but less abundant plankton species per measured volume. Therefore, it is not surprising that if one large particle passes the laser beam, several other, small particles pass simultaneously. The lack of the Flow CAM software to recognize the fluorescence of simultaneously passing particles separately is the main reason that we measured so much non-living particles in the fluorescence triggered image mode (based on co-captures, double measurements). The adjustable Flow CAM parameter which defines the particle size range which should be captured by the Flow CAM for each flow cell size enhanced this problem additionally. Therefore, it is highly recommended not to measure particles in the whole size range of the used flow cell size, but rather in several, shorter defined size steps.

All of this critical analysis of our used methods emphasize that many factors have to be considered when the Flow CAM has to be employed in the field. It is interesting that we obtained correlations between chlorophyll and the abundance of large particles. Furthermore, we found correlations between Flow CAM counts and microscopic counts on the base of selected taxa, albeit with underestimations of the Flow CAM when compared with the microscopic counts.

The Flow CAM technology is certainly of interest, but needs to be developed further. This applies also for the Flow CAM user. The Flow CAM which is sold as a ready-to-use piece of equipment has so many different possibilities to change parameters such as the fluorescent gain and its threshold which determines at which fluorescent signal a particle is captured. The possibility to adapt the fluorescent signal per se might be a good chance to exclude non fluorescent particles during the measurement. Consequently, the proportion of non living particles and the selection of these particles might take less time for data re-processing after the measurement has been finished. Since we know that fluorescence is strongly coupled with cell volume and its chlorophyll content, we think that the

underestimation of the smallest particles (3- 15 μm) which were measured with the 100 μm flowcell might depend on their weak fluorescent signal and the relatively high fluorescent threshold of the fluorescence detector. Although we could exclude a huge proportion of non-living material in the fluorescence triggered image mode (in comparison to the AutoImage mode), we also excluded a huge proportion of fluorescent cells. That might be the reason for Ide et al. (2008) setting the threshold at 12 (standard 100) and the gain at 4,095 (standard 4) of the fluorescent detector. Unfortunately, in high detritus systems the result would also have been an even higher number of non-living particles showing at least some fluorescence and as a result captured by the Flow CAM. In fact, one needs to know one system before deploying the Flow CAM. Unfortunately, at the moment getting to know this system, and the resulting optimal settings of the instrument is so time-consuming, and so variable between sampling days, that we are a long way from using the Flow CAM as a (semi-)automatic measuring system for complete planktonic communities. Hopefully, new developments and methods will make this possible in future.

CHAPTER IV

Dietary induced responses in the phagotrophic flagellate *Oxyrrhis marina*

Florian Matthias Hantzsche & Maarten Boersma

ABSTRACT

Primary producers may be limited by different nutrients as well as by light availability, which in turn affects their quality as food for higher trophic levels. Typically, algae with high C:N and/or C:P- ratios are a low quality food for consumers. Heterotrophic protists are important grazers on these autotrophes, but despite their importance as grazers, knowledge of food quality effects on heterotrophic protists is sparse. In the present study we examined how differently grown *Rhodomonas salina* (nutrient replete, N-limited and P-limited) affected the phagotrophic flagellate *Oxyrrhis marina*. The functional response of *O. marina* (based on ingested biovolume) did not show significant differences between food sources, thus food uptake was independent of food quality. *O. marina* was weakly homeostatic which means that its C:N:P-ratio still reflected the elemental composition of its food to some extent. Food quality had a significantly negative effect on the numerical response of *O. marina*. Whereas nitrogen limited *R. salina* and nutrient replete *R. salina* resulted in similar growth rates, P-limited algae had a significantly negative effect on the specific growth rate of *O. marina*. Hence, the lack of elemental phosphorus of *O. marina* feeding on phosphorus limited algae caused a reduction in growth. Thus, despite their weaker homeostasis, heterotrophic protists are also affected by high C:P food in a similar way to crustacean zooplankton.

INTRODUCTION

Growth and production of all organisms is a function of resource uptake. Whereas primary producers are dependent on nutrients and light, heterotrophic organisms may be limited by carbon (energy), nutrients and essential biochemical elements. Indeed, for aquatic organisms several fatty acids, amino acids and sterols are essential for growth and reproduction (e.g. Ederington et al. 1995; von Elert 2002; Martin-Creuzburg and von Elert 2004). However, not only the biochemical composition of nutrition determines its quality as food for heterotrophic organisms, but also the amount, or more specifically the ratio, of several macronutrients, such as nitrogen and phosphorus. Especially in aquatic systems, ecological stoichiometry (Sterner and Elser 2002), the study of the ratios of different substances in organisms, has forwarded our knowledge on trophic transfer processes considerably. Typically, primary producers such as algae or higher plants show a large variation in C: N: P-ratios dependent on their growing conditions. In contrast, many secondary producers maintain some sort of homeostasis with respect to the elemental composition of their body, which means that they are often faced with food which is improperly balanced with respect to their own body tissue (Hessen et al. 2004).

A large body of literature exists, especially in freshwater environments, on the effect of different nutrient ratios on growth and reproduction of primary consumers both in the laboratory and in the field. For example the growth of *Daphnia* sp., the most important zooplankton in many freshwater lakes, may be limited by a high C:P- ratio of their food (DeMott et al. 2001; Hessen et al. 2002; Vrede et al. 2002) and surplus carbon may be partly released as CO₂ and/or as DOC (Plath and Boersma 2001; Darchambeau et al. 2003; Jensen and Hessen 2007). In marine food webs the main focus in food quality studies has been on the biochemical compounds of food (Jonasdottir 1994; Hazzard and Kleppel 2003; Tang and Taal 2005), and stoichiometric approaches are rare, even though there are several indications for potential stoichiometric imbalances between phyto- and zooplankton (Elser and Hassett 1994), with further consequences for higher trophic levels (Malzahn et al. 2007). In fact, for marine ecosystems only a few publications exist indicating how food quality in terms of its elemental composition affects secondary producers, such as calanoid copepods (Koski 1999; Augustin and Boersma 2006).

The stoichiometric studies on interactions between primary producers and their consumers in aquatic systems have focused almost exclusively on the algal-metazoan zooplankton (equals *Daphnia* in the majority of cases) interface, and other consumers have been virtually ignored, (but see Tarran 1991). Heterotrophic protists are, however, an important intermediary link between phytoplankton and mesozooplankton in pelagic food

webs. Furthermore, they compete with higher trophic levels for primary producers and simultaneously are consumed by a number of copepod species, some of which actually favour them over phytoplankton (Gismervik 2006).

As stated above, we know very little about the interface between algae and the smallest heterotrophes, in terms of food quality and stoichiometry. Based on some experimental data (Goldman et al. 1987; Nakano 1994) and a modelling study of Grover and Chrzanowski (2006) we would predict only weak homeostasis for heterotrophic protists, which could mean that they are not very strongly affected by different nutrient availabilities. Hence, in this study, we used the phagotrophic flagellate *Oxyrrhis marina* Dujardin and the cryptophyte *Rhodomonas salina* (Wislouch) Hill et Wetherbee as a model system. *O. marina* is an omnivorous cosmopolitan species, often found in rock pools (Johnson 2000). It is also described from the White Sea, the Western Baltic, the English Channel, the Mediterranean Sea and from Korean waters, where it can reach high abundances (Hansen et al. 1996; Jeong et al. 2003). *O. marina* ingests prey by engulfment and has been reported to feed on a wide range of particle sizes, from a completely soluble diet through bacteria, small algae to algae as large as *O. marina* itself. We set out to answer the following questions: 1). How dependent is the nutrient stoichiometry of *O. marina* on its prey. 2). What is the effect of nutrient-replete food vs. N- and P- depleted food on the ingestion and growth rate of the heterotrophic flagellate?

MATERIAL AND METHODS

Oxyrrhis marina was obtained from the Göttingen culture collection (Strain B21.89) and was reared semi-continuously in batch cultures in autoclaved f/2 medium (Guillard and Ryther 1962) without mixing at 20°C in dim light (18:6 light:dark cycle; 5 $\mu\text{mol m}^{-2} \text{s}^{-1}$). The food consisted of nutrient replete (f/2) batch cultures of the cryptophyte alga *Rhodomonas salina*, which were also grown at 20 °C, aerated gently, in high light conditions (185 $\mu\text{mol m}^{-2} \text{s}^{-1}$).

In the first experiment we fed *O. marina* nutrient replete (f/2), nitrogen limited (-N) and phosphorus limited (-P) *R. salina* to estimate the effect of food quality differences on the elemental composition of *O. marina* and its level of homeostasis. Next, we performed three separate functional response experiments to assess food quality dependent food uptake. These functional response experiments were carried out to assess the robustness of the results. The main difference between the experiments was the initial densities of the stock cultures of *O. marina* and their body volume. To investigate whether this difference could be responsible for the variability in the functional response, we performed an additional experiment with a range

of different stock culture conditions and one density of prey. Subsequently, we tested the population dynamical consequences of different food qualities for *O. marina*, with a numerical response experiment. In our last experiment we investigated one of the potential mechanisms explaining differences in numerical responses, by investigating the dependence of respiration rates of *O. marina* on the quality of the food.

Algal cultures and growth

The different *R. salina* cultures were grown for four days in 0.2 μm filtered seawater and kept in 5-L bottles under the same conditions as described above. One set of cultures was kept in full f/2 medium (treatment “f/2”) and the other two in f/2 medium without phosphorus (treatment “-P”) and with only 20% of normal nitrogen (treatment “-N”). This kind of treatment, which was checked in prior growth experiments, ensured algae growth and at the same time a limitation of the desired nutrient after four days. F/2- and N- depleted cultures were started with the same cell concentration (50,000 ind ml^{-1}), the P- limited culture had a higher start concentration (100,000 ind ml^{-1}) as algae grew slower under these conditions. After four days the nutrient depleted algal cultures showed signs of decreasing growth, whereas nutrient replete *R. salina* were still in the exponential growth phase (Augustin and Boersma 2006; Aberle and Malzahn 2007).

For each experiment *O. marina* and the three differently treated *R. salina* cultures were harvested and their cell concentrations were determined using a CASY particle counter (SCHÄRFE SYSTEMS, Reutlingen, Germany). All experiments were conducted in 500 ml glass bottles, which were filled with sterile artificial (P and N-free) sea water (Aqua Marin) with a final salinity of 32. Before the start of each experiment *O. marina* were left without food for 3 d to obtain a culture without prey. In preliminary experiments we could show that three days of starvation had no negative effect on the cell concentration of *O. marina*, only on its size (e.g. mean volume).

CN- and P- measurements in a simple feeding experiment

To evaluate the effect of nutrient replete, nitrogen and phosphorus depleted food on the stoichiometric composition of *O. marina* (start concentration 1,500 cells ml^{-1}), we fed them with f/2, -N and -P *R. salina* (start concentration 4×10^5 cells ml^{-1}) in ten replicates in dimmed light at 20°C to prevent further growth of prey. Each *R. salina* culture was filtered onto precombusted Whatman GF/C filters (estimated amount of 100 μg carbon) at the start of the experiment, and each *O. marina* culture after 4 d of growth. In this period all *R. salina* cultures were completely consumed by *O. marina* (*O. marina* was not starving), so that the

nutrient composition reflected only that of *Oxyrrhis marina* and not of its prey. The particulate carbon and nitrogen content of *R. salina* and *O. marina* were measured with a Europa 20/20 CN analyser (<http://stableisotopefacility.ucdavis.edu/>). Particulate phosphorus was analysed as orthophosphate after acidic oxidative hydrolysis with 5% H₂SO₄ (Grasshoff et al. 1999).

Functional response experiments

We used a concentration of *O. marina* in each bottle of 2,000 cells ml⁻¹ in combination with *R. salina* (f/2, -N and -P) densities in 16-20 concentrations between 2,000- 500,000 cells ml⁻¹ (~0.12- 30 µg C ml⁻¹) in three experimental runs. The experimental bottles were placed in a 20 °C water bath in dim light and only mixed at the start and the end of the experiment. In preliminary feeding experiments we could show that *O. marina* ingests prey very quickly and starts growing only ~9 h after receiving sufficient food. Therefore, the experimental duration of the functional response experiments was only one hour, thus preventing food exhaustion (max ~68% of offered food concentration was ingested) and growth of the predator. This allowed us to use simple calculations for ingestion, as we could avoid the corrections for changes in density of the predator (Skovgaard 1996). Ingestion was calculated as the number of prey items eaten per *O. marina* and hour (Frost 1972; Tarran 1991):

$$\text{Cell ingestion (cells h}^{-1} \text{ ind}^{-1}) = \frac{([\text{Prey}]_{t_1} - [\text{Prey}]_{t_0})}{[O. marina] * [t_1 - t_0]} \quad (1),$$

where [Prey]_t is the prey concentration at time t and [O. marina] is the *O. marina* concentration. This experiment was carried out three times to test the robustness of the different feeding responses. In order to compare the experiments, we used the Michaelis-Menten-equation:

$$V = \frac{V_{\max} * [\text{Prey}]}{K_M + [\text{Prey}]} \quad (2),$$

where V is the prey uptake per *O. marina* and per unit time [cells h⁻¹ ind⁻¹], V_{max} [maximum food cell ingestion] is the maximum observed rate and K_M [cells ml⁻¹] is a half-saturation constant equivalent to the prey concentration required to support ingestion equivalent to half the maximum rate. V_{max} and K_M were determined, and the standard error of these values was estimated during the iterative process with non-linear regression analysis using equation (2). These error estimates were used for testing the significance of food dependent ingestion rate

of *O. marina*, in pair wise Student's t- tests between algal treatments within each experiment. Ingestion was both calculated on a cell basis as well as on a biomass basis.

Effect of O. marina stock density on its feeding

To clarify the different results from the functional response for each experiment and algal treatment, a single feeding experiment with 13 different initial stock culture densities of *O. marina* was prepared in artificial seawater (2,000- 70,000 cells ml⁻¹) 24 h before the following feeding experiment with the same experimental conditions as described above. At the start of the experiment 2,000 *O. marina* ml⁻¹ (final concentration) from each different initial culture of *O. marina* were transferred to 100 ml experimental bottles, filled with artificial seawater and mixed with a f/2- *R. salina* culture (final concentration 100,000 cells ml⁻¹). The cell density of *R. salina* was measured after 1 h and after 2 h and the ingestion of *O. marina* was then plotted versus the original densities of the stock cultures of *O. marina*.

Effects on growth rate

We used the same experimental design as in the functional response experiments with the same *O. marina* start culture and the three different *R. salina* cultures and let it run for 48 h after a defined food pulse (10 food concentrations; 3,000- 500,000 cells ml⁻¹) in one single experimental run. The experimental bottles were mixed every 3 hours (except between 24:00 and 6:00) to prevent sedimentation and to guarantee proper predator-prey contact. The specific population growth rate μ (d⁻¹) of *O. marina* was calculated (Tarran 1991):

$$\mu \text{ (d}^{-1}\text{)} = \frac{\ln [O. marina]_{t_1} - \ln [O. marina]_{t_0}}{(t_1 - t_0)/24} \quad (3),$$

where $[O. marina]_{t_1}$ (h) is the concentration at the end of the experiment and $[O. marina]_{t_0}$ the concentration at the start. The numerical response was also fitted using a Michaelis-Menten-model (equation (2)), to estimate the effect of diet dependent growth rate of *O. marina* as described above.

Respiration rate experiment

We performed a respiration experiment to estimate the possible excretion of excess carbon indirectly as a function of O₂- consumption of ingested food particle by *O. marina* under different diet conditions. The experiment ran in dim light (5 μmol m⁻² s⁻¹), 20°C, in 4 replicates and 5 hours. The respiration rate was measured with a 4 channel microsensor oxygen meter (PreSens- Precision Sensing GmbH, Germany) using an oxygen microoptode, which was inserted through the lid into the middle of a 500 ml glass bottle. Each replicate bottle was filled with artificial seawater. Water blanks (~1% of total O₂ consumption), *O. marina* controls (14,000 cells ml⁻¹; in f/2 treatment ~34%, in -N ~13% and -P ~24% of total O₂ consumption), as well as algal controls were measured (f/2 ~4%, -N ~20%, -P ~21% of total O₂ consumption; for each treatment 280,000 cells ml⁻¹). For the actual measurements, *O. marina* were mixed with the three differently treated *R. salina* cultures with the same concentrations as described above (*O. marina* : *R. salina* = 1:20). After filling, the bottles were incubated for 15 min to adapt *O. marina* and *R. salina* to the experimental conditions. The oxygen content of each replicate was then measured and repeated after 1 h, 3 h and 5 h. The respiration rates per hour in each treatment were calculated by linear regression analysis. Simultaneously the food particle concentration was measured at the same time interval with a CASY particle counter to determine the concentration of *R. salina*. The ingestion rate of *R. salina* by *O. marina* was calculated by negative exponential regression analysis.

The food source- dependent respiration rate of *O. marina* per hour was determined after the respiration rate of the water blank and control *O. marina* was subtracted. Additionally, the respiration rates of the algae controls were used to calculate the respiration rate per algae cell and hour. Then, we used the mean algae concentration in the experimental set-ups to estimate the fraction of algal respiration in the *O. marina* + *R. salina* mixed treatments. After subtraction we obtained the food source dependent respiration rate of *O. marina* per hour and per ingested food particle.

RESULTS*C:N:P stoichiometry*

Rhodomonas salina grown under nitrogen limitation (-N) showed the highest molar C:N ratios and differed significantly from nutrient rich (f/2) and phosphorus limited (-P) algae; the C:N ratios were not significantly different between f/2 and P- limited algae (ANOVA, followed by Tukey-Post-hoc tests; Fig. 1 and Tab. 1). The highest molar C:P-ratios were detected in algae under phosphorus limitation and they differed significantly from f/2 and N- limited algae. The C:P- ratios of f/2 and N- limited algae did not differ. Similar to

the C:P- ratios we observed the highest N:P- ratios under P limitation, significantly different from the algae of the f/2 and -N treatment; N:P- differences between f/2 and N- limited algae were not significant (Fig. 1).

Oxyrrhis marina- Highest molar C:N ratios were detected in *O. marina* fed nitrogen limited algae. Nitrogen limited *O. marina* differed significantly from the f/2 and -P- treatments, the C:N ratios of the latter two did not differ significantly (ANOVA, followed by Tukey-Post-hoc tests; Table 1). Highest molar C:P ratios were observed in *O. marina* fed P- limited algae, differing significantly from *O. marina* under N-limitation or nutrient sufficient conditions; no significant differences between the latter could be detected. Similar to the molar C:P ratios, the molar N:P ratios were highest in *O. marina*, fed with *R. salina* under phosphorus limitation and they differed significantly from *O. marina*, fed with nutrient replete or nitrogen depleted algae. In all cases the carbon to nutrient ratios of *O. marina* showed less variation than the ratios of the algae they were feeding on (Fig. 1 and Tab. 1).

Table 1: Summary of analyses of variance (ANOVA). C:N, C:P and N:P of *R. salina* and *O. marina* were analysed each in a one- factorial ANOVA, using treatment (f/2, -N und - P) as the independent factor and C:N, C:P and N:P as the dependent variable.

Factor		MS	Df	F	p-value	
<i>Rhodomonas salina</i>	C:N	Treatment	77.523	2	20.5466	<0.001
		Error	3.773	27		
	C:P	Treatment	996,135	2	23.4164	<0.001
		Error	42,540	27		
	N:P	Treatment	17,739.71	2	28.4459	<0.001
		Error	623.63	27		
<i>Oxyrrhis marina</i>	C:N	Treatment	5.656	2	22.894	<0.001
		Error	0.247	27		
	C:P	Treatment	118,925	2	27.1799	<0.001
		Error	4,375	27		
	N:P	Treatment	2,425.98	2	29.4596	<0.001
		Error	82.35	27		

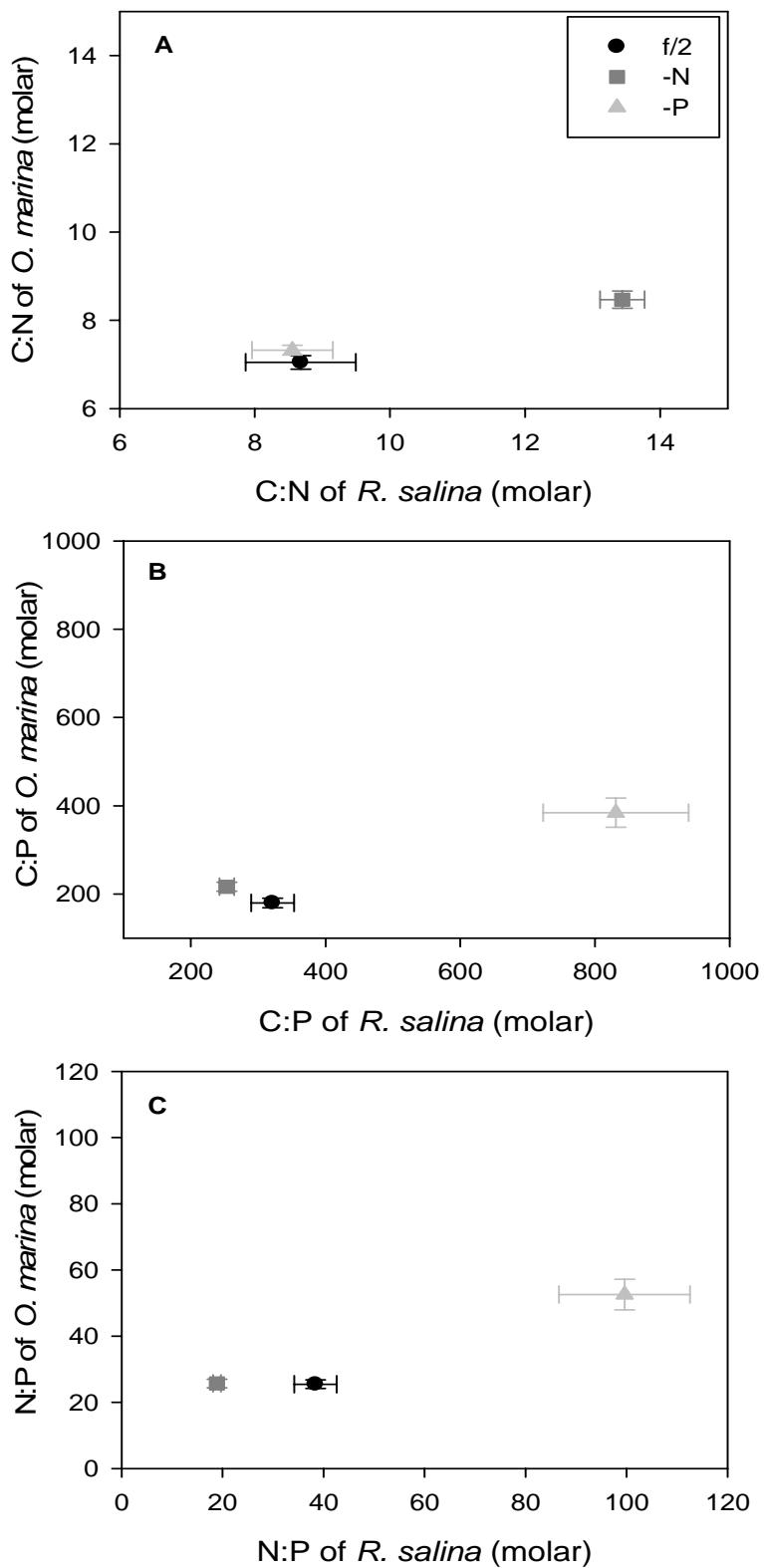


Figure 1: (A) Molar C:N, (B) C:P, and (C) N:P ratios of *R. salina* and *O. marina* under nutrient sufficient (f/2), N- limited (-N) and P- limited (-P) conditions. Error bars show the standard error of 10 measurements.

Functional and numerical response experiments

In the first functional response experiment the cell ingestion of *O. marina* ($R. salina$ h^{-1} $O. marina^{-1}$) fed f/2 *R. salina* and nitrogen limited *R. salina* showed very similar curves and maximum cell ingestions h^{-1} (V_{max}) were $\sim 17 R. salina$ h^{-1} in both treatments (Fig. 2 A). The maximum food uptake of *O. marina* when fed phosphorus limited *R. salina* was significantly lower ($\sim 9 R. salina$ h^{-1}) compared to f/2 and nitrogen limited *R. salina* fed by *O. marina* (Tab. 2). The calculated K_M - values from the Michaelis- Menten- model showed no significant differences between the three treatments. After correcting for the differences in size of the differently grown *R. salina* (Tab. 3), food uptake (in terms of biovolume) was not significantly different between the food sources (Fig. 2 B and Tab. 4).

Table 2: Summary of estimations of V_{max} and K_M - values from the Michaelis-Menten-Model (R^2 and p-value) in the functional and numerical response experiments with pair wise t-test (cell ingestion). Different letters (^a, ^b, ^c) indicate significant differences of V_{max} and K_M - values between the different algal treatments.

	experiment	treatment	V_{max}	s.e.	K_M	s.e.	R^2	p-value
functional response	1	f/2	16.85 ^a	1.127	36,896.54 ^a	7,915.328	0.91	<0.0001
		-N	16.81 ^a	1.45	38,040.77 ^a	10,865.41	0.84	<0.0001
		-P	9.45 ^b	1.076	15,615.38 ^a	7,403.072	0.61	<0.0001
	2	f/2	11.22 ^a	0.796	28,005.87 ^a	9,947.574	0.89	<0.0001
		-N	9.35 ^a	1.14	38,459.61 ^a	20,062.56	0.77	<0.0001
		-P	4.62 ^b	0.333	11,988.19 ^a	5,618.061	0.74	<0.0001
	3	f/2	9.36 ^a	1.67	94,937.93 ^a	32,005.85	0.93	<0.0001
		-N	5.2 ^b	0.59	51,074.39 ^a	13,970.03	0.92	<0.0001
		-P	6.09 ^{a,b}	0.54	32,426.15 ^a	8,449.286	0.91	<0.0001
numerical response	1	f/2	1.08 ^a	0.06	93,753.11 ^a	14,463.25	0.98	<0.0001
		-N	0.94 ^a	0.047	49,496.38 ^b	8,583.113	0.98	<0.0001
		-P	0.5 ^b	0.05	15,389.62 ^c	6,977.618	0.83	0.0002

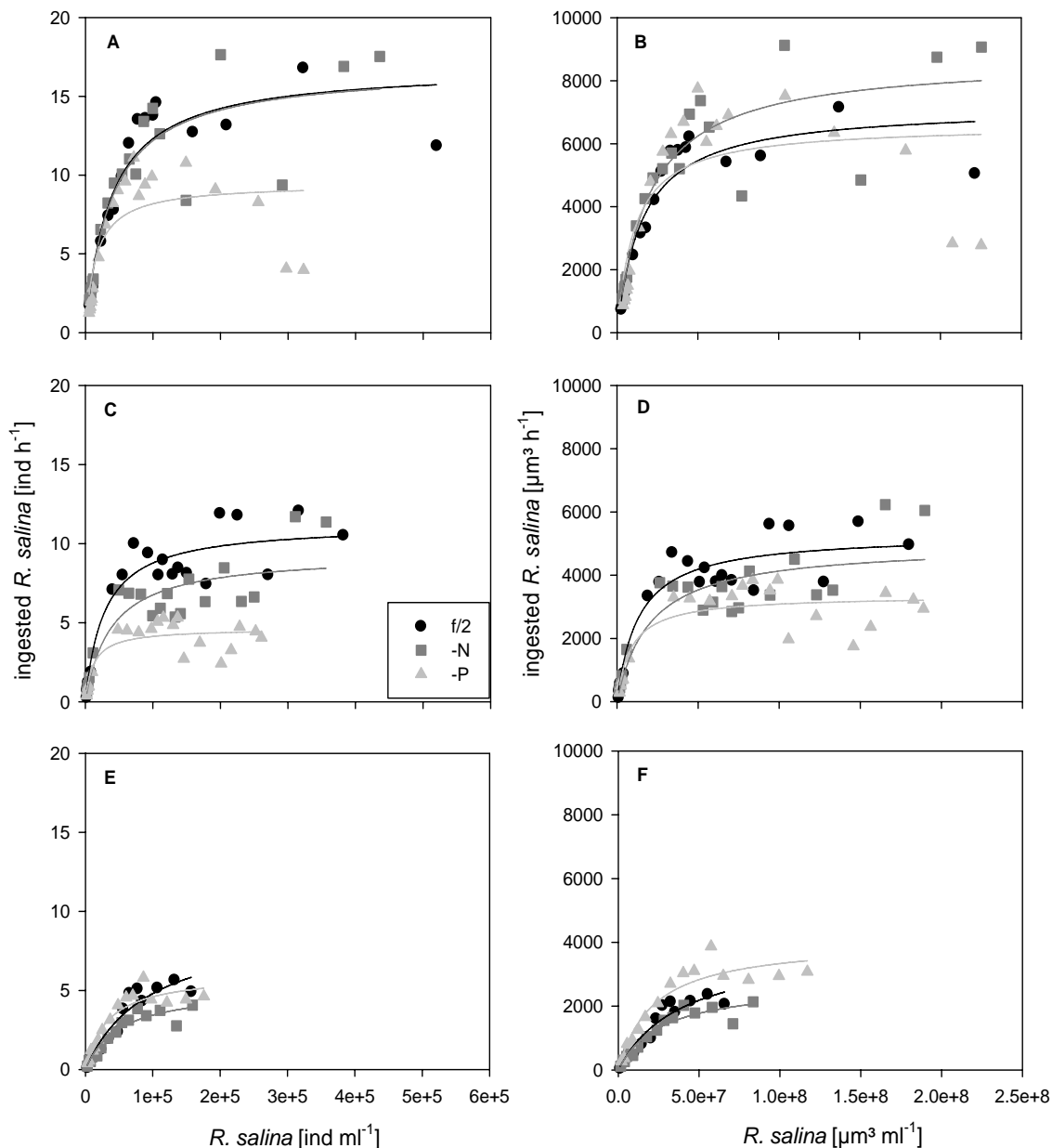


Figure 2: Ingestion rate h^{-1} of *O. marina* (in 3 functional response experiments) fed with sufficient (f/2), N- depleted (-N) and P- depleted (-P) *R. salina*. (A) cell ingestion in experiment 1 (B) cell volume ingestion in experiment 1 (C) cell ingestion in experiment 2 (D) cell volume ingestion in experiment 2 (E) cell ingestion in experiment 3 (F) cell volume ingestion in experiment 3.

The second functional response experiments (Fig. 2 C) showed less ingestion of prey in all three treatments compared to the results of the first experiment, even though the results were qualitatively similar. Highest ingestion of *O. marina* was again observed when fed nutrient replete ($V_{max} = \sim 11 R. salina h^{-1}$) and nitrogen depleted *R. salina* ($V_{max} = \sim 9 R. salina h^{-1}$). Phosphorus depleted *R. salina* ($V_{max} = \sim 5 R. salina h^{-1}$) were again ingested significantly less by *O. marina*. Again, we observed no significant differences between the calculated K_M -

values of the three algal treatments (Tab. 2). Based on the biovolume uptake these differences remained significant (Tab. 4 and Fig. 2 D).

The feeding results of the third functional response experiment (Fig. 2 E) showed the lowest cell ingestion of *O. marina* in all three experiments. Highest cell ingestion was observed again for *O. marina* fed nutrient replete algae ($V_{\max} = \sim 9 R. salina h^{-1}$) which differed significantly from *O. marina* fed nitrogen depleted *R. salina* ($V_{\max} = \sim 5 R. salina h^{-1}$) as well as fed phosphorus depleted *R. salina* ($V_{\max} = \sim 6 R. salina h^{-1}$). The calculated K_M -values were again not significantly different between algal treatments (Tab. 2). Based on biovolume, we observed no significant differences between the uptake of P-limited and nutrient replete cells, both were significantly higher than the maximum uptake of nitrogen limited cells (Tab. 4).

Table 3: Mean biovolume ($\mu m^3 cell^{-1}$) of used *R. salina* and *O. marina*, used in the functional response experiments.

	experiment	f/2 (std)	-N (std)	-P (std)
<i>R. salina</i>	1	426 (6)	517 (5)	698 (30)
	2	471 (5)	532 (4)	725 (10)
	3	418 (2)	525 (6)	666 (24)
<i>O. marina</i>	1	5,442 (86)	5,032 (79)	6,477 (25)
	2	6,370 (133)	6,006 (48)	5,711 (96)
	3	5,360 (131)	5,360 (131)	5,360 (131)

The three experiments showed that especially phosphorus limited *R. salina* were consumed less than the other algae, at least in two out of three experiments. After correction for the differences in biovolume, however, the differences in uptake became small, and the total biovolume taken up by the predators was similar for the different quality algae. However, the absolute differences in uptake rates between experiments were large. The main difference between the experiments was the pre- experimental stock culture density of *O. marina* with corresponding differences in size (Tab. 3). We correlated the calculated V_{\max} and K_M values of each functional response experiment with the pre- experimental densities of *O. marina*, *i.e.* those densities before the start of the experiment; experimental densities were all the same at $2,000 ind. ml^{-1}$. With increasing original population size of *O. marina* the maximum cell ingestion decreased (Fig. 3 A, B), the K_M values however remained relatively constant (Fig. 3 C, D). In the gradient of different initial densities of *O. marina* (2,000- 70,000 cells ml^{-1}), from which 2,000 cells ml^{-1} final concentration was used the next day for the

feeding experiment with nutrient replete *R. salina* (f/2) (100,000 cells ml⁻¹), we observed a significantly negative correlation between stock population density and cell ingestion after 1 h food incubation (Fig. 4).

Table 4: Summary of estimations of V_{\max} and K_M - values from the Michaelis-Menten-Model in the functional and numerical response experiments with pair wise t-test (biovolume ingestion). Different letters (^a, ^b) indicate significant differences of V_{\max} and K_M - values between the different algal treatments.

	Experiment	treatment	V_{\max}	s.e.	K_M	s.e.
functional response	1	f/2	7,176 ^a	480	15,714,074 ^a	3,370,184
		-N	8,698 ^a	748	19,679,841 ^a	5,620,582
		-P	6,597 ^a	751	10,902,590 ^a	5,161,259
	2	f/2	5,289 ^a	375	13,200,882 ^a	4,689,400
		-N	4,975 ^a	605	20,468,392 ^a	10,677,632
		-P	3,351 ^b	242	8,685,626 ^a	4,074,375
	3	f/2	3,917 ^a	700	39,716,390 ^a	13,394,557
		-N	2,727 ^b	312	26,800,958 ^a	7,329,525
		-P	4,055 ^a	359	21,583,377 ^a	5,621,803

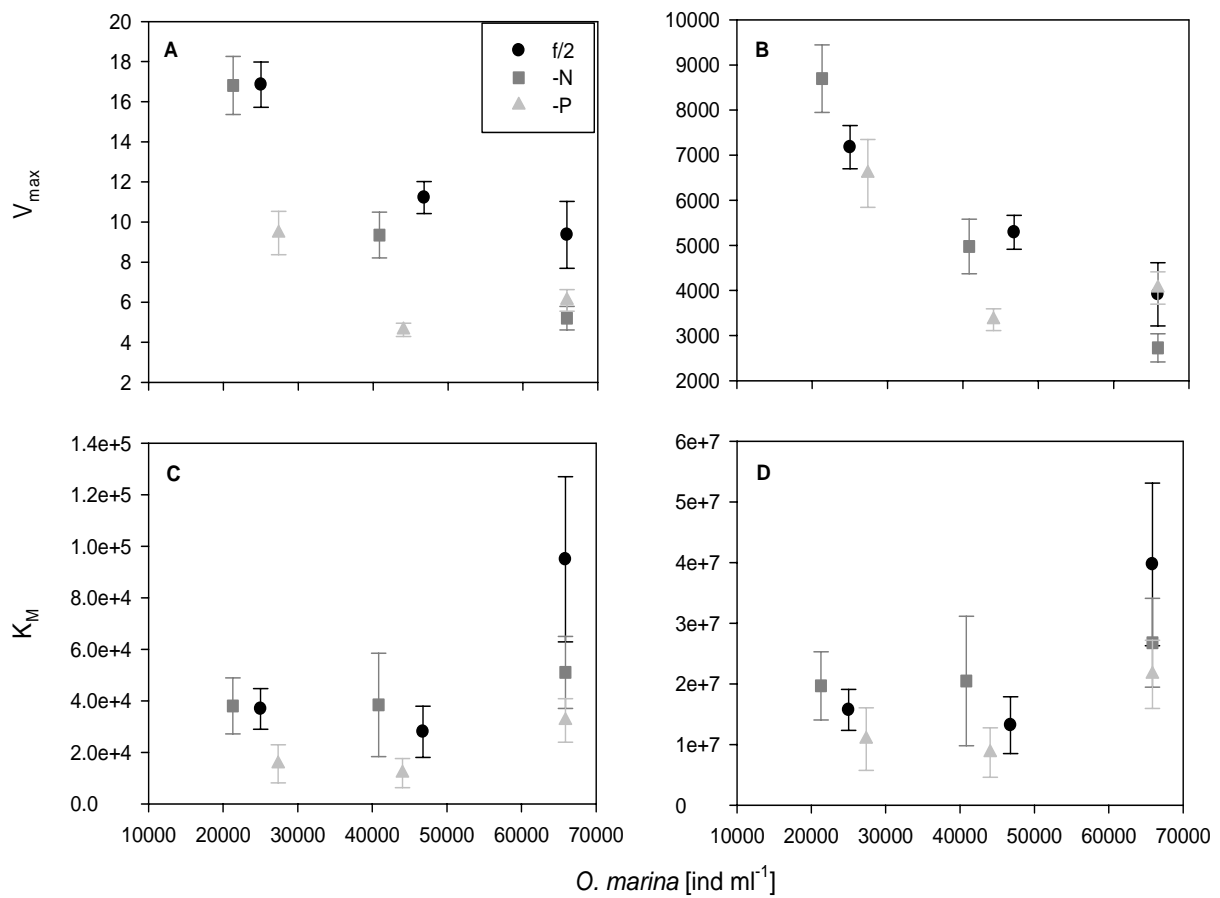


Figure 3: V_{\max} (ingested *R. salina* h^{-1} *O. marina* $^{-1}$) and K_M - values (*R. salina* ml^{-1}) of the used Michaelis-Menten-equation from functional response experiments vs. stock culture start concentrations of *O. marina*. (A+C) V_{\max} and K_M derived from cell ingestion (B+D) V_{\max} and K_M derived from cell volume ingestion. Error bars show the standard error.

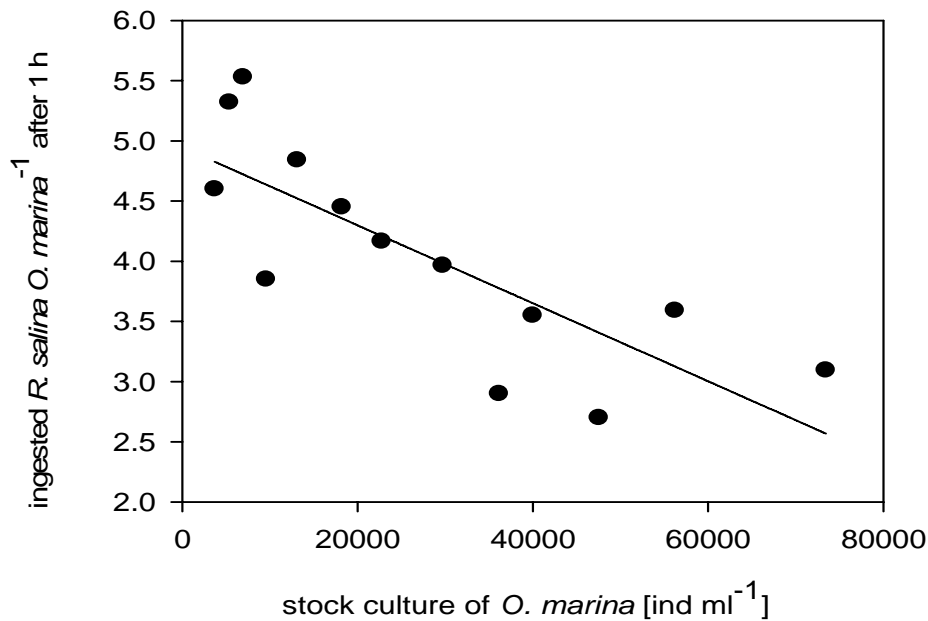


Figure 4: Stock culture dependent ingestion rate of *O. marina* fed with f/2 *R. salina*: $f(x) = y_0 + aXx$; $y_0 = 4.9466$ (s.e. = 0.2610); $a = -3.2394 \times 10^{-5}$ (s.e. = 7.484×10^{-6}) after 1 h food incubation ($R^2 = 0.63$; $p = 0.0012$).

We observed significant differences in the numerical response experiment with *O. marina* (Fig. 5). Similar to its functional response, the growth rate was fitted using a Michaelis-Menten model. μ_{\max} was highest in the f/2 treatment ($\mu_{\max} = 1.08 \text{ d}^{-1}$) and did not differ significantly from the N limited treatment ($\mu_{\max} = 0.94 \text{ d}^{-1}$), both were significant higher than in the P limited treatment ($\mu_{\max} = 0.5 \text{ d}^{-1}$). The K_M values between the three different algal treatments were significantly different ($K_M = \sim 94,000 \text{ R. salina ml}^{-1}$ (f/2); $K_M = \sim 50,000 \text{ R. salina ml}^{-1}$ (-N); $K_M = \sim 15,000 \text{ R. salina ml}^{-1}$ (-P)) (Tab. 2). At lower food concentrations ($< \sim 15,000 \text{ R. salina ml}^{-1}$) the growth rates of *O. marina* were similar in all treatments, only at food concentration above this food concentration threshold, food quality played a role.

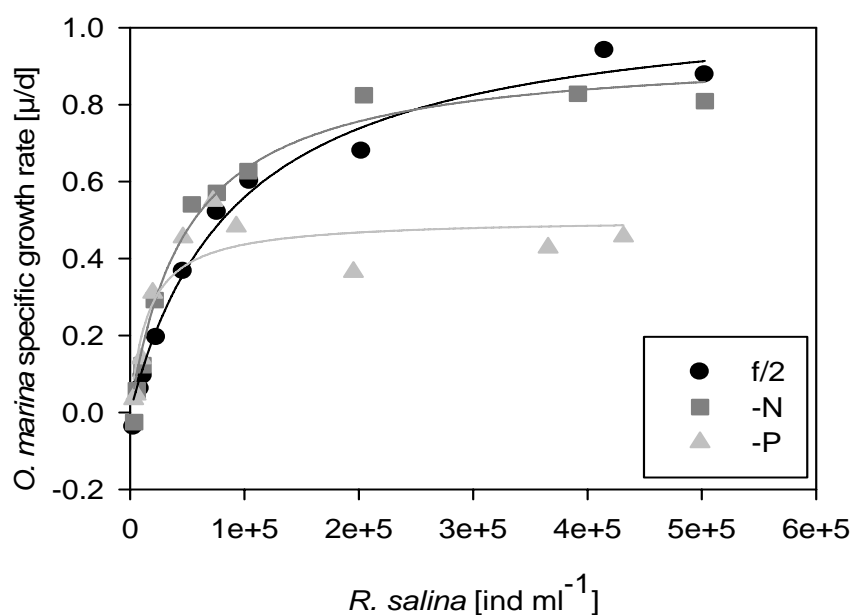


Figure 5: Specific growth rate d^{-1} of *O. marina* fed with sufficient (f/2), N- depleted (-N) and P- depleted (-P) *R. salina*.

Respiration rate experiment

We observed significant differences in the respiration rates of *O. marina* fed nutrient replete food (f/2) and the N- limited and P- limited *R. salina* treatments, whereas differences in respiration rate between N- and P- limited treatments were not significant (Tab. 5, Fig. 6). *O. marina* respired $\sim 5.98 \text{ pg O}_2 \text{ h}^{-1} \text{ ind}^{-1} \text{ prey}^{-1}$ when fed nutrient replete prey, $\sim 16.14 \text{ pg O}_2 \text{ h}^{-1} \text{ ind}^{-1} \text{ prey}^{-1}$ feeding on N-limited *R. salina* and $\sim 15.35 \text{ pg O}_2 \text{ h}^{-1} \text{ ind}^{-1} \text{ prey}^{-1}$ on P- limited algae. Higher respiration rates of *O. marina* when fed high C: nutrient food is a cell physiological consequence of carbon excretion.

Table 5: Respiration rates of *O. marina* were analysed in a one- factorial ANOVA, using treatment (f/2, -N und -P) as the independent factor and the respiration rates as the dependent variable.

	MS	Df	F	p-value
Treatment	127.604	2	11.6407	<0.01
Error	10.962	9		

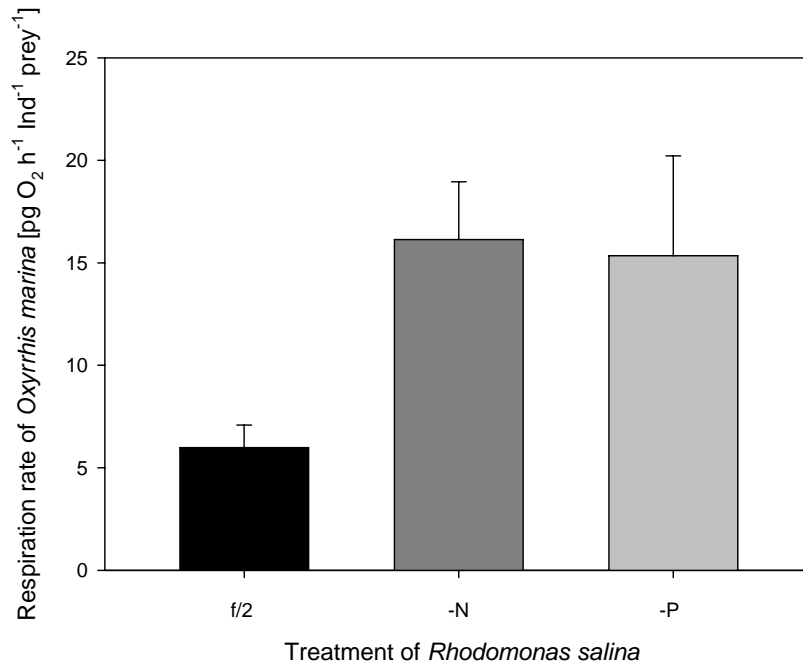


Figure 6: Respiration rate of *O. marina* h^{-1} per ingested *R. salina* in treatment f/2, -N and -P. Error bars show the standard deviation.

DISCUSSION

In this paper we have shown that important aspects of the life history of *O. marina* are affected by the quality of the food. *R. salina* with different stoichiometric composition (C:N:P) affected reproduction of *O. marina*. Especially phosphorus depleted algae seem to be a food source of low quality, whereas growth of *O. marina* was less affected by N-limited *R. salina* compared to nutrient replete algae (f/2). These results emphasize that phosphorus supply and a balanced C:P ratio are important also for phagotrophic flagellates like *O. marina*. Additionally, *O. marina* reacted to ‘adverse’ food conditions (N- and P-limited food) with higher respiration rates compared to nutrient replete food, thus a percentage of the total energy intake was excreted. Secondly, we could show that at low food concentrations food quality plays a less important role, and especially when algal concentrations were lower than $15,000 \text{ cells ml}^{-1}$ food quality did not seem to matter, suggesting that at these lower quantities the carbon (energy) content of the food is more important (Sterner and Robinson 1994; Boersma and Kreutzer 2002). Third, we observed that the initial conditions influenced the outcome of experiments quantitatively. Maximal uptake is lower when animals were kept under crowding conditions, which until now has only been described with the cladoceran *Daphnia* as “crowding effect” (Helgen 1987; Burns 1995; Burns 2000).

Various workers have already used *O. marina* as a model organism for grazing and growth experiments with different food algae (Tillmann and Reckermann 2002; Jeong et al. 2003; Kimmance et al. 2006), for food selection experiments either with different food algae

or artificial inert particles (Tarran 1991; Flynn et al. 1996; Hammer et al. 2001) and for physiological studies in terms of food digestion and release of in- and organic compounds (Klein et al. 1986; Barlow et al. 1988; Flynn and Davidson 1993). Although in some of these investigations nitrogen depleted food was considered to influence food uptake and growth of *O. marina*, to our knowledge no investigations exist on the effects of phosphorus depletion on *O. marina*. This might be a result of the widespread presumption that P-limitation is not of importance in marine environments (Howarth 1988), but is strange in the light of the P-growth rate hypothesis where animals that have high growth rates also have high requirements for phosphorus (Elser 2002). Moreover, there is considerable evidence that phosphorus can be a limiting nutrient especially in oligotrophic marine surface waters and coastal seas (Clark et al. 1998) and both nitrogen and phosphorus limitation may cause the decay of phytoplankton blooms.

Ingestion and growth rate of *Oxyrrhis marina* were fitted using a Michaelis- Menten equation, typical for heterotrophic protists with engulfment food uptake modus (Verity 1985; Verity 1991). Several authors already published ingestion and growth rates of *O. marina* fed different species of food algae (e.g. Goldman et al. 1989; Hansen et al. 1996; Jeong et al. 2007) as well as the effects of changes in temperature or pH on these rates (Pedersen and Hansen 2003; Kimmance et al. 2006), but to date almost no studies exist on the effects of nutrient depletion. Here, we showed that differently grown *R. salina* had strong effects in terms of ingestion of *O. marina* on a per cell basis which could be explained with cell volume differences of the different algae. Thus, food uptake in terms of biomass was largely quality independent. Differently grown *R. salina* however had a strong effect on the growth rate of the phagotrophic predator. Clearly, growth was lowest on P-limited algae, whereas the difference between those *O. marina* feeding on N- limited algae and nutrient replete ones was not significant. These differences in growth cannot be attributed to differences in uptake, but are most likely caused by the imbalances of the macronutrients in the food. From their modelling exercise Grover and Chrzanowski (2006) predicted a weak homeostasis in heterotrophic protists, which indeed was verified in our C:N:P measurements. Nutrient limitation signals from the autotrophic alga *R. salina* were transferred to *O. marina*, but in an alleviated form.

We did not measure the gross growth efficiencies of *O. marina*, nor is there much known in the literature. However, based on the studies of Selph et al. (2003), Uitto (1997) and Gonzalez (1993) we assume a gross growth efficiency for carbon of around 35%, and for nitrogen of around 50% (Davidson et al. 2005). Obviously, these both change under different

feeding conditions, but they might be an approximation of the non-stoichiometric excretion processes as defined by Anderson et al (2005). For P we assume a maximum growth efficiency of 70% (Anderson et al. 2005). If we then estimate (Fig. 1 A- C) that the optimal C:N:P ratio for *O. marina* is around 175:25:1, this would mean that the optimal food, given the different efficiencies, has a C:N:P ratio of around 350:35:1, which should result in as little stoichiometrically excreted material as possible, and the highest growth rates. It is clear, that the C:N:P stoichiometry of P-limited algae is not even close to this optimal food ratio, which explains the slow growth on this food source. At the same time, this optimal food ratio is intermediate between those of the nutrient replete and the N-limited algae. This could explain why growth on nutrient replete and nitrogen depleted *R. salina* was not significantly different, and would imply that *O. marina* growing on N-limited algae would have to excrete excess carbon to some extent, and those growing on nutrient replete algae would have to excrete some excess nitrogen. We did not measure N excretion, but several authors have indeed demonstrated that *O. marina* excrete inorganic compounds like NH_4^+ when fed with high-N prey (Davidson et al. 2005). Carbon excretion was measured using oxygen uptake as a proxy. We indeed observed higher respiration rates in the heterotrophic flagellate fed nutrient limited algae, which was to be expected based on the stoichiometric considerations, and found by several others (Darchambeau et al. 2003; Jensen and Hessen 2007). Of course, *O. marina* may have other alternative possibilities to egest excess carbon and nitrogen, through free amino acids (Opik and Flynn 1989) and carbohydrates excretion (Strom et al. 1997) or as dissolved organic carbon. Little is known about the excretion of excess phosphorus, but phosphonates and P- esters (DOP) (Kolowitz et al. 2001) should be taken in account, although in our study we would have not expected *O. marina* to excrete any excess phosphorus. We expect that if we had had another treatment with *R. salina* with only a gentle N limitation, these would have been the best food source for *Oxyrrhis marina*.

Our results indicate that the stoichiometry of the food is of vital importance not only for the growth of protist populations, but also for the fate of carbon and energy that entered the system through primary production. In systems with low nutrient inputs, we expect high amounts of the available carbon to dissipate directly as CO_2 , even if heterotrophic protists and not higher organisms are the primary consumers.

CHAPTER V

No food selection, but compensatory feeding in the phagotrophic flagellate *Oxyrrhis marina*

Florian M. Hantzsche, Cedric Meunier, Julia Haafke, Arne M. Malzahn & Maarten Boersma

ABSTRACT

The phagotrophic flagellate *Oxyrrhis marina* shows only weak homeostasis when fed food sources with different nutrient concentrations. Hence, we tested whether *O. marina* displayed selective feeding behaviour in mixtures of nitrogen and phosphorus depleted *Rhodomonas salina*. This was not the case; *O. marina* reacted however with different ingestion rates. When *O. marina* was fed nitrogen or phosphorus depleted *R. salina* and re-fed with one of these food treatments, the phagotrophic flagellate displayed compensatory feeding; feeding more on the source they were not given before, which means that *O. marina* recognizes the nutritional status both in its own cells and its prey. Thus, *O. marina* might handle bad quality food via post-ingestion selection rather than pre-ingestion selection.

Keywords: food quality, stoichiometry, compensatory feeding, food selection, *Oxyrrhis marina*, Flow CAM

INTRODUCTION

Studies on food selectivity between interacting trophic levels, such as selective grazing behaviour of a predator for or against a specific prey, have contributed substantially to our understanding of food webs. Not only higher trophic levels, but also heterotrophic organisms such as phagotrophic protists are often faced with a huge variety of potential food items with different qualities. Therefore, it is not surprising that selective feeding behaviour of heterotrophic flagellates and ciliates has been widely documented. Prey size (Andersson et al. 1986; Chrzanowski and Simek 1990) and prey motility (Gonzalez et al. 1993) are some of the factors which may affect a predator's choice. Food quality, however, is not only determined by the physical properties of the prey, but also by its elemental and biochemical composition. Lee (1980) defined food quality as the nutritional value of the food relative to the energetic and molecular needs of the consumer. The framework of ecological stoichiometry by Sterner and Elser (2002) developed this definition further and defines food quality in elemental ratios (mostly in terms of C:N:P). Optimal food quality is defined as the food composition matching the consumer's elemental ratios most closely, thus resulting in the lowest amounts of excreted products. Flexible stoichiometry of the consumer as well as luxury consumption can make it difficult to determine these optimal ratios. Ultimately, the quality of certain food sources for a consumer can only be measured in terms of growth rates and reproductive success of the consumer.

To feed selectively distinct physiological mechanisms are needed to identify suitable prey (physical and/or chemical cues emitted by the prey) in an accessible area (Verity 1991), or the ability by the predator to follow the (biochemical) trail of these potential food sources (Fenchel and Blackburn 1999). Depending on their nutritional status or growth stage algae excrete certain substances (Wetz and Wheeler 2007), which are composed of different biochemical compounds such as carbohydrates and amino acids (Granum et al. 2002). Some of those compounds may serve as attractors, while others might be inhibitors for herbivores (Davidson et al. 2005; Martel 2006). Our knowledge about chemosensory-receptors in marine protists which allow these organisms to detect areas of elevated prey densities is poor (Buskey and Stoecker 1988; Verity 1988; Fenchel and Blackburn 1999). The biochemical mechanism responsible for the ingestion or rejection of food particles, however, has been identified recently. Roberts et al. (2006) and Wootton et al. (2007) found a variety of lectins, which are highly specific carbohydrate-binding proteins, along the cell surface of the phagotrophic protist *O. marina*. These glycoconjugate-binding lectins are responsible for coupling with

species specific glycoconjugates of the prey and thus initiate phagocytosis of the prey (Martel 2009).

In the studies cited above the main focus was on differences between prey species, not differences within species. However, it is suspected that the nutritional status (e.g. nutrient replete or nutrient stressed) of algal cells modifies their structural or species-specific glycoconjugates on the cell surface. Therefore the phagotrophic protist may be able to “taste” the prey cells’ nutritional status during cell-to-cell contact via the detection of these glycoconjugates (Martel 2006; Martel 2009). In feeding experiments with *Oxyrrhis marina*, Martel (2009) showed a discrimination against nitrogen depleted cells of the alga *Isochrysis galbana* compared to nitrogen replete *I. galbana*, but the mechanisms in this interaction remain unclear.

Further studies in this field need to be done to clarify this capability of food selection in heterotrophs in general. Whereas, for example, crustacean mesozooplankton has been described to switch to food with a more favourable stoichiometric (Cowles et al. 1988) or biochemical composition such as fatty acid content (e.g. Vargas et al. 2006) there is a lack of such information where heterotrophic protists are concerned. While some information exists on the ability of predators to discern the biochemical food quality of their prey, we have almost no data on whether the predators are also capable of distinguishing the food quality in terms of elemental composition. Furthermore it is unclear if predators are able to balance elemental deficiencies through compensatory feeding. This is surprising since we know that fast growing organisms such as heterotrophic protists need phosphorus rich diets for RNA synthesis in order to maintain their rapid growth. Therefore, it is necessary to focus not only on the capability of a predator to select between food species. Studies focussing on how food with different nutritional status affects the nutrition of the predator and consequently how predators use their selection behaviour to improve their elemental balance are needed. It is therefore important to understand whether heterotrophic protists are able to recognize a shortage of a certain element in their own cells and consequently adjust their feeding behaviour accordingly. This could be achieved by discriminating against such low quality food (high C:nutrient) when better food (low C:nutrient) is available. Two mechanisms might allow heterotrophs to achieve a balanced nutrition even when food quality is suboptimal (Mittra and Flynn 2005). The first is a decrease of ingestion rate on unfavourable food to use more time for extracting the limiting element efficiently. Alternatively, food uptake of sub-optimal food might be higher, extracting only the easily available parts of the limiting nutrient, thus allowing for a high throughput with a short gut passage time (White 1993).

Since the nutritional state of one single alga species is very difficult to discern in microscopic surveys, we used the Flow CAM in the fluorescence triggered image mode (Sieracki et al. 1998). In previous studies Hantzsche et al. (in prep.) showed that the Flow CAM was capable of discriminating between nitrogen depleted and nutrient replete *Rhodomonas salina* due to differences in several traits. Fluorescent properties, for example, varied between algae from the nutrient defined cultures.

In the following study we used the phagotroph *Oxyrrhis marina* as consumer and the phototroph *Rhodomonas salina* as algal prey. In previous functional response experiments Hantzsche and Boersma (2010) fed starved *O. marina* with nutrient replete, nitrogen depleted and phosphorus depleted *R. salina* cultures. The authors observed that food uptake was independent of food quality in terms of biovolume. Furthermore, only phosphorus depleted *R. salina* had a significantly negative effect on the growth rate of *O. marina* compared to nitrogen depleted and nutrient replete *R. salina*, confirming that phosphorus is an important element for fast growing consumers (Boersma and Kreutzer 2002; Frost et al. 2006).

We hypothesize that food selectivity is dependent on the nutritional pre-condition of *O. marina*, as well as the nutrient status of the prey. Hence we pre-fed *O. marina* with *R. salina* cultures of varying nutrient composition. Then, we offered each pre-conditioned *O. marina* culture a mixture of 50% nitrogen-depleted and 50% of phosphorus-depleted *R. salina* and investigated feeding selectivity.

In a second experiment we investigated the capability of nitrogen- and phosphorus-stressed *O. marina* to compensate for the deficiency of the respective element through changes in food uptake. This was tested by re-feeding each of the two nutrient-stressed *O. marina* cultures with *R. salina* of different nutrient composition. Here, we hypothesize that nutrient-limited organisms should take up the limiting nutrient in greater amounts.

MATERIAL AND METHODS

Experimental cultures

Oxyrrhis marina Dujardin was obtained from the Göttingen culture collection (Strain B21.89) and maintained on exponential-phase *Rhodomonas salina* (Wislouch) Hill et Wetherbee as food. *R. salina* was reared in gently aerated batch cultures at 20°C in an 18:6h light : dark cycle ($185 \mu\text{mol m}^{-2} \text{s}^{-1}$) using sterile filtered f/2 medium (Guillard and Ryther 1962).

Three *Rhodomonas salina* cultures were grown for four days in 0.2 μm filtered seawater in 1L bottles under the conditions described above. One set of cultures was kept in

full f/2 medium (treatment “Rho f/2”) and the other two in f/2 medium without phosphorus (treatment “Rho-P”) and with only 20% of normal nitrogen addition (treatment “Rho-N”). Rho f/2 cultures were started with 25,000 cells ml⁻¹, Rho-N cultures with 200,000 cells ml⁻¹ and Rho-P cultures with 300,000 cells ml⁻¹. This treatment ensured that Rho f/2 was still in the exponential growth phase after four days of growth whereas Rho-N and Rho-P were in the stationary phase at which a significant limitation of the desired nutrient was obtained (see also Hantzsche and Boersma 2010).

O. marina's preconditions

Cell number and mean biovolume of *O. marina* and *R. salina* cultures were determined using a CASY particle counter (SCHÄRFE SYSTEMS, Reutlingen, Germany). To establish different pre-conditioning regimes the original *O. marina* (Oxy) culture was split into four cultures. Each preconditioned culture was then re-fed with nutrient replete (“Oxy f/2”), nitrogen depleted (“Oxy-N”) and phosphorus depleted *R. salina* (“Oxy-P”) for 2.5 days in 12 h intervals. The fourth culture of *O. marina* remained starved (treatment “Oxy-starved”). All Oxy cultures were kept without mixing by aeration at 20°C in dim light (18:6 light : dark cycle; 5 μmol m⁻² s⁻¹).

Since there is no means to separate *O. marina* from *R. salina*, we had to ensure that all *R. salina* in the preconditioned *O. marina* cultures had been eaten before the “selection or compensation experiment” began. In pre-experiments we found that *O. marina* feeds ~6 *R. salina* cells h⁻¹. The amount of food required to ensure that all algae were eaten in 2.5 days without inducing severe starvation effects in *O. marina* was calculated based on these numbers. Due to significant cell density differences between the three different *R. salina* cultures, resulting in different volumes of algal suspension added to the different *O. marina* treatments, the differences in water volume (ml) between the cultures were compensated through addition of artificial, sterile and nutrient free seawater (Aqua Marin). Each *R. salina* and preconditioned *O. marina* culture was filtered onto pre-combusted Whatman GF/F filters at the start of the experiment. The particulate carbon and nitrogen content of *R. salina* and *O. marina* were measured with a Vario Micro Cube/CN- analyser (Elementar). Particulate phosphorus was analysed as orthophosphate after acidic oxidative hydrolysis with 5% H₂SO₄ (Grasshoff et al. 1999).

Selection experiments with Rho-N and Rho-P

At the start of the experiment, nitrogen- and phosphorus-depleted *R. salina* were centrifuged (2,000 rpm; 5 min), the supernatant was discarded and the pellet re-suspended in artificial (N- and P-free) seawater. This procedure was repeated twice to ensure that nutrient limited algae remained nutrient stressed. After cell density determination, a mixture of 50% nitrogen depleted and 50% phosphorus depleted *R. salina* was prepared in 100 ml plastic beakers (four replicates) and diluted with artificial seawater to final cell concentration of 50,000 cells ml⁻¹. We used a high cell density (prey : predator = 25 : 1) because we expected that, if *O. marina* feeds selectively, this effect would be strengthened at high food concentrations. Furthermore we wanted to ensure that feeding rates higher than the expected six cells *O. marina*⁻¹ h⁻¹ did not lead to a quantity effect due to low food availability. Prior to the addition of *O. marina* we used 0.2 ml of this algae mixture and diluted it (10 ml end volume) with artificial seawater to 1,000 cells ml⁻¹ for the start measurement with the Flow CAM. In earlier method studies Hantzsche et al. (in prep.) found that the Flow CAM in the fluorescence triggered image modus was able to differentiate between Rho-N and Rho-P and produced reliable data at this cell concentration within a short time (~10 min for 400 pictures measurement⁻¹), using the 100 µm flow cell and the 20X objective (pump rate 0.47 ml min⁻¹; camgain 700; fluorescent gain 4; fluorescent threshold 1).

Directly after the first Flow CAM measurement (start), all four preconditioned *O. marina* cultures were transferred into each prepared food treatment (2,000 cells ml⁻¹ final concentration) and the selection experiment was run for 1 h. Total densities after one hour were measured with the particle counter. After dilution to approximately 1,000 cells ml⁻¹ we performed a second Flow CAM measurement as described above (end measurement). To define and to identify both nutrient defined *R. salina* treatments (Rho-N and Rho-P) in the 50:50 mix treatments we took 400 pictures of each individual culture and performed a discriminant analysis (Statistica 7.1) using all Flow CAM parameters (20 parameters). After determination of the significant variables in the discriminant analysis, the factor loadings were used to establish the classification function for both N- depleted and P-depleted *R. salina*. Selectivity could then be measured as the deviation of the start distribution of Rho-N and Rho-P from the final distribution, using a two-way-ANOVA. The two independent factors were the pre-conditions of *O. marina* (Oxy f/2, Oxy-N, Oxy-P and Oxy starved) and the time (start and end of the experiment). The dependent variables were the percentage of Rho-N and Rho-P found in the discriminant analysis, described above.

Food compensation experiment

In the second experiment we prepared preconditioned Oxy-N and Oxy-P as described above (2,000 cells ml⁻¹) and re-fed them either with Rho-N or with Rho-P in four different cell concentrations (7,500; 15,000; 25,000 and 50,000 cells ml⁻¹) in five replicates for 1 h. Cell ingestion rates were analysed for the two preconditioned *O. marina* with respect to offered food source and food concentration (3-way ANOVA; factor A= precondition of *O. marina* (Oxy-N, Oxy-P), factor B= food treatment (Rho-N, Rho-P), factor C= offered cell density of *R. salina* [cells ml⁻¹]. Cell ingestion [*R. salina O. marina*⁻¹ h⁻¹] was the dependent variable).

RESULTS*Selection experiment with the Flow CAM*

We were able to discriminate between nitrogen (Rho-N) and phosphorus depleted *R. salina* (Rho-P) and found that they were significantly different in five of twenty Flow CAM parameters (Tab. 1). Best discriminating factors were the fluorescence signal in channel 2 for phycoerythrin, followed by the fluorescence signal in channel 1 for chlorophyll a, since Rho-P tended to have a higher fluorescence in both channels than Rho-N. Further parameters were the cell length and cell width of *R. salina*, which were greater under phosphorus limitation than under nitrogen limitation. Lastly the cell transparency of nitrogen depleted *R. salina* was higher than the one of phosphorus depleted *R. salina*. We used these five parameters for the classification equation (Tab. 2) and were able to correctly classify ~79% of Rho-N and ~96% of Rho-P (Tab. 3) in the single cell treatments.

Table 1: Summary of discriminant analysis between nitrogen (Rho-N) and phosphorus (Rho-P) depleted *R. salina* (n=609) in the selection experiment. Five of twenty potential Flow CAM parameters contributed significantly to discriminate between Rho-N and Rho-P (ch 2 peak, ch 1 peak, length, width and transparency) and used in the classification model.

Variable/ parameter	Wilks'Lambda	Part.Lambda	F	p-value	Tolerance	R ²
Ch 2 Peak	0.751440	0.575340	445.0758	<0.0001	0.285354	0.71
Ch 1 Peak	0.500946	0.863035	95.6974	<0.0001	0.289264	0.71
Length	0.438803	0.985256	9.0239	0.0028	0.337594	0.66
Width	0.436972	0.989385	6.4695	0.0112	0.171290	0.83
Transparency	0.436137	0.991278	5.3055	0.0216	0.342808	0.66

Table 2: Summary of the five parameters which defined the classification equation ($f(x) = \text{constant} + ax + bx + cx + dx + ex$) for each algal treatment (Rho-N and Rho-P) in the selection experiment.

Parameter	Rho-N (p=0.44663)	Rho-P (p=0.55337)
A=Ch 2 Peak	-0.0075	-0.0035
B=Ch 1 Peak	0.0168	0.0134
C=Length	1.8998	2.2401
D=Width	6.2197	5.8125
E=Transparency	211.1850	202.9028
Constant	-70.3832	-68.2366

Table 3: Classification matrix: Percentage and number of cases where the classification model estimates the correct contribution to one of both groups (Rho-N or Rho-P).

Group	Percent correct	Rho-N	Rho-P
Rho-N	78.67647	214	58
Rho-P	95.84570	14	323
Total	88.17734	228	381

The stoichiometry of the preconditioned *O. marina* reflected the stoichiometry of their food sources (Fig. 1, Tab. 4) which means that *O. marina* is only weakly homeostatic. The pre-feeding condition had a significant effect on the total ingestion of *O. marina* (ANOVA, $F_{3,12}=8.9$; $p<0.01$), with highest food uptake by starved *O. marina* ($\sim 9 R. salina h^{-1}$, Fig. 2), and the lowest by P-limited *O. marina*. None of the differently pre-conditioned *O. marina* showed selective feeding behaviour towards the food containing the limiting nutrient of the pre-conditioning (Tab. 5).

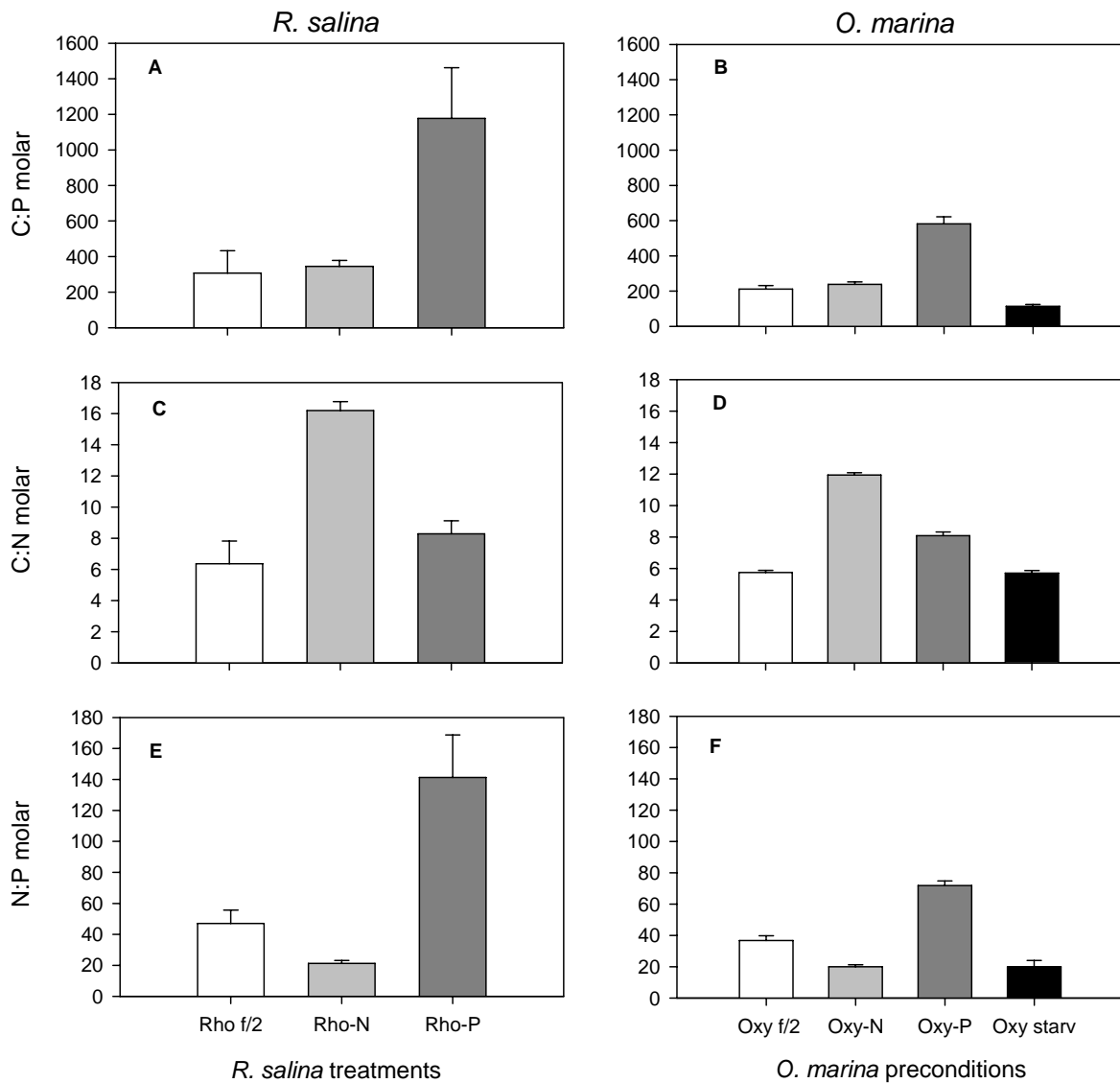


Figure 1: Stoichiometrical differences between *R. salina* (left hand) and preconditioned *O. marina* (right hand). (A, B) molar C:P; (C, D) molar C:N, and (E, F) molar N:P of *R. salina* and *O. marina* under nutrient replete (f/2), N- depleted (-N) and P- depleted (-P) conditions. Bars show the mean and error bars show the standard deviation of five measurements.

Table 4: Mean carbon, nitrogen, phosphorus cell content (pg cell⁻¹) and mean biovolume (µm³ cell⁻¹) of used *R. salina* cultures and of preconditioned *O. marina* in paired t-tests (n=5; FG=8; p<0.05). Different letters (a, b, c, d) indicate significant differences between the different *R. salina* and *O. marina* treatments.

	Treatment	f/2	-N	-P	Starved
		mean (±std)	mean (±std)	mean (±std)	mean (±std)
<i>Rhodomonas salina</i>	C [pg cell ⁻¹]	54 (18) ^a	92 (4) ^b	83 (3) ^c	-
	N [pg cell ⁻¹]	9.69 (1.37) ^a	6.59 (0.29) ^b	11.74 (0.85) ^c	-
	P [pg cell ⁻¹]	0.46 (0.07) ^a	0.69 (0.05) ^b	0.19 (0.05) ^c	-
	Vol [µm ³ cell ⁻¹]	499 (182) ^a	531 (70) ^a	583 (48) ^a	-
	C:P (molar)	308 (125) ^a	345 (34) ^a	1,177 (285) ^b	-
	C:N (molar)	6.36 (1.46) ^a	16.20 (0.57) ^b	8.29 (0.84) ^c	-
	N:P (molar)	47 (9) ^a	21 (2) ^b	141(27) ^c	-
<i>Oxyrrhis marina</i>	C [pg cell ⁻¹]	1,568 (239) ^a	1,818 (85) ^a	1,491 (109) ^a	487 (44) ^b
	N [pg cell ⁻¹]	318 (43) ^a	178 (8) ^b	215 (18) ^c	100 (8) ^d
	P [pg cell ⁻¹]	19.23 (2.95) ^a	19.70 (0.59) ^a	6.64 (0.76) ^b	11.04 (0.69) ^c
	Vol [µm ³ cell ⁻¹]	6,713 (1,212) ^a	6,172 (1,017) ^a	6,337 (1,051) ^a	3,996 (771) ^b
	C:P (molar)	211 (20) ^a	238 (14) ^b	582 (40) ^c	114 (10) ^d
	C:N (molar)	5.74 (0.14) ^a	11.94 (0.15) ^b	8.09 (0.23) ^c	5.70 (0.16) ^{a,d}
	N:P (molar)	36.76 (2.98) ^a	19.96 (1.26) ^b	71.85 (2.94) ^c	19.98 (1.66) ^{b,d}

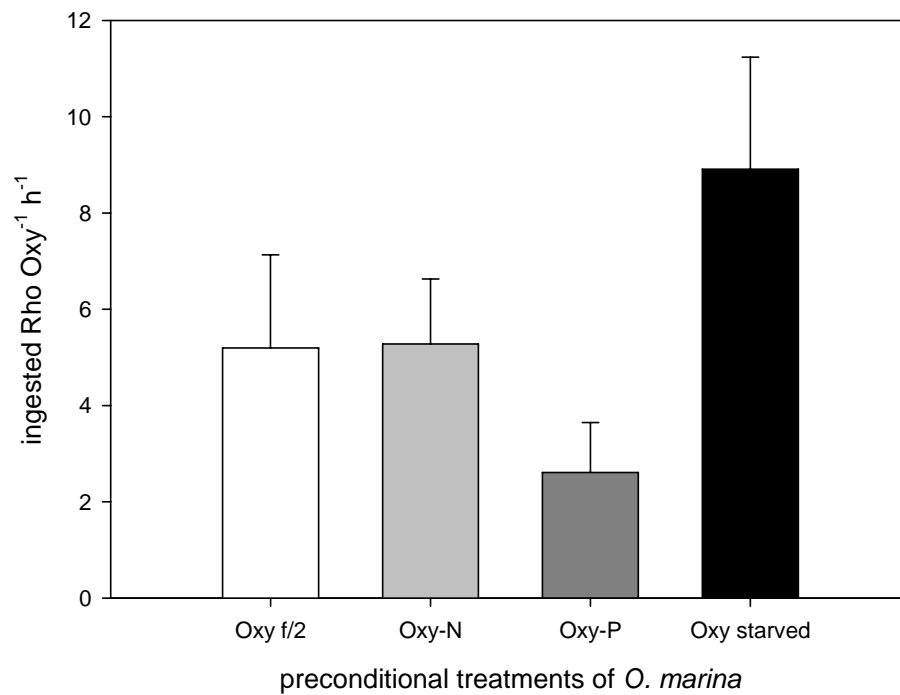


Figure 2: Food ingestion rate of *O. marina* depending on their precondition during the 50:50 selection experiment with nitrogen and phosphorus depleted *R. salina* (Rho-N and Rho-P). Bars show the mean and error bars the standard deviation of four measurements.

Table 5: Summary of the selection experiment using a two-way-ANOVA. The two independent factors were the pre-conditions of *O. marina* (Oxy f/2, Oxy-N, Oxy-P and Oxy starved) and the time (start and end of the experiment). The dependent variable was the ratio between Rho-N and Rho-P (and vice versa) found in the discriminant analysis.

Food	factors	MS	Df	F	p-value
treatment					
Rho-N :	Pre-condition	0.001570	3	1.0001	0.4114
Rho-P	Time	0.000043	1	0.0274	0.8701
	Pre-	0.001178	3	0.7505	0.5337
	condition*time				
	Error	0.001570	22		
Rho-P :	Pre-condition	1.1085	3	1.0856	0.3758
Rho-N	Time	0.1663	1	0.1629	0.6904
	Pre-	0.6459	3	0.6326	0.6018
	condition*time				
	Error	1.0211	22		

Food compensation experiment

Although we did not detect any selective feeding behaviour of *O. marina* in a mixture of nitrogen and phosphorus depleted *R. salina*, we observed a slight but significant food uptake increase of *O. marina* when they were re-fed with the opposite *R. salina* treatment (Fig. 3, Tab. 6; ANOVA Result Interaction between Pre-condition and food type; $F_{1,64}=4.004$; $p=0.05$). Thus, *O. marina* recognized its nutritional imbalance caused by its preconditioning treatment (fed either on nitrogen or phosphorus depleted *R. salina*) and seemed to have simultaneously recognized apparently the nutritional composition of *R. salina*. On average, Oxy-N grazed ~5% more on phosphorus depleted *R. salina* which were rich in nitrogen, whereas Oxy-P grazed ~19% more on nitrogen depleted *R. salina* which were rich in phosphorus. *O. marina* seemed to be capable to compensate its nutritional imbalance through

compensatory feeding (Fig. 4 A). As a result of feeding algae with different limitations, the N:P ratio of *O. marina* changed rapidly: within 18 hours the N:P ratio of P-limited *O. marina* feeding on N-limited (P-rich) algae was identical to those individuals feeding on a F/2 diet (Fig. 4 B). Thus, *O. marina* seems to be very flexible and capable of compensating for the deficiency of elements through compensatory feeding.

Table 6: Summary of the “compensation experiment” of nitrogen and phosphorus stressed *O. marina* (Oxy-N and Oxy-P), re- fed with nitrogen and phosphorus depleted *R. salina* (3-way ANOVA; precondition of *O. marina*, food treatment of Rho-N or Rho-P, offered prey density as independent factors and ingestion rate [*R. salina* Oxy⁻¹h⁻¹] as dependent variable).

	FG	MQ	F	p-value
Precondition	1	0.0195	0.038	0.846469
Food	1	0.5637	1.094	0.299626
Prey density	3	31.2556	60.630	0.000000
Precondition*Food	1	2.0642	4.004	0.049633
Precondition*Prey density	3	0.2796	0.542	0.654977
Food*Prey density	3	0.3520	0.683	0.565751
Precondition*Food*Prey density	3	0.1165	0.226	0.878024
Error	64	0.5155		

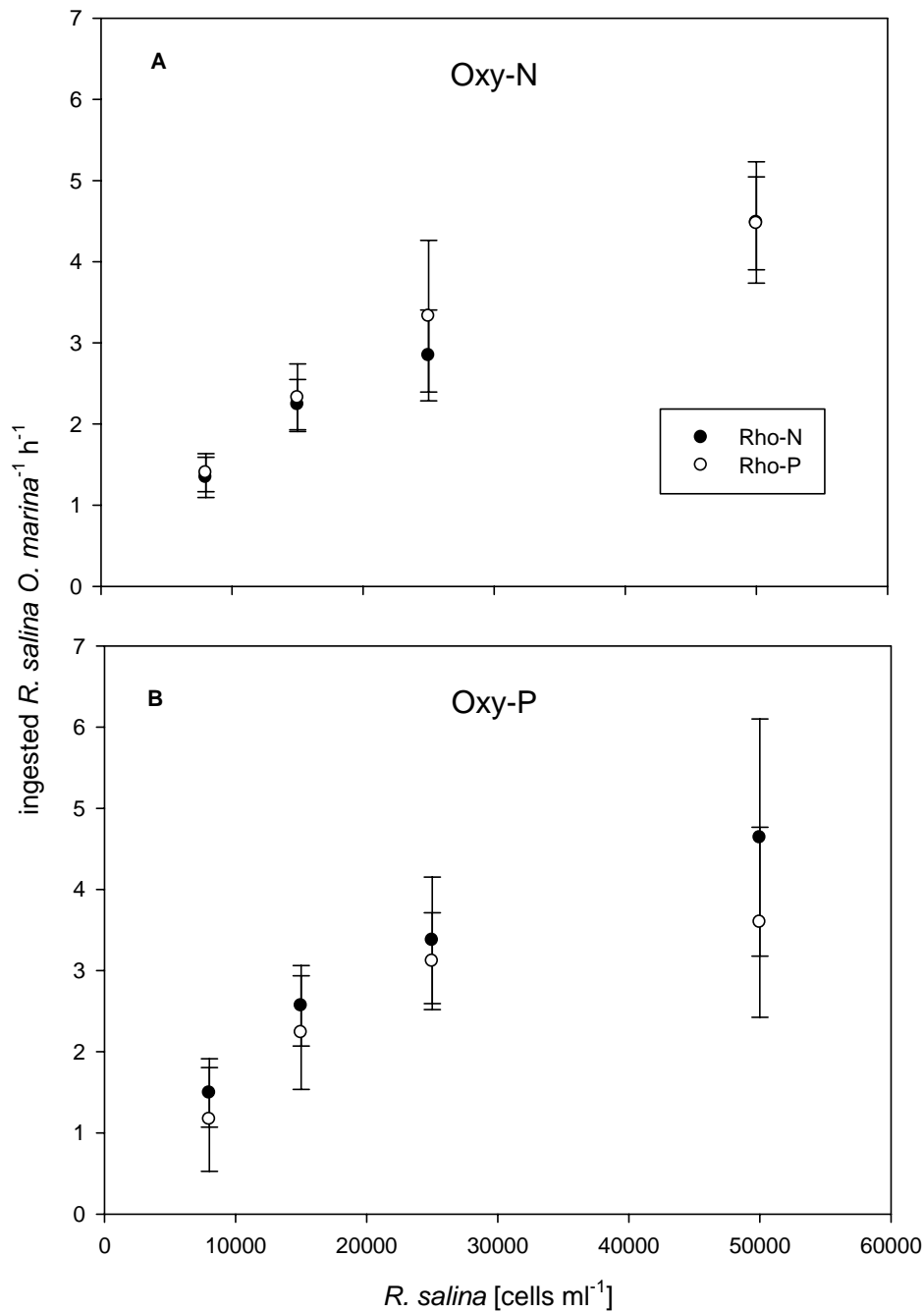


Figure 3: Compensation experiment: cell ingestion of *O. marina* h⁻¹, (A) preconditioned either on nitrogen depleted *R. salina* (Oxy-N) or (B) on phosphorus depleted *R. salina* (Oxy-P), re-fed either with nitrogen depleted (Rho-N) and phosphorus depleted *R. salina* (Rho-P). Error bars show the standard deviation of five measurements.

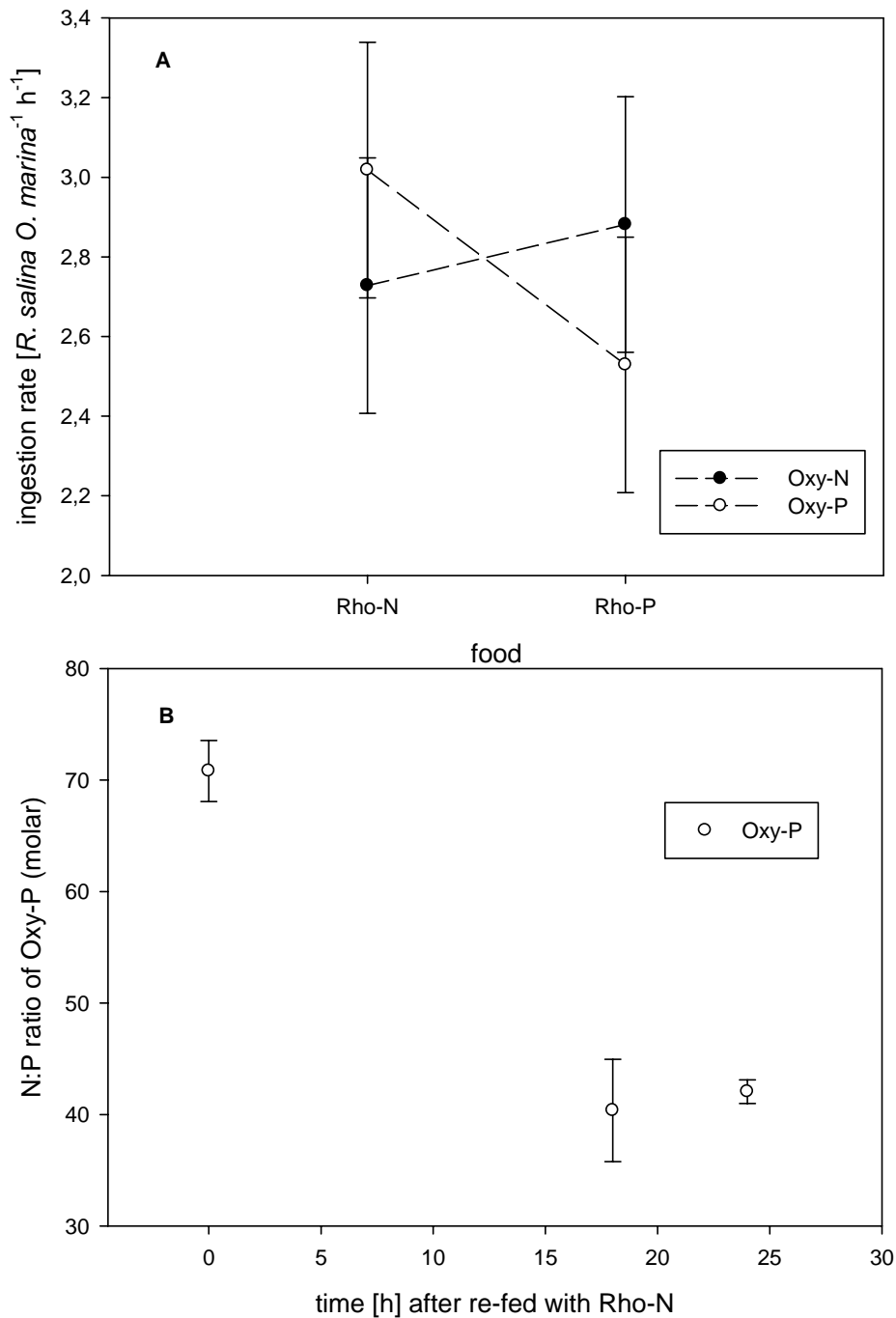


Figure 4: (A) Compensatory feeding of preconditioned *O. marina* (Oxy-N and Oxy-P) re-fed with nitrogen (Rho-N) and phosphorus depleted *R. salina* (Rho-P). Cell ingestion of *O. marina* h^{-1} derived from 3-way ANOVA (Tab. 6) and the compensation experiment (Fig. 3). Error bars show the standard error of five measurements. (B) Change of molar N:P ratio of Oxy-P after re-fed with nitrogen depleted *R. salina* (Rho-N). Error bars show the standard deviation of four measurements.

DISCUSSION

The framework of ecological stoichiometry by Sterner and Elser (2002) predicts that the elemental composition of photoautotrophic organisms is characterized by high plasticity whereas the carbon:nutrient (N and P) content of herbivores is much more constant. Consequently, herbivores are often faced with imbalanced food which has effects on the somatic growth and reproduction of the consumer. The consumer, however, may have the possibility to adapt to unfavourable food conditions either through positive or negative food selection. Moreover, Mitra and Flynn (2005) suggested that herbivores could change their feeding behaviour either through lowering the ingestion rate of unfavourable food, thus using more time for extracting the limiting element efficiently, or through an increase of food uptake, and a shortening of the handling time to extract only the easily available parts of the limiting nutrient. A third possible behaviour of herbivores is to compensate for low nutritional quality of one food item via compensatory feeding on a second food item which contains the limiting element (Raubenheimer and Jones 2006). These mechanisms are measurable as food uptake behaviour of consumers which can be summarized as pre-ingestion selection. Alternatively, post-ingestion mechanisms, such as selective transfer efficiencies of ingested elements and excretion of elements which are in excess might also be effective mechanisms to balance unbalanced food (Anderson et al. 2005; Frost et al. 2005).

Our study on food selectivity of *O. marina* show that this phagotrophic protist does not actively select between different food qualities presented to them in a mixture. Given the relatively relaxed form of homeostasis of *O. Marina*, it apparently is capable of dealing with different food qualities and compensates its nutritional imbalance through general changes in food uptake rather than through selecting between different food qualities. A mixed food uptake of nitrogen depleted and phosphorus depleted *R. salina* treatment compensates the lack of one element from the one algal treatment through food uptake of the other algal treatment. This feeding strategy is typical for omnivorous or opportunistic animals such as cockroaches (Raubenheimer and Jones 2006) and aquatic filter feeders such as *Daphnia* sp. (DeMott 1998) which compensate the biochemical (carbohydrates vs. proteins) or elemental deficiencies (low P vs. high P food) through compensatory feeding.

In our compensation experiment with single food treatments (either nitrogen depleted or phosphorus depleted *R. salina*) we could indeed show that *O. marina* grown on nitrogen depleted *R. salina* compensated its lack of elemental nitrogen by an increased uptake of phosphorus depleted *R. salina*, rich in elemental nitrogen. *O. marina* which was grown on phosphorus depleted *R. salina* showed higher food uptake of nitrogen depleted *R. salina*,

which are, in turn, rich in elemental phosphorus. This compensatory feeding behaviour of *O. marina* corresponds very well with the experimental findings of Hantzsche and Boersma (2010) who showed that at high food concentrations nitrogen depleted *R. salina* had less of an effect on the growth rate of *O. marina* than phosphorus depleted *R. salina*. Even though phosphorus depleted *R. salina* can therefore be considered poor quality food source for *O. marina*, *O. marina* fed more on this food source when preconditioned on nitrogen depleted *R. salina* to compensate for the lack of nitrogen. *O. marina* suffering phosphorus depletion compensated for the lack of elemental phosphorus with higher ingestion rates of nitrogen depleted *R. salina* which are phosphorus rich. This feeding strategy permitted *O. marina* to change its elemental composition within a few hours.

The fact that *O. marina* continued feeding on the same algal treatment on which it had been preconditioned before shows, however, that food uptake of *O. marina* depends rather on food availability than on food quality, as Hantzsche and Boersma (2010) already described. Hence, we suggest that *O. marina* digests its prey very efficiently to extract the elements it needs at constant grazing rates rather than increasing food uptake to extract only the easily available parts of the limiting nutrient as described by Mitra and Flynn (2005). Food quality-induced cell physiological processes in *O. marina* to handle unfavourable food and post-ingestion selection of elements might play thereby a more important role than pre-ingestion selection. Hantzsche and Boersma (2010) showed that a higher respiration rate is one potential mechanism for *O. marina* to excrete surplus carbon. The excretion of ammonium and amino acids might be a possible mechanism to excrete surplus nitrogen. To which extent *O. marina* excretes elemental phosphorus which is so important for its further growth is still very much unknown.

Thus, food quality per se for *O. marina* is not easily definable through food uptake differences since its ingestion rate is highly depend on its pre-condition. The ability of *O. marina* to recognize the nutritional composition and deficiency both inside its own cells and its potential prey organisms provides a sophisticated mechanism which enables *O. marina* to compensate nutritional imbalance via compensatory feeding. Differences of cell surface structures and bio-chemicals released by the food might be responsible for food recognition.

CHAPTER VI

General Discussion

Employing Flow CAM technology in planktological surveys

Doubtless, the Flow CAM is state-of-the-art technology with respect to its innovative approach and technical finesses, as it enables the user to measure and visualise particles in water samples. In contrast to most other particle counters the user can actually see which kind of particles are captured and to which extent such particles contribute to total particle distribution and frequency in water samples. The quality of the images taken by the Flow CAM is high and sufficient to identify particles $>10\ \mu\text{m}$ without restrictions, provided that suitable flowcell sizes and objective magnifications are used. Unfortunately, even using the highest magnification (200X) the resolution of the images of particles with a size range of 2-10 μm is rather low, (e.g. Ide et al. 2008), making the visual identification of such small particles very difficult (Fig. 1).

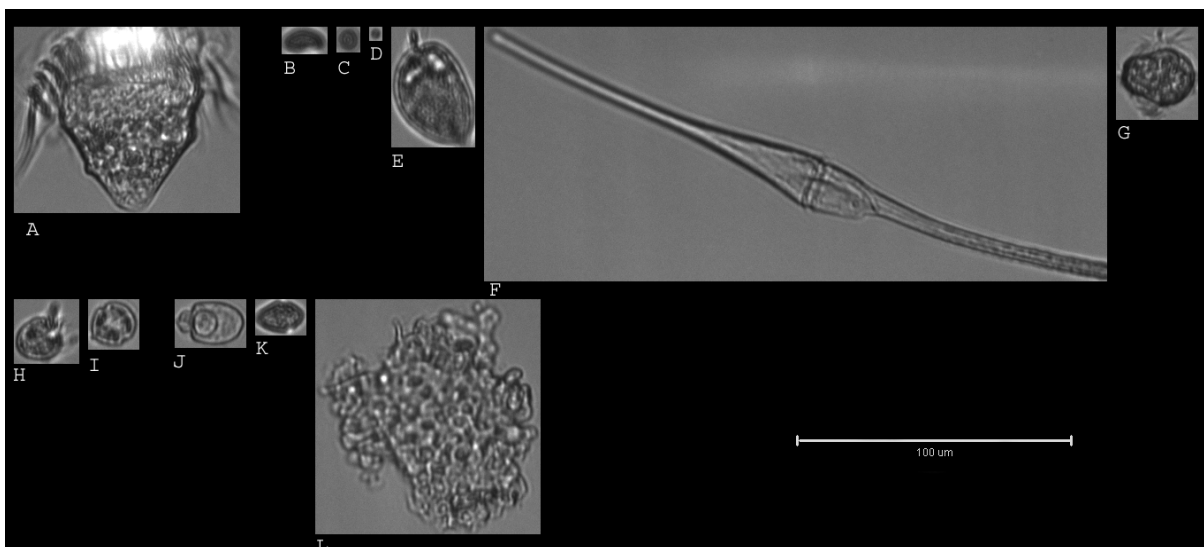


Figure 1: Particles captured by the Flow CAM in the fluorescence triggered image mode using the 100 μm flowcell and the 20X objective (200X magnification): (A) undefined ciliate ($\sim 65\mu\text{m}$); (B) “Flagellata indeterminata” ($\sim 15\mu\text{m}$); (C) round undefined particle ($\sim 9\mu\text{m}$); (D) round undefined particle ($\sim 4\mu\text{m}$); (E) *Prorocentrum micans* ($\sim 45\mu\text{m}$); (F) *Ceratium fusus* ($\sim 245\mu\text{m}$); (G) *Myrionecta rubra* ($\sim 35\mu\text{m}$); (H) undefined ciliate ($\sim 20\mu\text{m}$); (I) undefined dinoflagellate ($\sim 17\mu\text{m}$); (J) *Amphidinium* group ($\sim 35\mu\text{m}$); (K) *Gymnodinium* group ($\sim 20\mu\text{m}$); (L) detritus ($\sim 80\mu\text{m}$).

Moreover, especially when non-living particles are co-captured together with algal cells it is difficult to discern between the different particle types as size and particle shape are often very similar. This is, however, also complicated under the light microscope and is the reason why these small plankters are often classified in terms of cell shape and size only (e.g. Wiltshire and Dürselen 2004). Right there, the Flow CAM could have huge potential. Since size and shape as well as the fluorescent properties of such small phytoplankton are determined by the Flow CAM, the identification of such small cells in water samples should be possible. Each captured particle is digitalized and characterized with twenty Flow CAM parameters, which can be transferred into Excel sheets for further data analysis, as well as pattern recognition software. These species specific data and pictures can be used to build a library which should allow the automatic identification of specific cells in Flow CAM measurements (e.g. Buskey and Hyatt 2006). After a complete set of species is deposited in the picture library, an easy and time efficient, almost automatic recognition of plankton samples should be possible. Unfortunately, as is clarified below this is not so easy, and perhaps not possible at all with the current instrument.

Testing the Flow CAM

The Flow CAM is sold as a ready-to-use-instrument and advertised as a means to eradicate traditional, tedious methods such as microscopic counts, waiting for appropriate applications in planktological surveys. Therefore, the expectations for this relatively new technology as an automated plankton recognition system were high, brought about by the picture quality and the high recognition value of captured plankton individuals (Fig. 1). In Chapter II of this thesis, I investigated the effects of changing some of the many parameters which can be manipulated on the measurement success of the Flow CAM in the fluorescence triggered image mode. This mode is in the main interest for planktological studies since only fluorescent particles are supposedly captured. Already the measurement of one single algal species (*Rhodomonas salina*) in different densities was anything but trivial, essentially leading to the conclusion that one needs to know the exact density of the cells of interest before counting the densities with the Flow CAM. The huge variety of Flow CAM adjustments like camera exposure (camgain), amplifier (gain) and threshold of the fluorescence detector, pump rate and particle density, have indeed an enormous effect on the accuracy of the Flow CAM measurements in the fluorescence triggered image mode. It is very important to know the effects of all of these adjustments before using the system. Furthermore, the way the Flow CAM calculates cell density in the fluorescence triggered

image mode based on cell counts in a sub-sample of the whole flow cell width (field of view) may cause bias. Apparently cells are not homogeneously distributed in the flowcell. At low cell densities and low pump rates, long periods of non-captures are combined with low amounts of captured particles which sometimes pass through the field of view together (double measurements/co-captures). Based on the low cell captures in the field of view, the Flow CAM calculates the amount of particles which should have gone through the whole flowcell.

We still do not understand why these low numbers of counts should have lead to an overestimation of the real densities at low pump speeds. Rather, it could have been expected that the variation between counts should have been higher at those speeds. Therefore, it is certainly necessary to further investigate why at low cell counts the Flow CAM overestimates the actual densities. At higher pump speeds, I observed a strong underestimation of the actual densities. With increasing pump speeds the amount of captured particles per time is increasing, but the risk that particles are not captured is enhanced as well, since capture per time unit did not linearly increase with increasing pump speeds. This means that the risk to underestimate the real cell densities becomes larger with increasing pump speeds. Unexpectedly, this is not caused by an overload of the fluorescence detector, but most likely by the time the particles spend in the flowcell, which is too short for them to be captured. With increasing cell densities the Flow CAM captures more particles in a shorter time; hence the amount of images per time is larger at lower pump rates. Thus, the counting error based on the amount of captured particles with increasing pump speed is stronger even at lower pump speeds.

The risk of co-captures of two passing cells with increasing cell densities is not so important when using only one algal species with more or less the same fluorescence property. However, when using the Flow CAM in the field (Chapter III) where fluorescent particles (phytoplankton) and non fluorescent particles (detritus) occur in different ratios, co-captures are the main reason why the Flow CAM captured such large amount of detritus in the fluorescence triggered image mode. This was caused by the fact that the Flow CAM does not measure particles and their individual fluorescence separately when such particles pass the field of view simultaneously. The Flow CAM takes pictures of both but assigns the fluorescent signal from the one particle which has triggered the Flow CAM to all other particles in the field of vision at the same time. Even though it is a relatively easy (as two particles in the Data sheets have identical fluorescence signals), but very tedious (going through thousands of data lines) exercise to remove these (one needs to exactly know which

was the living particle and which was the hitchhiker particle), this is certainly a major shortcoming of the Flow CAM system.

Also, if the Flow CAM is to be used in experimental setups (Chapter V) where the Flow CAM is supposed to discriminate between different fluorescent algae of the same species, co-captures of algae with different fluorescence have to be prevented. Therefore, low cell densities have to be prepared for such measurements. One other feature of the fluorescence measurements with the Flow CAM is of importance. The magnitude of the fluorescence signal obtained by the Flow CAM (Chapter II) is not an absolute value but rather dependent on the used pump speed, with higher values at higher speeds. Hence, discriminating between different fluorescent algae is easier when the pump rate is high. This, of course, has also consequences for the fluorescence signal of fluorescent particles obtained in the field, since densities vary greatly throughout the year. Thus, keeping the number of detections per second more or less constant by varying pump rates might not be the best experimental approach. Therefore using the fluorescence parameters to characterize a specific algal species in the library as described above is only possible if the pump speed used is constant over the whole experimental period. Even then, however, it has to be considered that the fluorescence of different algae species changes between different growth phases. The remaining Flow CAM parameters which might be used for characterizing different species are mostly based on length and width (e.g. ESD, ABD) and are therefore auto-correlated. This indicates that an establishment of a species library is at the moment of lower importance than a sophisticated elaboration of the many pitfalls which influence the measurement success of the Flow CAM in the fluorescence triggered image mode.

Hence, my results show that at this moment it is very difficult to use the Flow CAM as a standard instrument for plankton surveys, as very much needs to be known about the sample beforehand. It is certainly not ready to be used as a stand-alone instrument to count plankton densities in an autonomic mode. At the moment, the Flow CAM might be best used in controlled laboratory studies using the Flow CAM's potential to measure the relative fluorescence of e.g. differently grown algal cells of the same species or different algal species in experimental setups. There is a great need for caution even in this case, as, for example, the relative fluorescence is highly dependent on the used pump rate. False measurements are therefore pre-programmed if pump rates are changed between the measurements (see Buskey and Hyatt 2006).

The Flow CAM in the field

Despite the potential pitfalls described above, I also tested the instrument in field situations. In Chapter III of this thesis the Flow CAM performance in the field was tested using two measurement modes: the AutoImage (-laser) and the fluorescence triggered image mode (+laser). At Helgoland Roads, the particle concentrations of non fluorescent particles (detritus) greatly exceed those of the fluorescent particles (phytoplankton). The frequency of both particle types in water samples is an inverse power function of size. Thus, the AutoImage mode which measures particles unselectively (fluorescent and non fluorescent), may be suitable to determine total particle concentration in distinct size classes correctly. In contrast to the fluorescence triggered image mode, the AutoImage mode is less vulnerable with respect to the Flow CAM adjustment issues, but in this mode the Flow CAM is essentially just a particle counter and the feature of the laser is not used. Moreover, in the field samples I obtained almost exclusively pictures of non-living particles. Thus, the AutoImage mode of the Flow CAM is useful if field surveys focusing on particle concentrations and distributions in the water column in general. At Helgoland Roads, however, the AutoImage is less useful for counting plankton due to the high amount of non-living particles. While measurements in the small size range can be done relatively quickly, the time needed for larger particles is much longer, as larger particles are less abundant. Nevertheless, the results of the AutoImage mode show that the density of particles, especially in the size range between 2-15 μm , correlates well with the Secchi Depth at Helgoland Roads. Attempts to explain Secchi Depth with chlorophyll a concentrations or total algal biomass have not been successful as of yet, which indicates that, in contrast to lakes, phytoplankton in the German Bight does not determine the water transparency, but rather that non-fluorescent particles determine the attenuation of the light around Helgoland.

The successful use of the AutoImage mode for plankton abundance estimations requires water samples in which plankton cells (not detritus) dominate in adequate numbers ($>1,000 \text{ ml}^{-1}$). Candidates which might occur in such high cell numbers in natural waters are small sized flagellates (2-15 μm), haptophytes and, during blooming conditions, small sized dinoflagellates and small sized diatoms. Microzooplankton densities, however, are far below 1,000 cells ml^{-1} even at blooming conditions, which implies that when using the AutoImage mode several hundred images of the most abundant species will have to be taken before the less abundant species can be assessed. The work by See et al. (2005) is the only available publication which investigated a possible Flow CAM application for plankton abundance estimations in the field using the AutoImage mode. Their investigation focused only on

phytoplankton which was larger than 15 μm . They concluded that the Flow CAM was not sensitive enough to describe the complete phytoplankton community, but claimed that larger diatoms and dinoflagellates were enumerated as precisely with the Flow CAM as with traditional methods. Most likely, in blooms of single species this is indeed the case.

To exclude the detritus in the samples the fluorescence triggered image mode is used. This mode is supposed to capture only fluorescent (living) particles. This is the mode of interest for planktological surveys (Buskey and Hyatt 2006). In contrast to the AutoImage mode, the fluorescence triggered image mode is highly dependent on cell density and pump rate, as described above. Furthermore, this mode is the suitable choice if expected particle concentrations are low (<100 cells ml^{-1}). At high particle concentrations the fluorescence triggered image mode is highly dependent on the capability of the fluorescence detector, which is the bottleneck of the Flow CAM and allows only two particle detections s^{-1} (Sieracki et al. 1998). This means that water samples have either to be diluted or the pump speed has to be adapted to expected particle concentrations. Since dilution of water samples in automated plankton recognition systems is very difficult, especially if the dilution factor is changing between samples, an automated adaptation of the pump rate combined with an automatic exchange of flowcell sizes and objectives are needed if particle concentrations are too high for the capacity of the fluorescence detector. Again the problem of changing fluorescence signals with different passing speed through the flow cell needs to be overcome. Moreover, although the fluorescence triggered image mode is supposed to capture only fluorescent particles, a huge proportion of detritus particles were also captured. The reason is either that detritus particles also contain some fluorescent properties or that detritus particles passed through the field of view at the same time as a phytoplankton cell, and were given the fluorescent properties of the algal cells as described above and in Chapter II.

Unfortunately, there is a considerable lack of precise descriptions of methods used for Flow CAM measurements in the literature, which is very difficult for new Flow CAM users as they need to decide which methods to use. The measurements of specific cell or plastic bead concentrations in the AutoImage mode to evaluate the capability of the Flow CAM for exact enumerations do not help here either, as in the fluorescence triggered image mode pump speeds and used cell concentrations for each flowcell size and objective combination additionally affect the accuracy of the measurements. The expected size of used particles largely determines the flowcell/objective combination. Hence to count the complete community in one sample it is necessary to use more than one magnification, which is rather time consuming. A critical evaluation of the few papers that have been published using the

Flow CAM showed that indeed all of the authors had considerably problems with the Flow CAM. These ranged from not mentioning microscopic countings for reference (Sieracki et al. 1998) to considerable differences between the methods (See et al. 2005; Ide et al. 2008). Moreover, most of the authors are quite unspecific in the exact methodology that was used (Buskey and Hyatt 2006; Littman et al. 2008). This might be the reason why actually so very few papers have appeared using the Flow CAM methodology.

In conclusion, if we are to use the Flow CAM to replace or support traditional counting methods, several improvements are necessary. First and foremost, the relative fluorescence of the particles needs to become independent of the pump speed. Only then will a certain algal cell have the same properties in different samples, and species libraries can be used. As different samples have different densities, changing the pump speed will be necessary to avoid very long handling times. The fluorescence detector will have to be improved in order to prevent that particles are not captured when passing the flowcell too rapidly. Furthermore, it is of vital importance to improve the software and the fluorescence detector so as to separate fluorescence recognition of simultaneously passing particles to prevent co-captures (=fluorescence double measurements). A standard protocol needs to be established which describes the approach of Flow CAM parameter adjustments (camgain, fluorescent gain and threshold) to expected particle properties. A further Flow CAM development could consist of a mix of both measurement modes which would enable the system to measure particles correctly at any cell concentration “live”. If the fluorescence detector is overstrained, the machine should diminish pump speed or the field of view automatically. If the Flow CAM takes less than two pictures s^{-1} , the system should react automatically and increase either pump speed or the field of view. Since I used hours for the field measurements and hours to reprocess Flow CAM images after each measurement (to discriminate between detritus and plankton particles) this might be the chance for the Flow CAM to be used as an automated plankton recognition system in the future.

The effect of food quality on the phagotrophic flagellate *Oxyrrhis marina*

Experimental approach

The impact of light and nutrients on phytoplankton and the assessment of algal food quality for higher trophic levels are mainly based on findings in pelagic food webs of lakes and have nearly exclusively been tested on mesozooplankters, such as *Daphnia* sp. (Sterner 1993; DeMott 1998; DeMott and Gulati 1999; Darchambeau et al. 2003) and rotifers (Rothhaupt 1995; Jensen and Verschoor 2004). Effects of elemental composition in primary

producers on higher trophic levels in marine pelagic food webs, such as copepods, larval fish and gelatinous zooplankton were highlighted recently (Malzahn et al. 2007; Boersma et al. 2008; Malzahn et al. 2010). Not only the quantity but also the quality of food determines growth and reproduction of consumers. There is still considerable debate as to which compounds actually determine food quality - either the balanced elemental composition with respect to the elemental composition of the consumer (elemental stoichiometry) or the balanced biochemical composition such as essential fatty acids, proteins and sterols (see Tang and Dam 1999), or possibly a combination of both. Although it has been generally accepted that phagotrophic protists are an important component linking the microbial to the classical food web, virtually nothing is known about their stoichiometry and nutritional quality except for some studies on their biochemical composition (Klein-Breteler et al. 1999; Tang and Taal 2005). In Chapter IV of this thesis I aimed to close this gap. Different food qualities in terms of nutritional composition were presented to phagotrophic protists, which affected their food uptake, their corresponding growth and their physiological processes to handle food with different qualities.

Oxyrrhis marina was used as a model organism. *O. marina* is an omnivorous phagotrophic nanoflagellate which has been used in several studies on the uptake of different algae species and their subsequent growth potential (e.g. Flynn et al. 1996; Tillmann and Reckermann 2002). Starved *O. marina* fed nutrient replete, nitrogen depleted and phosphorus depleted *Rhodomonas salina* showed food quality independent food uptake at low and high food concentrations. This means that *O. marina* simply filled its food vacuoles unselectively as soon as food was offered. This is similar to observations from rotifers fed with different nutrient defined algal treatments (Rothhaupt 1995) but different to food uptake behaviour of *Daphnia* sp., which decreased when phosphorus depleted algae were offered (Sterner and Smith 1993).

The nutrient stoichiometry of *O. marina* is not strictly homeostatic. The elemental composition of *O. marina* reflects the nutritional composition of its food, albeit in a dampened form. The explanation for this might be that a fairly primitive, single celled, heterotroph such as *O. marina* does not possess any highly developed organs or storage tissues. Simultaneously, the turnover of ingested food is higher in one single cell compared to highly developed multi-cellular organisms. Elements which are ingested in excess are quickly excreted, whereas elements which are limiting for further growth are retained. *O. marina* respired significantly more when fed nitrogen-depleted and phosphorus-depleted *R. salina*, than when fed nutrient replete *R. salina*. This has already been observed in different *Daphnia*

species fed phosphorus depleted algal cells (Darchambeau et al. 2003; Jensen and Hessen 2007), whereas no higher respiration rates of the rotifer *Brachionus calyciflorus* could be detected when these were fed with nitrogen and phosphorus depleted food. Jensen et al. (2006), however, suggested other excretion mechanisms for rotifers to excrete surplus carbon like DOC release or high carbon content of fecal pellets. Therefore, higher respiration rates are an effective cell metabolism mechanism for *O. marina* to excrete surplus carbon of ingested food.

Food uptake of pre-fed *O. marina* was lower than that of starved *O. marina*. This indicates that food uptake in general is a function of food vacuole capacity (Chapter V). Nevertheless, I expected that *O. marina* might behave selectively dependent on its nutritional status when re-fed with more favourable food. In a mixture of different food cells *O. marina* did not select between different nutritional *R. salina* cells, but fed significantly more when only (not in a mixture) more favourable food were re-offered. This indicates that *O. marina* recognizes its own nutritional state, as well as the quality of its food as described in Wootton et al. (2007) and Martel (2006). In a mixture of different food qualities, however, nutritional selection might occur in the food vacuole of *O. marina* dependent on the precondition of *O. marina*. Consequently, *O. marina* probably has a high cell metabolic rate which extracts essential elements of its food depending on its needs and simultaneously excretes surplus elements very efficiently.

Here, I showed that the growth of *O. marina* is negatively affected only when fed with phosphorus depleted *R. salina* at high food concentrations, whereas nitrogen depleted and nutrient replete *R. salina* had similar effects on growth rate. This explicitly emphasizes the role of elemental phosphorus for fast growing organisms when food quantity is high (Elser 2002). At low food concentrations, however, growth of *O. marina* was food quality independent which means that ingested food of low quality is sufficient for cell metabolism maintenance and low growth as described for *Daphnia* (Sterner and Robinson 1994) and rotifers (Rothhaupt 1995).

The role of heterotrophic protists in the marine pelagic food web

Based on my main findings of food quality effects on the used model organism *O. marina*, one might try to extrapolate this to the field, knowing full well that this is a fairly dangerous endeavour as the experimental evidence is based on one species only. Nevertheless, we know that heterotrophic protists do not only play an important role as grazers on primary producers in the marine pelagic food web (Landry and Calbet 2004), but

actually are important both as nutrient recyclers and simultaneously as a crucial link in terms of nutrients to higher trophic levels such as copepods.

Before the spring phytoplankton bloom, algal cells are light limited since nutrients are available through recycling and water mixing during the winter months. Low standing crops of herbivores, such as micro- and mesozooplankton, have overwintered either as cysts, resting eggs or other resting stages. As soon as the days are getting longer and the light intensity increases, the phytoplankton grows at high rates and continues to build up the phytoplankton bloom as long as the major nutrient elements (Si, N or P) are not depleted (Sommer 1996). Additionally, the water temperature starts to increase which positively influences heterotrophic processes (Montagnes and Lessard 1999). Thus, heterotrophic protists which are able to grow as fast as their phytoplankton prey respond very quickly to increasing food availability since algae growing at high growth rates are rich in nitrogen and phosphorus. Most of the fixed carbon (and phosphorus) from primary producers is therefore channelled into the microbial loop. Depending on the absolute concentration of available nutrients, either nitrogen or phosphorus depletion limits further phytoplankton production. If the available phosphorus concentration is already low, nitrogen recycling from heterotrophic protists causes additional phosphorus limitation of phytoplankton. If the phosphorus concentration is still high, nitrogen recycling from the microbial loop supports further growth of primary producers until nitrogen fixation in primary producers is higher than the nitrogen recycling of the heterotrophs.

The nutritional quality of phytoplankton changes as soon as either nitrogen or phosphorus is depleted. Herbivores which ingest such phytoplankton have to cope with a high C:nutrient content. Essentially, the excess carbon needs to be excreted, either as dissolved organic carbon or as CO₂ through increased respiration rates. My results suggest that nitrogen limitation of primary producers is probably less detrimental for heterotrophic protists than phosphorus limitation. Most likely, the phenomenon that heterotrophic protists disappear as fast as they have appeared after the spring bloom is caused both by food quality aspects in terms of phosphorus depletion as well as depletion of algal biomass.

In contrast, crustacean mesozooplankton such as copepods are not able to respond to food availability as fast as heterotrophic protists. Consequently, the response of copepods to enhanced food quantity and increasing temperature during spring takes longer (~two weeks) since the small stock of overwintering copepods have either to mate or to hatch from resting eggs. The first developmental stage of copepods, the naupliar stage, is as vulnerable with respect to phosphorus limitation as heterotrophic protists (Malzahn et al. 2010) and competes

with heterotrophic protists for available resources. Small nauplii are, however, not as voracious grazers as their already abundant protist competitors. With increasing developmental stage of copepods, however, food ingestion increases exponentially and since heterotrophic protists are also ingested by copepods the competition for food ends with the copepods winning (“eat your competitor”).

The phenomenon that copepods switch from autotrophic food to heterotrophic food is well described but rather in terms of prey recognition based on higher prey motility and more favourable biochemical composition such as fatty acids and proteins (Gismervik and Andersen 1997; Klein-Breteler et al. 1999; Gismervik 2006). Food quality, however, in terms of nutritional composition has been neglected so far. Phosphorus depleted algal cells have strong negative effects on the growth and the developmental rate of copepods. Copepods which are faced with low food quality in the autotrophs (end of spring bloom) can switch to heterotrophic prey to balance their nutrition composition in terms of phosphorus. So, while the microbial loop was often considered as a sink for energy, it might play a more important role as a concentrating mechanism of limiting nutrients. If the primary producers are nutrient depleted, the protists feeding on them will have ‘burnt’ much of the carbon already, thus making them a very interesting food source for higher trophic levels. Thus, I expect that especially in systems where carbon is in ample supply, copepods should feed mainly on protists. Alternatively, if nutrients are not limiting it might be better to feed on the primary producers directly. In fact, in the North Sea we see a shift with the change in nutrient availability (Martens and van Beusekom 2008). With decreasing nutrient loading in the past years, we see an increase in a more carnivorous copepod feeding mostly on protists. This is exactly what is to be expected.

Outlook

In this thesis I have elaborated on the effect of different food qualities in terms of elemental composition on the model organism *Oxyrrhis marina* with special emphasis on phosphorus limitation and the fate of fixed carbon from primary producers to higher trophic levels within the pelagic marine food web. The classical view that the production of higher trophic levels such as fish is highly dependent on the length of the food chain and the amount of trophic levels might be applicable as soon as primary producers are not nutrient depleted. Since this refers almost exclusively to upwelling systems, nutrient depletion occurs almost in all shelf seas in temperate waters during the plankton growth phase. Hence food-chain-elongation through additional members of the microbial loop dampens unfavourable autotrophic food during nutrient depletion and enhances the nutritional quality for copepods

and potentially also higher trophic levels. Further research is certainly needed to assess whether and under which circumstances the negative (carbon loss) and positive (concentrating favourable substances) effects of the microbial loop prevail.

Furthermore, studies on the capability of zooplankters to recognize the nutritional status of their prey and on the physiological mechanisms used to assimilate ingested elements or to excrete surplus elements depending on the nutritional needs of the consumers are needed. We still know practically nothing on these mechanisms. How do herbivores taste what is good food and what is bad food, when (and how) do organisms regulate their stoichiometry, and what are the excretory pathways are examples of burning issues that need to be dealt with in the future.

Based on my results, I suggest that growth of heterotrophic protists is phosphorus limited rather than nitrogen limited, or more precisely, that protists suffer more from phosphorus limitations than from nitrogen limitations. One explanation for this could be that being able to deal with phosphorus limitations is not necessary in a sea where nitrogen is normally the limiting nutrient. Alternatively, phosphorus limitations in the sea might be real, and in one system some consumers might be limited by one nutrient and others by another one, much the same as has been described for phytoplankton. In fact, recent evidence has even shown that rather than single nutrients the ratios of the nutrients might be the determining factors. Most likely, our simple assertions that the sea is nitrogen limited and lakes are phosphorus limited need to be replaced by more detailed and subtle conclusions, the database of which needs to be established by much more experimental work.

SUMMARY

In this thesis the Flow CAM is examined for possible applications in the field as well as for experimental setups under controlled conditions. The Flow CAM is supposed to replace tedious, traditional methods like microscopic counting in planktological surveys. The daily routine sampling and measurement program of important parameters such as microscopic counts and chlorophyll measurements at the sampling station “Helgoländer Reede” provide the best background against which to test the reliability of Flow CAM measurements. The expectation on this technology was high since the Flow CAM, in contrast to other particle counters, takes pictures of each particle. Thus, it is possible not only to measure the distribution of particles in water samples but also enables the identification of each particle. Each captured particle on the digitalized picture is characterized by twenty Flow CAM parameters (e.g. length, width, fluorescence) assigned to it. This kind of particle signature is supposed to help to identify such a particle in new subsequent measurements, which would shorten time for particle quantification tremendously. In some cases this might be possible. The results presented here, however, show that much more effort has to be used for appropriate data acquisition with the Flow CAM.

Therefore, several factors are illustrated in Chapter II which determine the accuracy of Flow CAM measurements in the fluorescence triggered image mode, such as camera and fluorescence settings which are of great importance in this measurement mode. Particles are potentially not photographed, and thereby missed, because they are not recognized by the camera or because their fluorescence is too low. The most serious factors which determine the measurement success of the Flow CAM are particle concentration and pump speed. The ability of the Flow CAM to measure the fluorescence of particles is not absolute but rather dependent on pump speeds.

The Flow CAM performance on field samples is presented in Chapter III. In order to be able to measure the wide size range of phytoplankton and microzooplankton, three different flowcell sizes were used. All of these were measured in two of the three available measurement modes, the AutoImage and the fluorescence triggered image mode. The results in the AutoImage mode showed that the Flow CAM measures particle densities correctly. The main proportion of these particles, however, consisted almost exclusively of detritus. The fluorescence triggered image mode, which is supposed to measure fluorescent particles selectively, captured also a large amount of detritus due to co-captures of fluorescent particles. In comparison to microscopic counts the Flow CAM underestimates the abundances

of plankton species in most cases. This is due to the relatively high threshold of the fluorescence detector and the different pump speeds which were used to increase the contact probability with fluorescent particles.

The effect of food quality on the phagotrophic flagellate *Oxyrrhis marina* is presented in Chapter IV. Up to date little is known about how such primitively single-celled heterotrophs are affected. Feeding experiments showed that *O. marina* does not distinguish between food of different qualities; feeding seemed to be food quality independent. The growth rate, however, was lower when *O. marina* was fed with phosphorus depleted food. Nitrogen depleted food on the other hand had no effect on growth. The attempt to explain this by comparing enhanced respiration rates failed since *O. marina* fed nitrogen or phosphorus depleted food respired at similarly enhanced rates to excrete the surplus carbon. Therefore, the elemental phosphorus may be the limiting element for such fast growing heterotrophs.

The extent to which *O. marina* select between different food qualities depending on its precondition is presented in Chapter V. For this purpose the Flow CAM was used to discriminate between phosphorus and nitrogen depleted food. *O. marina*, however, did not feed selectively but rather reacted with different ingestion rates depending on its precondition. When *O. marina* fed in single food treatments containing that element which was limiting in its precondition treatment, *O. marina* reacted with compensatory feeding. This shows that *O. marina* can perceive the limiting nutrient in its own cell as well as in the nutrient composition of its food source. The fact that *O. marina* continued feeding on the food source with which it was fed before indicated that post-gut ingestion play a higher role in *O. marina* than pre-gut ingestion.

This present thesis is aimed at revealing some of the weak points of the Flow CAM. These shortcomings are to be further identified in order to ensure that the Flow CAM can possibly be used for automatic counting processes in the future. The role which heterotroph protists can play in the food web and the effect food of different qualities can have on them is shown in the experiments presented here using the model organism *O. marina*. Further investigations are needed to establish whether these results can be transferred to other protists.

ZUSAMMENFASSUNG

Die vorliegende Arbeit beschäftigt sich sowohl mit der Einsetzbarkeit der Flow CAM für planktologische Untersuchungen im Feld, als auch für experimentelle Fragestellungen unter kontrollierten Laborbedingungen. Ursprünglich war die Flow CAM als geeignetes Hilfsmittel gedacht, Wasserproben und deren Planktonbestandteile in kürzester Zeit zu messen, um gegebenenfalls die zeitintensiven, traditionellen Zählmethoden mit dem Mikroskop abzulösen. Die langen Erfahrungen und die täglichen Arbeiten an der Helgoländer Messstation „Reede“ sollten deshalb beste Voraussetzungen bieten, um die Fähigkeiten der Flow CAM mit einigen Routineparametern (z.B. Mikroskopzählungen und Chlorophyll-Messungen) zu vergleichen und ihre Glaubwürdigkeit zu testen. Große Erwartungen wurden in die Flow CAM gesetzt, da sie im Vergleich zu bisherigen Partikelzählern digitale Bilder macht, die es qualitativ ermöglichen, Verteilungsmuster von erkennbaren Partikeln zu bestimmen. Jeder digital erfasste Partikel erhält eine Art Signatur bestehend aus zwanzig verschiedenen Flow CAM Parametern (z.B. Länge, Breite, Fluoreszenz), die es theoretisch ermöglichen sollten eine Gruppe oder eine Art eindeutig zu charakterisieren. Anhand der Signatur sollte es in erneuten Messungen leicht möglich sein die so definierten Partikel wieder zu finden, was eine Quantifizierung enorm vereinfachen würde. In manchen Fällen dürfte dies auch funktionieren, jedoch zeigen die hier vorliegenden Ergebnisse, dass eher darauf zu achten ist, wie die Flow CAM in den einzelnen Messmodi Partikel misst, um glaubhafte Zählraten überhaupt zu erhalten.

In Kapitel II werden deshalb verschiedenste Faktoren präsentiert, die die Flow CAM Ergebnisse im Fluoreszenz-Modus enorm beeinträchtigen. Dazu zählen bestimmte Einstellungen der digitalen Kamera bzw. Einstellungen des Fluoreszenz-Detektors, die für diesen Messmodus sehr wichtig sind. Es besteht die Gefahr, dass Partikel deshalb nicht fotografiert werden, weil sie entweder von der Kamera nicht erkannt werden oder weil sie zu wenig Fluoreszenz besitzen. Viel wichtiger sind aber noch die Auswirkungen von Partikeldichten und Pumpgeschwindigkeiten, die über den Erfolg der Flow CAM Messungen entscheiden. Zudem darf die gemessene Fluoreszenz von einem Partikel nicht als absolute Fluoreszenz gewertet werden, sondern ist auch hier abhängig von der Pumpgeschwindigkeit.

In Kapitel III wird die Fähigkeit der Flow CAM im Feld unter Beweis gestellt. Um das gesamte Größenspektrum des Phytoplanktons und Mikrozooplanktons abdecken zu können, mussten drei verschiedene Größenfraktionen gemessen werden. Alle drei Größen wurden mit zwei der drei möglichen Messmodi der Flow CAM gemessen (AutoImage Modus und

Fluoreszenz-Modus). Die Ergebnisse zeigen, dass der AutoImage modus der Flow CAM zur Bestimmung der Gesamtpartikelkonzentration im Wasser zuverlässige Ergebnisse erzielt. Jedoch werden in diesem Messmodus hauptsächlich Detrituspartikel aufgenommen. Der Fluoreszenz-Modus hingegen sollte theoretisch nur fluoreszierende Partikel aufnehmen, um die Anzahl an Detritus zu verringern. Dies ist jedoch nicht der Fall, weil eine Vielzahl an Detrituspartikeln mit fluoreszierenden Partikeln mit gemessen wird. Im Vergleich zu den Zählraten unter dem Mikroskop unterschätzt die Flow CAM die Abundanz von einzelnen Planktonarten in fast allen Fällen. Dies lässt sich hauptsächlich auf den relativ hohen Schwellenwert des Fluoreszenz-Detektors und auf die variablen Pumpgeschwindigkeiten zurückführen, die verwendet wurden, um die Kontaktraten mit fluoreszierenden Partikeln (Plankton) zu erhöhen.

Kapitel IV beschäftigt sich zunächst mit den Auswirkungen von unterschiedlichen Futterqualitäten auf den phagotrophen Flagellaten *Oxyrrhis marina*. Bis jetzt ist wenig bekannt darüber, inwieweit solch primitiv organisierten Einzeller von unterschiedlichen Futterqualitäten betroffen sind. In mehreren Fraßexperimenten zeigt sich dass dieser Einzeller nicht zwischen unterschiedlichen Futterqualitäten unterscheidet; somit scheint die Futteraufnahme qualitätsunabhängig zu sein. Allerdings wirkt sich Phosphor limitiertes Futter negativ auf die Wachstumsraten von *O. marina* aus. Stickstoff limitiertes Futter hat dagegen keine negativen Auswirkungen. Der Versuch dies anhand von unterschiedlichen Respirationsraten zu erklären, klappt jedoch nicht, da *O. marina* in beiden Fällen mehr respiriert, um den überschüssigen Kohlenstoff auszuscheiden. Deshalb scheint Phosphor der begrenzende Faktor zu sein, der schnell wachsende Einzeller limitiert.

In wie weit *O. marina* abhängig von seiner elementaren Ausstattung zwischen Stickstoff und Phosphor limitierendem Futter selektieren kann, wird mit Hilfe der Flow CAM in Kapitel V gezeigt. Die Ergebnisse zeigen jedoch keine Selektion, sondern nur unterschiedliche Aufnahmeleistungen abhängig davon, was vorher gefressen wurde. Wenn *O. marina* allerdings das Futter nicht in einer Mischung erhält, sondern einzeln, dann fressen sie signifikant mehr von dem Futter, das sie zuvor nicht bekommen haben. Das bedeutet, dass *O. marina* sowohl den Mangel eines limitierenden Elementes in der eigenen Zelle, aber auch die Nährstoffzusammensetzung des Futters erkennt. Die Tatsache, dass *O. marina* aber auch weiterhin das Futter frisst, das zuvor schon gefressen wurde, zeigt, dass Zellvorgänge, die die Exkretion überschüssiger bzw. das Zurückhalten limitierender Nährstoffe bestimmen, entscheidender sind als die Selektion zwischen unterschiedlichen Futterqualitäten.

Die vorliegende Arbeit soll dazu dienen, um einige wichtige Schwachpunkte der Flow CAM aufzuzeigen. Diese Schwachpunkte gilt es weiter auszuarbeiten, um sicherzustellen, dass die Flow CAM eventuell in Zukunft automatische Zählaufgaben übernehmen kann. Welche Rolle heterotrophe Protisten im marinen Nahrungsnetz spielen können und in wie weit sie von unterschiedlichen Futterqualitäten betroffen sind zeigen die hier durchgeführten Experimente mit dem Modellorganismus *O. marina*. Weitere Untersuchungen sind notwendig um herauszufinden inwiefern sich diese Ergebnisse auf andere Protisten übertragen lassen.

REFERENCES

- Aberle N, Malzahn AM (2007) Interspecific and nutrient-dependent variations in stable isotope fractionation: experimental studies simulating pelagic multitrophic systems. *Oecologia* 154: 291-303
- Anderson TR, Hessen DO, Elser JJ, Urabe J (2005) Metabolic stoichiometry and the fate of excess carbon and nutrients in consumers. *Am Nat* 165: 1-15
- Andersson A, Larsson U, Hagström A (1986) Size-selective grazing by a microflagellate on pelagic bacteria. *Mar Ecol Prog Ser* 33: 51-57
- Augustin CB, Boersma M (2006) Effects of nitrogen stressed algae on different *Acartia* species. *J Plankton Res* 28: 429-436
- Azam F, Fenchel T, Field JG, Gray JS, Meyerreil LA, Thingstad F (1983) The ecological role of water-column microbes in the Sea. *Mar Ecol Prog Ser* 10: 257-263
- Barlow RG, Burkill PH, Mantoura RFC (1988) Grazing and degradation of algal pigments by marine protozoan *Oxyrrhis marina*. *J Exp Mar Biol Ecol* 119: 119-129
- Benfield MC, Grosjean P, Culverhouse PF, Irigoien X, Sieracki ME, Lopez-Urrutia A, Dam HG, Hu Q, Davis CS, Hansen A, Pilskaln CH, Riseman EM, Schultz H, Utgoff PE, Gorsky G (2007) RAPID Research on Automated Plankton Identification. *Oceanography* 20: 172-187
- Boersma M (2000) The nutritional quality of P-limited algae for *Daphnia*. *Limnol Oceanogr* 45: 1157-1161
- Boersma M, Aberle N, Hantzsche FM, Schoo KL, Wiltshire KH, Malzahn AM (2008) Nutritional limitation travels up the food chain. *International Review of Hydrobiology* 93: 479-488
- Boersma M, Kreutzer C (2002) Life at the edge: Is food quality really of minor importance at low quantities? *Ecology* 83: 2552-2561
- Burns CW (1995) Effects of crowding and different food levels on growth and reproductive investment of *Daphnia*. *Oecologia* 101: 234-244
- Burns CW (2000) Crowding-induced changes in growth, reproduction and morphology of *Daphnia*. *Freshw Biol* 43: 19-29
- Buskey EJ, Hyatt CJ (2006a) Use of the FlowCAM for semi-automated recognition and enumeration of red tide cells (*Karenia brevis*) in natural plankton samples. *Harmful Algae* 5: 685-692

- Buskey EJ, Hyatt CJ (2006b) Use of the FlowCAM for semi-automated recognition and enumeration of red tide cells (*Karenia brevis*) in natural plankton samples. *Harmful Algae* 5: 685-692
- Buskey EJ, Stoecker DK (1988) Locomotory patterns of the planktonic ciliate *Favella* sp.: Adaptations for remaining within food patches. *Bull Mar Sci* 43: 783-796
- Caron DA, Lim EL, Sanders RW, Dennett MR, Berninger UG (2000) Responses of bacterioplankton and phytoplankton to organic carbon and inorganic nutrient additions in contrasting oceanic ecosystems. *Aquat Microb Ecol* 22: 175-184
- Chrzanowski TH, Simek K (1990) Prey-size selection by freshwater flagellated protozoa. *Limnol Oceanogr* 35: 1429-1436
- Clark LL, Ingall ED, Benner R (1998) Marine phosphorus is selectively remineralized. *Nature* 393: 426-426
- Claustre H, Hooker SB, Van Heukelem L, Berthon JF, Barlow R, Ras J, Sessions H, Targa C, Thomas CS, van der Linde D, Marty JC (2004) An intercomparison of HPLC phytoplankton pigment methods using in situ samples: application to remote sensing and database activities. *Marine Chemistry* 85: 41-61
- Cowles TJ, Olson RJ, Chisholm SW (1988) Food selection by copepods: Discrimination on the basis of food quality. *Mar Biol* 100: 41-49
- Culverhouse PF (2007) Human and machine factors in algae monitoring performance. *Ecological Informatics* 2: 361-366
- Cushing DH (1995) The long-term relationship between zooplankton and fish. *ICES J Mar Sci* 52: 611-626
- Darchambeau F, Faerovig PJ, Hessen DO (2003) How *Daphnia* copes with excess carbon in its food. *Oecologia* 136: 336-346
- Davidson K, Roberts EC, Wilson AM, Mitchell E (2005) The role of prey nutritional status in governing protozoan nitrogen regeneration efficiency. *Protist* 156: 45-62
- DeMott WR (1998) Utilization of a cyanobacterium and a phosphorus deficient green alga as complementary resources by daphnids. *Ecology* 79: 2463-2481
- DeMott WR, Gulati RD (1999) Phosphorus limitation in *Daphnia*: Evidence from a long term study of three hypereutrophic Dutch lakes. *Limnol Oceanogr* 44: 1557-1564
- DeMott WR, Gulati RD, Siewertsen K (1998) Effects of phosphorus-deficient diets on the carbon and phosphorus balance of *Daphnia magna*. *Limnol Oceanogr* 43: 1147-1161

- DeMott WR, Gulati RD, Van Donk E (2001) Effects of dietary phosphorus deficiency on the abundance, phosphorus balance, and growth of *Daphnia cucullata* in three hypereutrophic Dutch lakes. *Limnol Oceanogr* 46: 1871-1880
- Diehl S (2002) Phytoplankton, light, and nutrients in a gradient of mixing depths: Theory. *Ecology* 83: 386-398
- Dubelaar GBJ, Geerders PJF, Jonker RR (2004) High frequency monitoring reveals phytoplankton dynamics. *Journal of Environmental Monitoring* 6: 946-952
- Ederington MC, Mcmanus GB, Harvey HR (1995) Trophic transfer of fatty acids, sterols, and a triterpenoid alcohol between bacteria, a ciliate, and the copepod *Acartia tonsa*. *Limnol Oceanogr* 40: 860-867
- Elser JJ (2002) Biological stoichiometry from genes to ecosystems: ideas, plans, and realities. *Integrative and Comparative Biology* 42: 1226-1226
- Elser JJ, Hassett RP (1994) A stoichiometric analysis of the zooplankton-phytoplankton interaction in marine and freshwater ecosystems. *Nature* 370: 211-213
- Fenchel T (1982a) Ecology of heterotrophic microflagellates. I. Some important forms and their functional morphology. *Mar Ecol Prog Ser* 8: 211-223
- Fenchel T (1982b) Ecology of heterotrophic microflagellates. II. Bioenergetics and growth. *Mar Ecol Prog Ser* 8: 225-231
- Fenchel T (1982c) Ecology of heterotrophic microflagellates. IV. Quantitative occurrence and importance as bacterial consumers. *Mar Ecol Prog Ser* 9: 35-42
- Fenchel T (1988) Marine plankton food chains. *Annual Review of Ecology and Systematics* 19: 19-38
- Fenchel T (2008) The microbial loop-25 years later. *J Exp Mar Biol Ecol* 366: 99-103
- Fenchel T, Blackburn N (1999) Motile chemosensory behaviour of phagotrophic protists: Mechanisms for and efficiency in congregating at food patches. *Protist* 150: 325-336
- Flynn KJ, Davidson K (1993) Predator-prey interactions between *Isochrysis galbana* and *Oxyrrhis marina* II. Release of nonprotein amines and faeces during predation of *Isochrysis*. *J Plankton Res* 15: 893-905
- Flynn KJ, Davidson K, Cunningham A (1996) Prey selection and rejection by a microflagellate: Implications for the study and operation of microbial food webs. *J Exp Mar Biol Ecol* 196: 357-372
- Frost BW (1972) Effects of size and concentration of food particles on feeding behavior of marine planktonic copepod *Calanus pacificus*. *Limnol Oceanogr* 17: 805-815

- Frost PC, Benstead JP, Cross WF, Hillebrand H, Larson JH, Xenopoulos MA, Yoshida T (2006) Threshold elemental ratios of carbon and phosphorus in aquatic consumers. *Ecol Lett* 9: 774-779
- Frost PC, Evans-White MA, Finkel ZV, Jensen TC, Matzek V (2005) Are you what you eat? Physiological constraints on organismal stoichiometry in an elementally imbalanced world. *Oikos* 109: 18-28
- Gismervik I (2006) Top-down impact by copepods on ciliate numbers and persistence depends on copepod and ciliate species composition. *J Plankton Res* 28: 499-507
- Gismervik I, Andersen T (1997) Prey switching by *Acartia clausi*: experimental evidence and implications of intraguild predation assessed by a model. *Mar Ecol Prog Ser* 157: 247-259
- Goldman JC, Caron DA, Dennett MR (1987) Nutrient cycling in a microflagellate food chain: IV. Phytoplankton-microflagellate interactions. *Mar Ecol Prog Ser* 38: 75-87
- Goldman JC, Dennett MR, Gordin H (1989) Dynamics of herbivorous grazing by the heterotrophic dinoflagellate *Oxyrrhis marina*. *J Plankton Res* 11: 391-407
- Gonzalez JM, Sherr EB, Sherr BF (1993) Differential feeding by marine flagellates on growing versus starving, and on motile versus nonmotile, bacterial prey. *Mar Ecol Prog Ser* 102: 257-267
- Goransson B (1990) Improved accuracy in the measurement of particle size distribution with a Coulter Counter equipped with a hydrodynamically focused aperture. *Particle & Particle Systems Characterization* 7: 6-10
- Granum E, Kirkvold S, Mykkestad SM (2002) Cellular and extracellular production of carbohydrates and amino acids by the marine diatom *Skeletonema costatum*: diel variations and effects of N depletion. *Mar Ecol Prog Ser* 242: 83-94
- Grasshoff K, Kremling K, Ehrhardt M (1999) *Methods of Seawater Analysis*. Wiley-VCH, Weinheim, New York, Chicester, Brisbane, Singapore, Toronto
- Grover JP, Chrzanowski TH (2006) Stoichiometry and growth kinetics in the "smallest zooplankton" - phagotrophic flagellates. *Arch Hydrobiol* 167: 467-487
- Guillard RRL (1975) *Culture of phytoplankton for feeding marine invertebrates*. Plenum Press, New York
- Guillard RRL, Ryther JH (1962) Studies of marine planktonic diatoms. I. *Cyclotella nana* Hustedt and *Detonula confervacea* Cleve. *Can J Microbiol* 8: 229-239
- Haeckel E (1890) *Plankton Studien. Vergleichende Untersuchung über die Bedeutung und Zusammensetzung der pelagischen Fauna und Flora*

- Hammer A, Gruttner C, Schumann R (2001) New biocompatible tracer particles: use for estimation of microzooplankton grazing, digestion, and growth rates. *Aquat Microb Ecol* 24: 153-161
- Hansen FC, Witte HJ, Passarge J (1996) Grazing in the heterotrophic dinoflagellate *Oxyrrhis marina*: Size selectivity and preference for calcified *Emiliana huxleyi* cells. *Aquat Microb Ecol* 10: 307-313
- Hantzsche FM, Boersma M (2010) Dietary-induced responses in the phagotrophic flagellate *Oxyrrhis marina*. *Mar Biol* 157: 1641-1651
- Harfield JG, Wharton RA (1988) Increased resolution of size distributions with the Coulter Counter. *Particle & Particle Systems Characterization* 5: 29-37
- Hazzard SE, Kleppel GS (2003) Egg production of the copepod *Acartia tonsa* in Florida Bay: role of fatty acids in the nutritional composition of the food environment. *Mar Ecol Prog Ser* 252: 199-206
- Helgen JC (1987) Feeding rate inhibition in crowded *Daphnia pulex*. *Hydrobiologia* 154: 113-119
- Hessen DO, Agren GI, Anderson TR, Elser JJ, De Ruiter PC (2004) Carbon sequestration in ecosystems: The role of stoichiometry. *Ecology* 85: 1179-1192
- Hessen DO, Faerovig PJ, Andersen T (2002) Light, nutrients, and P : C ratios in algae: Grazer performance related to food quality and quantity. *Ecology* 83: 1886-1898
- Howarth RW (1988) Nutrient limitation of net primary production in marine ecosystems. *Annual Review of Ecology and Systematics* 19: 89-110
- Ide K, Takahashi K, Kuwata A, Nakamachi M, Saito H (2008) A rapid analysis of copepod feeding using FlowCAM. *Journal of Plankton Research* 30: 275-281
- Jensen TC, Anderson TR, Daufresne M, Hessen DO (2006) Does excess carbon affect respiration of the rotifer *Brachionus calyciflorus* Pallas? *Freshw Biol* 51: 2320-2333
- Jensen TC, Hessen DO (2007) Does excess dietary carbon affect respiration of *Daphnia*? *Oecologia* 152: 191-200
- Jensen TC, Verschoor AM (2004) Effects of food quality on life history of the rotifer *Brachionus calyciflorus* Pallas. *Freshw Biol* 49: 1138-1151
- Jeong HJ, Kim JS, Yeong DY, Kim ST, Kim TH, Park MG, Lee CH, Seong KA, Kang NS, Shim JH (2003) Feeding by the heterotrophic dinoflagellate *Oxyrrhis marina* on the red-tide raphidophyte *Heterosigma akashiwo*: a potential biological method to control red tides using mass-cultured grazers. *J Eukaryot Microbiol* 50: 274-282

- Jeong HJ, Song JE, Kang NS, Kim S, Yoo YD, Park JY (2007) Feeding by heterotrophic dinoflagellates on the common marine heterotrophic nanoflagellate *Cafeteria* sp. *Mar Ecol Prog Ser* 333: 151-160
- Johnson MP (2000) Physical control of plankton population abundance and dynamics in intertidal rock pools. *Hydrobiologia* 440: 145-152
- Jonasdottir SH (1994) Effects of food quality on the reproductive success of *Acartia tonsa* and *Acartia hudsonica*: Laboratory observations. *Mar Biol* 121: 67-81
- Jumars PA, Penry DL, Baross JA, Perry MJ, Frost BW (1989) Closing the microbial loop: Dissolved carbon pathway to heterotrophic bacteria from incomplete ingestion, digestion and absorption in animals. *Deep-Sea Research Part A: Oceanographic Research Papers* 36: 483-495
- Kimance SA, Atkinson D, Montagnes DJS (2006) Do temperature-food interactions matter? Responses of production and its components in the model heterotrophic flagellate *Oxyrrhis marina*. *Aquat Microb Ecol* 42: 63-73
- Kiorboe T (1998) Population regulation and role of mesozooplankton in shaping marine pelagic food webs. *Hydrobiologia* 363: 13-27
- Klein-Breteler WCM, Schogt N, Baas M, Schouten S, Kraay GW (1999) Trophic upgrading of food quality by protozoans enhancing copepod growth: role of essential lipids. *Mar Biol* 135: 191-198
- Klein B, Gieskes WWC, Kraay GG (1986) Digestion of chlorophylls and carotenoids by the marine protozoan *Oxyrrhis marina* studied by H.P.L.C analysis of algal pigments. *J Plankton Res* 8: 827-836
- Kleppel GS (1993) On the diets of calanoid copepods. *Mar Ecol Prog Ser* 99: 183-195
- Kleppel GS, Burkart CA (1995) Egg production and the nutritional environment of *Acartia tonsa*: The role of food quality in copepod nutrition. *ICES J Mar Sci* 52: 297-304
- Kolowitz LC, Ingall ED, Benner R (2001) Composition and cycling of marine organic phosphorus. *Limnol Oceanogr* 46: 309-320
- Koski M (1999) Carbon : nitrogen ratios of Baltic Sea copepods - indication of mineral limitation? *J Plankton Res* 21: 1565-1573
- Landry MR, Calbet A (2004) Microzooplankton production in the oceans. *ICES J Mar Sci* 61: 501-507
- Lee JJ (1980) Informational energy flow as an aspect of protozoan nutrition. *J Protozool* 27: 5-9

- Littman RA, van Oppen MJH, Willis BL (2008) Methods for sampling free-living *Symbiodinium* (zooxanthellae) and their distribution and abundance at Lizard Island (Great Barrier Reef). *J Exp Mar Biol Ecol* 364: 48-53
- Lund JWG, Kipling C, Le Cren ED (1958) The inverted microscope method of estimating algal numbers and the statistical basis of estimations by counting. *Hydrobiologia* 11
- Malzahn AM, Aberle N, Clemmesen C, Boersma M (2007) Nutrient limitation of primary producers affects planktivorous fish condition. *Limnol Oceanogr* 52: 2062-2071
- Malzahn AM, Hantzsche F, Schoo KL, Boersma M, Aberle N (2010) Differential effects of nutrient-limited primary production on primary, secondary or tertiary consumers. *Oecologia* 162: 35-48
- Martel CM (2006) Prey location, recognition and ingestion by the phagotrophic marine dinoflagellate *Oxyrrhis marina*. *J Exp Mar Biol Ecol* 335: 210-220
- Martel CM (2009) Conceptual bases for prey biorecognition and feeding selectivity in the microplanktonic marine phagotroph *Oxyrrhis marina*. *Microbial Ecology* 57: 589-597
- Martens P, van Beusekom JEE (2008) Zooplankton response to a warmer northern Wadden Sea. *Helgoland Marine Research* 62: 67-75
- Martin-Creuzburg D, von Elert E (2004) Impact of 10 dietary sterols on growth and reproduction of *Daphnia galeata*. *Journal of Chemical Ecology* 30: 483-500
- McCave IN (1984) Size spectra and aggregation of suspended particles in the deep ocean. *Deep Sea Research Part A* 31: 329-352
- Menden-Deuer S, Lessard EJ, Satterberg J (2001) Effect of preservation on dinoflagellate and diatom cell volume and consequences for carbon biomass predictions. *Marine Ecology-Progress Series* 222: 41-50
- Metfies K, Berzano M, Mayer C, Roosken P, Gualerzi C, Medlin L, Muyzer G (2007) An optimized protocol for the identification of diatoms, flagellated algae and pathogenic protozoa with phylochips. *Molecular Ecology Notes* 7: 925-936
- Mitra A, Flynn KJ (2005) Predator-prey interactions: is 'ecological stoichiometry' sufficient when good food goes bad? *J Plankton Res* 27: 393-399
- Montagnes DJS, Lessard EJ (1999) Population dynamics of the marine planktonic ciliate *Strombidinopsis multiaurisy*: its potential to control phytoplankton blooms. *Aquat Microb Ecol* 20: 167-181
- Nakano S (1994) Carbon : nitrogen : phosphorus ratios and nutrient regeneration of a heterotrophic flagellate fed on bacteria with different elemental ratios. *Arch Hydrobiol* 129: 257-271

- Opik H, Flynn KJ (1989) The digestive process of the dinoflagellate *Oxyrrhis marina* Dujardin feeding on the chlorophyte *Dunaliella primolecta* Butcher: a combined study of ultrastructure and free amino acids. *New Phyt* 113: 143-151
- Pedersen MF, Hansen PJ (2003) Effects of high pH on the growth and survival of six marine heterotrophic protists. *Mar Ecol Prog Ser* 260: 33-41
- Plath K, Boersma M (2001) Mineral limitation of zooplankton: Stoichiometric constraints and optimal foraging. *Ecology* 82: 1260-1269
- Pomeroy LR (1974) Ocean's food web, a changing paradigm. *Bioscience* 24: 499-504
- Raabe T, Wiltshire KH (2009) Quality control and analyses of the long-term nutrient data from Helgoland Roads, North Sea. *J Sea Res* 61: 3-16
- Raubenheimer D, Jones SA (2006) Nutritional imbalance in an extreme generalist omnivore: tolerance and recovery through complementary food selection. *Anim Behav* 71: 1253-1262
- Roberts EC, Zubkov MV, Martin-Cereceda M, Novarino G, Wootton EC (2006) Cell surface lectin-binding glycoconjugates on marine planktonic protists. *FEMS Microbiol Lett* 265: 202-207
- Rothhaupt KO (1995) Algal nutrient limitation affects rotifer growth rate but not ingestion rate. *Limnol Oceanogr* 40: 1201-1208
- Ryther JH (1969) Photosynthesis and fish production in the sea. *Science* 166: 72-76
- Sanders RW, Berninger UG, Lim EL, Kemp PF, Caron DA (2000) Heterotrophic and mixotrophic nanoplankton predation on picoplankton in the Sargasso Sea and on Georges Bank. *Mar Ecol Prog Ser* 192: 103-118
- Sanders RW, Caron DA, Berninger UG (1992) Relationships between bacteria and heterotrophic nanoplankton in marine and fresh waters: An inter-ecosystem comparison. *Mar Ecol Prog Ser* 86: 1-14
- See JH, Campbell L, Richardson TL, Pinckney JL, Shen R, Guinasso Jr. NL (2005a) Combining new technologies for determination of phytoplankton community structure on the northern Gulf of Mexico. *Journal of Phycology* 41: 305-310
- See JH, Campbell L, Richardson TL, Pinckney JL, Shen RJ, Guinasso NL (2005b) Combining new technologies for determination of phytoplankton community structure in the northern Gulf of Mexico. *Journal of Phycology* 41: 305-310
- Selph KE, Landry MR, Laws EA (2003) Heterotrophic nanoflagellate enhancement of bacterial growth through nutrient remineralization in chemostat culture. *Aquat Microb Ecol* 32: 23-37

- Sherr EB, Sherr BF (1994) Bacterivory and herbivory: Key roles of phagotrophic protists in pelagic food webs. *Microbial Ecology* 28: 223-235
- Sieracki CK, Sieracki ME, Yentsch CS (1998) An imaging-in-flow system for automated analysis of marine microplankton. *Marine Ecology Progress Series* 168: 285-296
- Simons JWIM (1970) Characterization of somatic cells by determination of their volumes with a Coulter Counter. *J Cell Biol* 46: 610-612
- Skovgaard A (1996) Mixotrophy in *Fragilidium subglobosum* (Dinophyceae): Growth and grazing responses as functions of light intensity. *Mar Ecol Prog Ser* 143: 247-253
- Sommer U (1996) Plankton ecology: The past two decades of progress. *Naturwissenschaften* 83: 293-301
- Sommer U, Stibor H, Katchakis A, Sommer F, Hansen T (2002) Pelagic food web configurations at different levels of nutrient richness and their implications for the ratio fish production: primary production. *Hydrobiologia* 484: 11-20
- Sterling Jr. MC, Bonner JS, Ernest ANS, Page CA, Autenrieth RL (2004) Characterizing aquatic sediment-oil aggregates using in situ instruments. *Marine Pollution Bulletin* 48: 533-542
- Sterner RW (1993) *Daphnia* growth on varying quality of *Scenedesmus*: Mineral limitation of zooplankton. *Ecology* 74: 2351-2360
- Sterner RW, Elser JJ (2002) *Ecological Stoichiometry: the biology of elements from molecules to the biosphere*. Princeton University Press, Princeton, New Jersey, USA
- Sterner RW, Robinson JL (1994) Thresholds for growth in *Daphnia magna* with high and low phosphorus diets. *Limnol Oceanogr* 39: 1228-1232
- Sterner RW, Smith RF (1993) Clearance, ingestion and release of N and P by *Daphnia obtusa* feeding on *Scenedesmus acutus* of varying quality. *Bull Mar Sci* 53: 228-239
- Stoecker DK, Capuzzo JM (1990) Predation on protozoa: Its importance to zooplankton. *J Plankton Res* 12: 891-908
- Stoecker DK, Gifford DJ, Putt M (1994) Preservation of marine planktonic ciliates - losses and cell shrinkage during fixation. *Mar Ecol Prog Ser* 110: 293-299
- Strom SL, Benner R, Ziegler S, Dagg MJ (1997) Planktonic grazers are a potentially important source of marine dissolved organic carbon. *Limnol Oceanogr* 42: 1364-1374
- Tang KW, Dam HG (1999) Limitation of zooplankton production: beyond stoichiometry. *Oikos* 84: 537-542

- Tang KW, Taal M (2005) Trophic modification of food quality by heterotrophic protists: species-specific effects on copepod egg production and egg hatching. *J Exp Mar Biol Ecol* 318: 85-98
- Tarran GA (1991) Aspects of the grazing behaviour of the marine dinoflagellate *Oxyrrhis marina*, Dujardin
- Thingstad TF, Skjoldal EF, Bohne RA (1993) Phosphorus cycling and algal-bacterial competition in Sandsfjord, western Norway. *Mar Ecol Prog Ser* 99: 239-259
- Tillmann U, Reckermann M (2002) Dinoflagellate grazing on the raphidophyte *Fibrocapsa japonica*. *Aquat Microb Ecol* 26: 247-257
- Tilman D, Kilham SS, Kilham P (1982) Phytoplankton community ecology: The role of limiting nutrients. *Annual Review of Ecology and Systematics* 13: 349-372
- Uitto A, Hallfors S (1997) Grazing by mesozooplankton and metazoan microplankton on nanophytoplankton in a mesocosm experiment in the northern Baltic. *J Plankton Res* 19: 655-673
- Urabe J, Clasen J, Sterner RW (1997) Phosphorus limitation of *Daphnia* growth: Is it real? *Limnol Oceanogr* 42: 1436-1443
- Utermöhl H (1958) Zur Vervollkommnung der quantitativen Phytoplankton-Methodik. *Mitt. Verein. Theor. Angew. Limnol.* 9: 1-38
- Vargas CA, Escribano R, Poulet S (2006) Phytoplankton food quality determines time windows for successful zooplankton reproductive pulses. *Ecology* 87: 2992-2999
- Verity PG (1985) Grazing, respiration, excretion, and growth rates of tintinnids. *Limnol Oceanogr* 30: 1268-1282
- Verity PG (1988) Chemosensory behavior in marine planktonic ciliates. *Bull Mar Sci* 43: 772-782
- Verity PG (1991a) Feeding in planktonic protozoans: evidence for non-random acquisition of prey. *J Protozool* 38: 69-76
- Verity PG (1991b) Measurement and simulation of prey uptake by marine planktonic ciliates fed plastidic and aplastidic nanoplankton. *Limnol Oceanogr* 36: 729-750
- von Elert E (2002) Determination of limiting polyunsaturated fatty acids in *Daphnia galeata* using a new method to enrich food algae with single fatty acids. *Limnol Oceanogr* 47: 1764-1773
- Vrede T, Persson J, Aronsen G (2002) The influence of food quality (P : C ratio) on RNA : DNA ratio and somatic growth rate of *Daphnia*. *Limnol Oceanogr* 47: 487-494

- Wenger J, Nowak JS, Kai O, Franklin RM (1982) Display and analysis of cell size distributions with a Coulter Counter interfaced to an Apple II microcomputer. *Journal of Immunological Methods* 54: 385-392
- Wetz MS, Wheeler PA (2007) Release of dissolved organic matter by coastal diatoms. *Limnol Oceanogr* 52: 798-807
- White TCR (1993) *The inadequate environment*. Springer Verlag, Berlin, New York
- Wiadnyana NN, Rassoulzadegan F (1989) Selective feeding of *Acartia clausi* and *Centropages typicus* on microzooplankton. *Mar Ecol Prog Ser* 53: 37-45
- Wiltshire KH, Dürselen CD (2004) Revision and quality analyses of the Helgoland Reede long-term phytoplankton data archive. *Helgoland Marine Research* 58: 252-268
- Wiltshire KH, Malzahn AM, Wirtz K, Greve W, Janisch S, Mangelsdorf P, Manly BFJ, Boersma M (2008) Resilience of North Sea phytoplankton spring bloom dynamics: An analysis of long-term data at Helgoland Roads. *Limnol Oceanogr* 53: 1294-1302
- Wiltshire KH, Manly BFJ (2004) The warming trend at Helgoland Roads, North Sea: Phytoplankton response. *Helgoland Marine Research* 58: 269-273
- Wootton EC, Zubkov MV, Jones DH, Jones RH, Martel CM, Thornton CA, Roberts EC (2007) Biochemical prey recognition by planktonic protozoa. *Environ Microbiol* 9: 216-222
- Zarauz L, Irigoien X (2008) Effects of Lugol's fixation on the size structure of natural nano-microplankton samples, analyzed by means of an automatic counting method. *Journal of Plankton Research* 30: 1297-1303
- Zimmermann U, Groves M, Schnabl H, Pilwat G (1980) Development of a new Coulter Counter System: Measurement of the volume, internal Conductivity, and dielectric breakdown voltage of a single guard cell protoplast of *Vicia faba*. *J Membr Biol* 52: 37-50

DANKSAGUNG

Mein erster Dank geht an Prof. Dr. Maarten Boersma für die Betreuung meiner Arbeit, seine fortwährende Unterstützung und Diskussionsbereitschaft, sowie sein äußerst menschliches Einfühlungsvermögen, wenn die Dinge mal nicht so laufen, wie man es sich gerne wünscht. Ich habe viel, sowohl Fachliches, als auch Menschliches hinzugelernt!

Herrn Dr. Friedhelm Schroeder danke ich für die Betreuung dieser Arbeit.

Dann möchte ich mich bei meinen Kolleginnen und Kollegen des Helgoländer Foodweb-Projektes für die gute Zusammenarbeit bedanken: Alexandra Kraberg, Antje Wichels, Arne Malzahn, Cedric Meunier, Christina Gebühr, Gunnar Gerdts, Karen Wiltshire, Katherina Schoo, Martin Löder, Nicole Aberle-Malzahn und Petra Brand. Außerdem danke ich den vielen Praktikanten, FÖJlern, Bachelor-, Master- Studenten und Diplomanden, sowie allen anderen Mitarbeitern der BAH.

Einen ganz besonderen Dank richte ich an die technischen Assistenten der BAH Bettina Oppermann, Daniel Schütz, Julia Haafke, Kristine Carstens, Michael Janke, Silvia Peters, Uwe Nettelmann, sowie den Haustechnikern Detlef Frier, Heino Peters, Helgo Denker, Joachim Kühn und Pio. Ihr seid das Rückgrat allen wissenschaftlichen Arbeitens!

Der Crew der „Aade“ danke ich für das unermüdliche Heranschaffen von Wasserproben!

Kathleen Herrig und Rebecca Störmer danke ich für ihre große Freundschaft, in guten und in schlechten Zeiten! Auch meinen anderen lieb gewonnenen Freunden auf der Insel Angel Urzua, Cedric Meunier, Christina Gebühr, Jan Knott, Judith Lucas, Karin Näpfel, Karin Röder, Katherina Schoo, Martin Löder, Nicole Hielscher, Nils Gülzow und Sonja Oberbeckmann danke ich für alles was wir zusammen erlebt haben. Ich bin immer für Euch da!!!

Meiner lieben Freundin Cathrien danke ich für die schöne Zeit auf der Insel, ihre Geduld und Bereitschaft mich in regelmäßigen Abständen zu besuchen. Wir beide werden nun viel mehr Zeit füreinander haben, versprochen!

Und zu guter letzt danke ich meiner lieben Familie, meinen Eltern und Uschi für ihre unablässige Unterstützung und Liebe, meinen Idealismus zu bewahren und ihn auch in Zukunft auszuleben. Ein großer Dank an Basti, Benedikt und Linda, die mir immer das gute Gefühl gegeben haben bei ihnen „zu Hause“ zu sein, auch wenn die Zeit, die man miteinander verbracht hat, viel zu kurz war.

CURRICULUM VITAE

PERSÖNLICHE ANGABEN

Familienstand:	ledig
Staatsangehörigkeit:	deutsch
Geburtsdatum:	17.04.1974
Geburtsort:	München

BERUFSERFAHRUNG

01.07.04- 31.10.05	Marie Curie Stipendiat an der Trondheimer Biologischen Station (TBS), NTNU Trondheim, Mitarbeit am „ <i>Calanus</i> -Projekt“ bei Prof. Dr. Olav Vadstein
15.09.06- heute	Doktorand im „Helgoländer Foodweb Projekt“ an der Biologischen Anstalt Helgoland (BAH), Alfred Wegener Institut für Polar- und Meeresforschung (AWI), finanziert vom GKSS Forschungszentrum in Geesthacht.

AUSBILDUNG

1985-1995	Reuchlin-Gymnasium Ingolstadt, Abiturfächer: Altgriechisch, Biologie, Geschichte, Deutsch
1996	Zivildienst im Klinikum Ingolstadt, chirurgische Intensivstation
1996-1998	Studium der Biologie an der Eberhard-Karls-Universität Tübingen; Vordiplom
1998-2003	Hauptstudium an der Ludwig-Maximilians-Universität München; Hauptfach: Ökologie, Nebenfächer: Botanik, Mikrobiologie, Landschaftsplanung und Naturschutz, Abschluss: Diplombiologe (Note: „sehr gut“, März 2003) Diplomarbeit bei PD Dr Herwig Stibor, Aquatische Ökologie (LMU): „Einfluss von Rippenquallen auf das pelagisch, marine Nahrungsnetz-Zooplankton“; Feldarbeiten und Mesokosmenversuch in Norwegen (TBS)

TÄTIGKEITEN NEBEN DEM STUDIUM

SS 1998	Tutor Botanischer Bestimmungskurs bei Prof. Dr. Meike Piepenbring
05/2006-08/2006	Tätigkeit als wissenschaftliche Hilfskraft bei Prof. Dr. Sebastian Diehl und PD Dr. Herwig Stibor

SPRACHKENNTNISSE

Englisch (fließend in Wort und Schrift)
Norwegisch(Grundkenntnisse)

PUBLIKATIONEN

Stibor H, Vadstein O, Diehl S, Gelzleichter A, Hansen T, **Hantzsche F**, Katechakis A, Lippert B, Loseth K, Peters C, Roederer W, Sandow M, Sundt-Hansen L, Olsen Y (2004) Copepods act as a switch between alternative trophic cascades in marine pelagic food webs. *Ecol Lett* 7: 321-328

Stibor H, Gelzleichter A, **Hantzsche F**, Sommer U, Striebel M, Vadstein O, Olsen Y (2006) Combining dialysis and dilution techniques to estimate gross growth rate of phytoplankton and grazing by micro- and mesozooplankton in situ. *Archiv für Hydrobiologie* 167: 403-419

Boersma M, Aberle N, **Hantzsche FM**, Schoo KL, Wiltshire KH, Malzahn AM (2008) Nutritional limitation travels up the food chain. *International Review of Hydrobiology* 93: 479-488

Malzahn AM, **Hantzsche F**, Schoo KL, Boersma M, Aberle N (2010) Differential effects of nutrient-limited primary production on primary, secondary or tertiary consumers. *Oecologia* 162: 35-48

Hantzsche FM, Boersma M (2010) Dietary-induced responses in the phagotrophic flagellate *Oxyrrhis marina*. *Mar Biol* 157: 1641-1651

ERKLÄRUNG

Hiermit erkläre ich, dass die vorliegende Dissertation, abgesehen von der Beratung meiner Betreuer, selbstständig von mir angefertigt wurde und dass sie nach Form und Inhalt meine eigene Arbeit ist. Sie wurde keiner anderen Stelle im Rahmen eines Prüfungsverfahrens vorgelegt. Dies ist mein einziges und bisher erstes Promotionsverfahren. Die vorliegende Arbeit entstand unter Einhaltung der Regeln guter wissenschaftlicher Praxis der Deutschen Forschungsgemeinschaft. Des Weiteren erkläre ich, dass ich Zuhörer bei der Disputation zulasse.



Helgoland, den 23.08.2010

Florian Hantzsch